NTNU – Trondheim
Norwegian University of
Science and Technology

Dynamic Stress due to End Effects in of Non-bonded Flexible Pipes

Miao Li

Marine Technology
Submission date: June 2015
Supervisor: Svein Sævik, IMT
Co-supervisor: Naiquan Ye, Marintek

Norwegian University of Science and Technology
Department of Marine Technology

NTNU – Trondheim
Norwegian University of
Science and Technology

Dynamic Stress due to End Effects in Non-bonded Flexible Pipes

Miao Li

Marine Technology

Submission date: June 2015

Supervisor: Svein Sævik, IMT

Co-supervisor: Naiquan Ye, Marintek

Abstract

In oil and gas industry, flexile riser is a crucial component for the production system which connected the seabed and the floating units. At the upper end of the flexible riser, bending stiffener is added to reduce the over bending. Flexible riser is mainly made of non-bonded flexible pipe, tensile amour layer is the crucial layer for sustain the longitudinal force. In this thesis, the maximum fatigue damage and stress components of the tensile amour layer are studied. The gap between the end fitting and the bending stiffener can decrease the end effects, in this thesis the effect of increasing the gap length is to be analyzed.

In this thesis two kinds of cross-section- ITCODE31 and ITCODE0 are analyzed. For each cross-section, two different load conditions are analyzed, one is with low longitudinal force (0.1MN) and the other one is with high longitudinal force (0.5MN). Under each load condition, models with different gap length (0, 0.25, 0.5 and 0.75 pitch) are analyzed to study the effects on fatigue and stress components. Under 0.5MN longitudinal force, two more cases (1.5 and 3pitch length) are analyzed to better study the convergence of the gap effect.

At last, friction sensitive study is performed. Three friction factors: 0.1, 0.15 and 0.3 are analyzed and compared.

Preface

This master thesis has been carried out during the spring semester of 2015 at the Department of Marine Technology, Norwegian University of Science and Technology (NTNU). The thesis is the completion of the two years Master program in Marine Technology.

This topic is very cutting-edge technology, and the work is creative and challenging. The work mainly includes literature study about flexible pipe, modeling in the BFLEX2010 software, fatigue and stress analysis and results discussion.

As the topic of research was different from the author's area of expertise and earlier research project work, initial phase of the research was slow. A large amount time was spent on identifying and understanding relevant theory and learning the BFLEX2010 software. Through this thesis work the author was able to gain a much deeper understanding of subsea technology and solid theory knowledge which has been very beneficial for the research work.

I would like to express my heartfelt thanks to my supervisor Prof. Svein Sævik for guiding me through the whole semester with great patience. During the course of this thesis, Prof. Svein Sævik explained the relevant literature and most apt research method for this research. I would also like to thank my co-supervisor Dr. Naiquan Ye from MARINTEK with his detailed and in-depth guidance in using the BFLEX2010 software and inspiring suggestions.

Miao Li

Trondheim, June 2015

Scope of work

The flexible riser represents a vital part of many oil and gas production systems. Failure in the riser section may cause loss of lives, environmental pollution and threaten the field economy. One of the most critical failure modes is corrosion fatigue in the tensile armour steel layers due to the combined action of dynamic loads and corrosion from the annulus and seawater environments. The fatigue stresses in the tensile armour is governed by the slip and friction behaviour of the tensile armours and is normally evaluated by models that assume that the stress at one location is uniquely determined by the curvature at the same location. This might not be the case if end effect is present or if curvature gradients occur. The purpose of the master thesis is to investigate under which circumstances this assumption hold.

The work shall be carried out as follows:

1. Literature study related to non-bonded flexible pipe technology, design standards etc. This is also to include methods for global and local response analysis focusing on the issue of calculating the stresses in flexible pipes and familiarization with the Bflex software.

2. Establish necessary input for flexible riser local stress and fatigue analysis for two cross-sections. This includes geometric and mechanical characteristics as well as a dynamic load scatter diagram. A full and detailed overview of the cross-section input and load cases analysis shall be included in the report.

3. Establish local Bflex models for the flexible pipe cross-section using ITCODE 0 and ITCODE31 for two cross-sections and for start BS at 0, 0.25, 0.5 and 0.75 pitch from end fitting.

4. Perform fatigue stress analysis in Bflex using the above models and compare the results in terms of stress history plots and fatigue contribution from each load case at different longitudinal force for a typical SN curve.

5. Conclusions and recommendations for further work

Nomenclature

E	Young's module
G	Shear module
L_0	Total pipe length
L_p	pitch length
R	radius of the outer circle
r	radius of the inner circle
α	lay angle of the helix of the tensile layer
θ_1	Radian corresponding to the whole pipe length along the helix
θ_0	Radian corresponding to the gap length along the helix
I_z	the area moment of inertia of the cross-section about the z axis
EI_y	the bending stiffness of the cross-section about the y axis
EI_z	the bending stiffness of the cross-section about the z axis
A	R: radius of the outer circle
I_y:	the area moment of inertia of the cross-section about the y axis
σ_{ax}	Axial stress of tendon
σ_{my}	Normal curvature stress of tendon
σ_{mz}	Transverse curvature stress of tendon
σ_{xx}	Total longitudinal stress of tendon

Contents

List of Tables

List of Figures

1 Introduction

1.1 Background

With the development of the oil and gas industry, exploration has been performed in progressively deeper and deeper locations under the water surface. The growth and development of deepwater and ultra-deepwater activity is apparently all around the world. With flexible pipe technology developing rapidly, flexible pipes are increasingly being used in offshore field even in harsh environments.

The main characteristic of a flexible pipe is its low relative bending stiffness so that it can provide more compliant performance which allows it to withstand both vertical and horizontal movement of the floating platform. This is achieved by using multiple layers of different material in the wall fabrication. These layers are able to slip past each other when under the influence of external and internal loads, and hence this characteristic gives a flexible pipe its property of a low bending stiffness.

1.2 Main contributions

This thesis is mainly focus on studying how the gap length (from the end fitting to the starting of the bending stiffener) affects the maximum fatigue damage on the tensile layer, including the damage location and the damage value. Furthermore the study also focuses on how the stress components affect the fatigue.

Models with two kinds of cross-section, ITCODE0 and ITCODE31, are built with gap length of 0, 0.25, 0.5, 0.75 pitch cases, respectively. Analysis is performed mainly on the inner tensile layer where will get the largest fatigue damage and stress components.

Two kinds of load conditions are analyzed to study the effect of different load condition, with 0.1MN and 0.5MN longitudinal force. Under 0.5MN longitudinal force condition, two more cases, 1.5 and 3.0 pitch cases are analyzed for fully control the fatigue damage changing trend as the gap length increasing.

Friction sensitive study is performed. Three friction factors: 0.1, 0.15 and 0.3 are analyzed and compared.

1.3 Structure of the contents

The thesis is carried out as the following:

Chapter 2: introduction of the flexible pipe technology which include the riser configurations, classifications, constructions, characteristics and failure modes

Chapter 3: description of the mechanical behavior of the flexible pipe, both axisymmetric and bending behavior

Chapter 4: introduction of BFLEX2010 program which include both the system and the theory under it

Chapter 5: introduction of the modeling method and the characteristics of the models

Chapter 6: stress and fatigue analysis and discussions

Chapter 7: summarizes of the conclusions and recommendations for future work

2 Introduction of flexible pipe

The flexible pipe composite structure combines steel armor layers with high stiffness to provide strength, and polymer sealing layers with low stiffness to provide fluid integrity. This construction gives flexible pipes a number of advantages over other types of pipelines (such as steel pipes). These advantages include prefabrication, storage in long lengths on reels, reduced transport and installation costs. Details see from [1].

2.1 Riser configuration

In harsh environmental conditions especially in deepwater, environmental loads become more and more complicated which lead to large dynamic motions of the floaters. Compliant risers are designed to absorb floater motions by changing of geometry without use of heave compensation systems, so that it allows highly dynamic flexibility. There are six ‘classical’ compliant riser configurations: Steep S, Lazy S, Steep Wave, Lazy Wave, Pliant Wave or Free Hanging Catenary. The selection of riser system configuration is according to the specific water depth, vessel movements, environmental conditions, number of risers and interference issues.

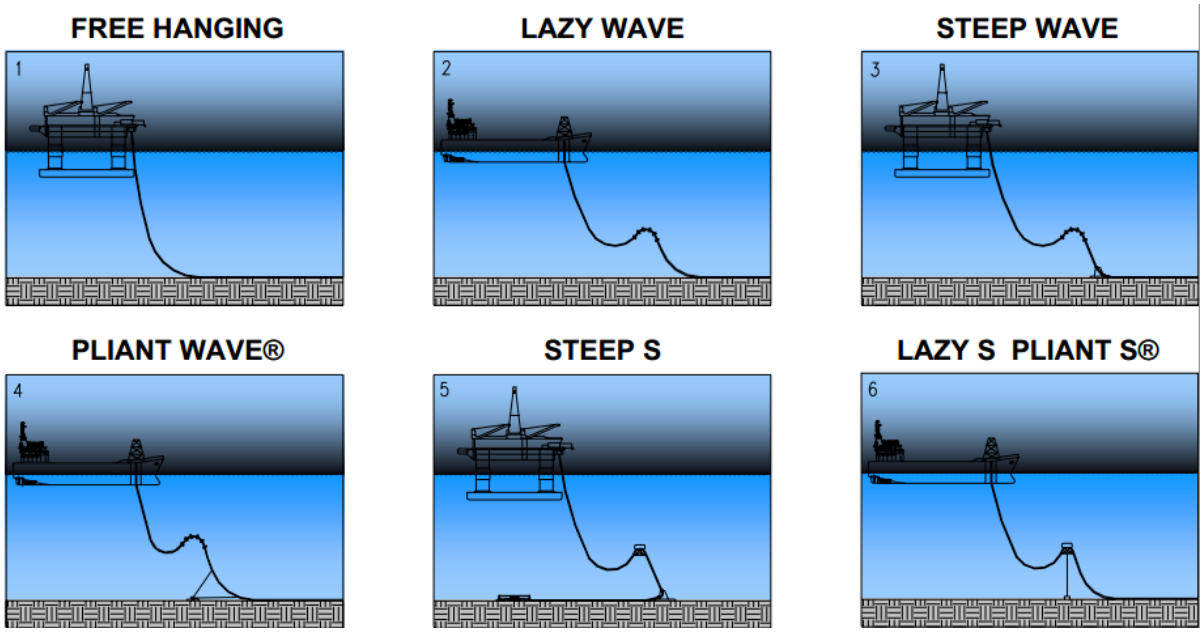

Figure 2-1 Classical Compliant Riser Configurations (Technip)

Free Hanging Catenary

In most cases, free hanging catenary is not only the simplest but also the cheapest solution among all the riser configurations. A free hanging catenary is very easy to install and does not need heave compensation equipment, which makes its use fairly common in deep water. Following the motion of the floater, the riser is just either lifted up from the seabed or lowered down on the seabed. As the water depth increases, the top tension also increases because of the growth of the riser length. The most critical point on the riser is the Tough Down Point (TDP), since the floater's motion is directly transferred to this point. Pipe compression may happen at this point for the downwards movements of the floater, which may lead to buckling and 'bird caging' of the armour wires.

Laze Wave and Steep Wave

To decouple the floater's motion transferred to TDP, added buoyancy and weight are added along the length of riser. With this distributed weight and buoyancy, the shape of riser can be decided. Compared with steep wave, lazy wave is preferred since it requires minimal subsea infrastructure. For steep wave, riser base on the seabed is needed which makes the installation process becomes more complex. However, steep wave riser can better maintain the original configuration even if the riser content density changes.

Lazy S and Steep S

To solve the problem at the TDP, a subsea buoy is added on the riser to get the S configuration, so that the subsea buoy absorbs the tension variation induced by the floater. Additionally, the requirements to the top tensioner are reduced because they reduce the free length of the riser.

There are two kinds of the subsea buoy, one is a fixed subsea structure, the other one is the anchored subsea buoy, also called Mid Water Arch.

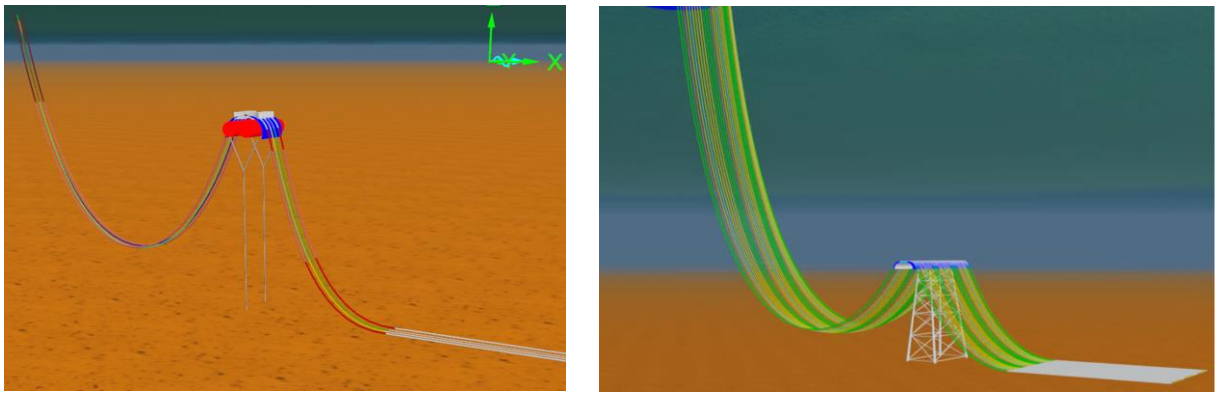

Figure 2-2 subsea buoy- fixed subsea structure (right) and anchored subsea buoy (left) Courtesy of 4subsea

Pliant Wave

In this configuration, a subsea anchor controls the TDP. The tension in the riser is directly transferred to the anchor instead of the TDP. Additionally, since the riser is directly tied to the well located beneath the floater, the well intervention become possible without additional vessel.

2.2 Bonded and non-bonded pipe

There are two kinds of flexible pipes bonded and non-bonded pipes. For non-bonded pipes, the cylindrical layer is able to slide relative to adjacent layers. While for bonded pipes, the armor elements and the pressure containing components are molded into a single structure and all the layers are glued together as an elastic composite material, which prevents it from slipping between layers.

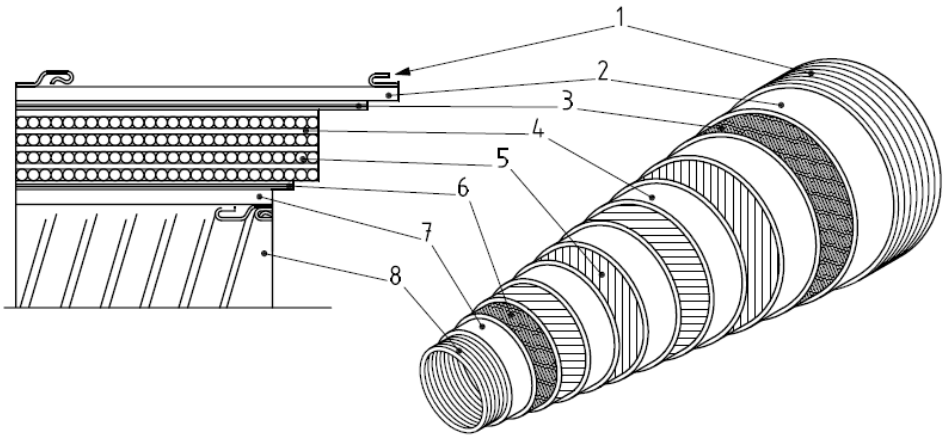

Key

1	outer wrap	5	reinforcement layer
2	cover	6	breaker layer
3	breaker layer	7	liner
4	cushion layer	8	carcass

Figure 2-3 Typical bonded flexible pipe [2]

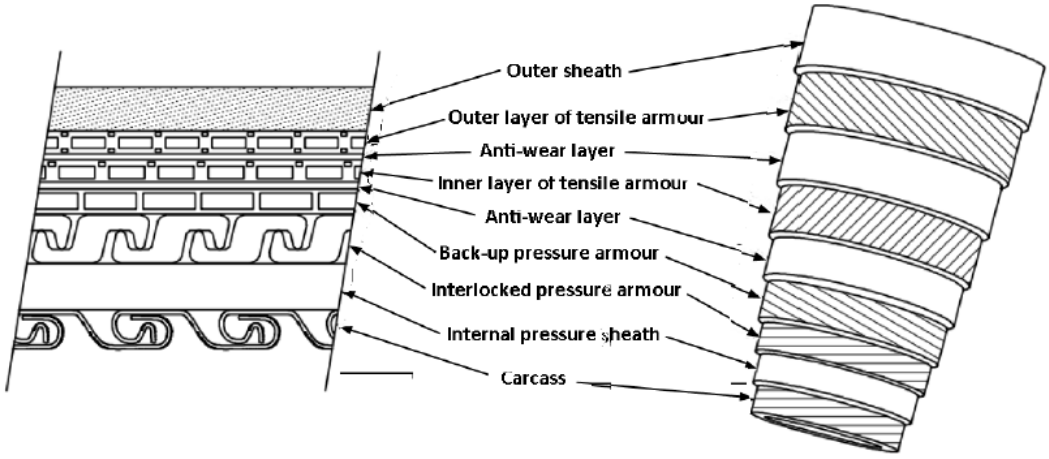

Figure 2-4 Typical non-bonded flexible pipe [3]

The bonded pipe is primarily used for short length (up to 100 meters) jumpers in high dynamic applications. Non-bonded pipes are widely used for long distance (up to several kilometers) transport pipes, such as flexible risers, flowlines, subsea jumpers and jumpers.

2.3 Main cross-section components of non-bonded pipe

Since non-bonded pipes are the main research focus in this thesis, in this part we mainly introduce the cross-section for the non-bonded flexible pipes. In general, Flexible pipe cross-

section is comprised of steel, polymer, insulation and tape materials. Six main layers from the inside to outside of the pipe radius direction are described below.

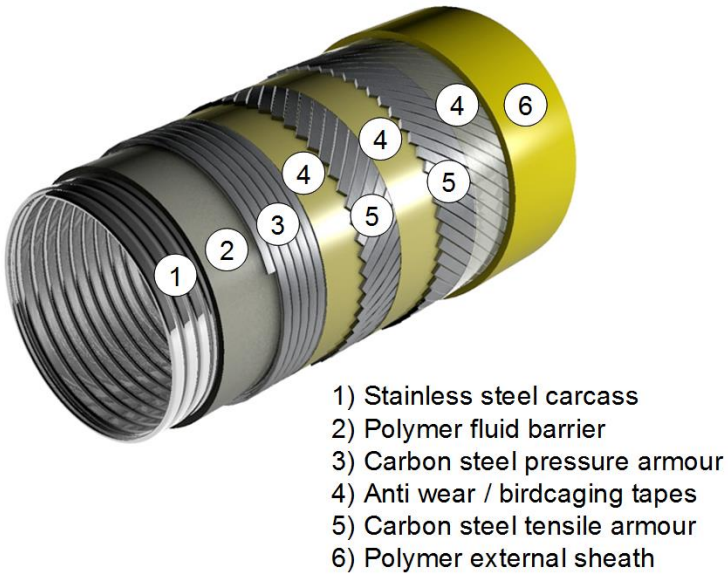

Figure 2-5 Typical cross section of a non-bonded flexible pipe. (Courtesy of GE Oil & Gas)

Carcass

The carcass forms the innermost layer of the non-bonded pipe cross-section. Typically, interlocking profile is fabricated from stainless steel flat strip. The inner bore fluid is free to flow through the carcass profile and therefore the carcass material needs to be corrosion-resistant to the bore fluid. The main function of the carcass is to provide strength to resist hydrostatic pressure and crushing loads during installation operations and handling of the pipe.

Polymer Fluid Barrier (Liner)

The liner is the sealing layer, made from a thermoplastic by extrusion over the carcass. The polymer sheath acts as a pressure barrier to maintain the bore fluid integrity.

Steel Pressure Armor

The function of the pressure armor is to back up the liner and to withstand the hoop stress in the pipe wall caused by the inner bore fluid pressure. The pressure armor is made of interlocking wires which allow bending flexibility and control the gap between the armor wires to prevent internal sheath extrusion through the armor layer.

The example profile Zeta/Flexlok shows in the following figure:

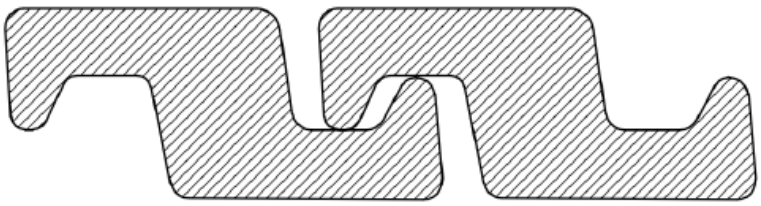

Figure 2-6 Zeta/Flexlok interlocking profile used as pressure armour [4]

Anti-wear tape & Anti-buckling tape

When the flexible pipe subjected to cyclic bending the tensile steel armour wires will slide cyclically relative to adjacent steel layers with significant contact stress. Anti-wear tape is applied between layers of steel armour to prevent direct contact between two steel armour layers.

Torsion and axial compression loading may lead to radial buckling or 'bird-caging' of the tensile armour. Anti-buckling tape provided outside the outer tensile armour layer to prevent buckling effect

Tensile Armor

The tensile armour formed by two or four layers (for high tension riser) of armor wires which provide strength against axial stress caused by internal pressure and by external loads. The layers are counter-wound in pairs to avoid torsion. In most cases, the lay angle of the wire helix is 30 to 35 deg.

Polymer External Sheath

This outer sheath (similar as the inter polymer sheath) is a seal layer to keep the seawater integrity. Additionally, the external polymer sheath protects the armor layers from clashing effects with other objects during installation.

2.4 Bending stiffener

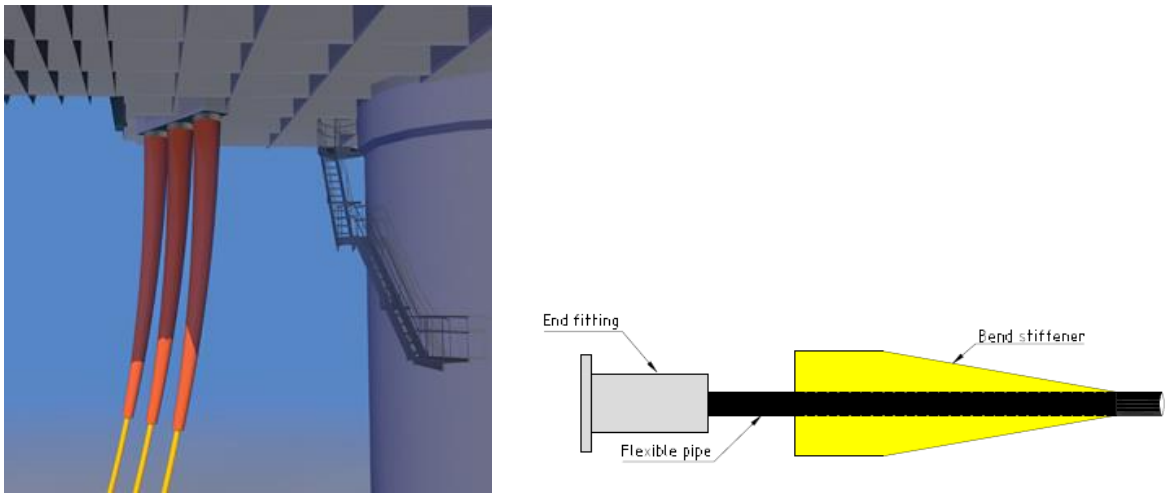

Figure 2-7 bending stiffener

Source from http://www.subseacableprotection.com/products/bend-stiffeners.cfm

A flexible pipe is terminated with an end fitting where all layers are anchored and clamped in a special end structure. Bending stiffeners are polymeric structures with a conical shaper that are added onto the flexible pipe at their uppermost connections to improve the pipe stiffness, so that they can limit the curvature of flexible risers, protecting them against overbending and from accumulation of fatigue damage. Therefore, bending stiffeners are very important to deep water oil and gas production systems. Bending stiffeners may have a large size, several metres in length and more than 1.5 m diameter at the base with a weight of more than 1.5 ton [4].

2.5 Failure modes

Flexible pipes mainly used in harsh working environment, they will experience loads from waves, internal fluid/gas and floating units. It is very important to have a comprehensive understanding of the failure modes of the flexible pipe both in the design phase and the operational phase.

Failure modes can stop the flexible pipe from transporting and have risk of large incident. Refer to [4], there are only two main failure modes:

• Leakage

• Reduction of internal cross section

Details are shown below:

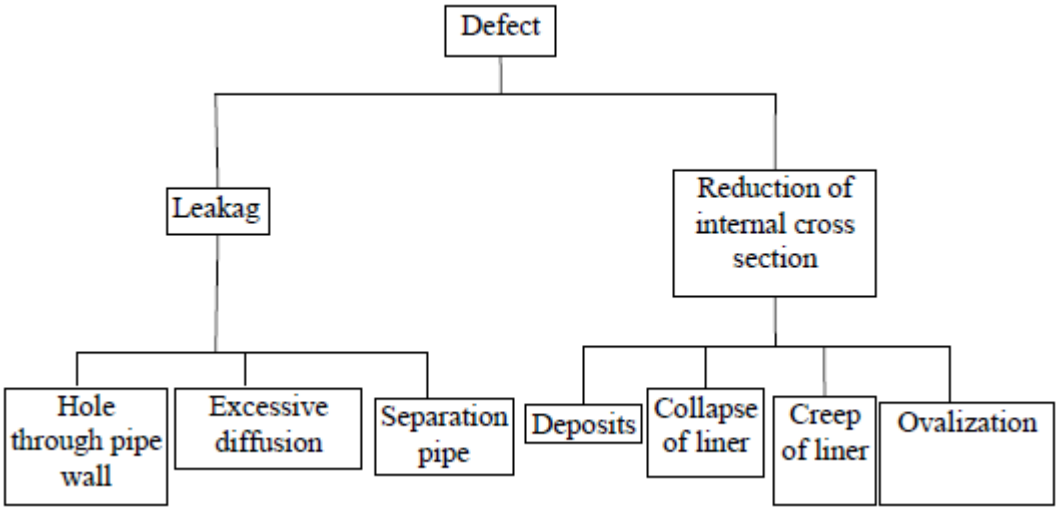

Figure 2-8 typical failure mode [5]

Due to over load tension, compression, bending, torsion, fatigue as well as erosion and diffused fluid, failures can happen in the tensile and pressure armours. the checklist for typical failure modes can be found in API Recommended Practice 17B [5].

Table 2-1 Checklist of Failure Modes for Structural Design of Unbonded Flexible Pipe

Pipe global failure mode	**Potential Failure Mechanisms**
Collapse	Collapse of carcass and/or pressure armour due to excessive tension, excessive external pressure, installation loads or ovalisation due to installation loads. Collapse of internal pressure sheath in smooth bore pipe. Collapse of carcass due to pressure build up in multilayer pressure sheaths followed by rapid decompression. Collapses of pipe due to carcass pull out from end fitting. Collapse of carcass due to the carcass fatigue.
Burst	Rupture of pressure armours due to excess internal pressure Rupture of tensile armours due to excess internal pressure

Tensile Failure	Rupture of tensile armors due to armour due to excessive tension Collapse of Carcass and/or pressure armors and/or internal pressure sheath due to excessive tension Snagging by fishing trawl board or anchor, causing over bending or tensile failure
Compressive Failure	Bird-caging of tensile armor wires. Compression leading to upheaval buckling and excess bending.
Over bending	Collapse of carcass and/or pressure armor or internal pressure sheath. Rupture of internal pressure sheath. Unlocking of interlocked pressure or tensile armor layer. Crack in outer sheath.
Torsional Failure	Failure of tensile armor wires. Collapse of carcass and/or internal pressure sheath. Birdcaging of tensile armor wires.
Fatigue Failure	Tensile armor wire fatigue. Pressure armor wire fatigue.
Erosion	Erosion of internal carcass
Corrosion	Corrosion of internal carcass. Corrosion of pressure of tensile armor exposed to seawater,if applicable. Corrosion of pressure of tensile armor exposed to diffused product

2.6 Design Criteria

The main source for requirements and criteria on flexible pipes are API and ISO. This thesis is mainly according to Specification for nonbonded Flexible Pipe. API.17J.

Relevant standards are shown as following:

DNV-RP-F204, Recommended practice for riser damage

DNV-RP-D101, Recommended practice for structural analysis of piping systems

Specification for bonded Flexible Pipe. API SPECIFICATION 17k.

Specification for nonbonded Flexible Pipe. API SPECIFICATION 17J.

Recommended Practice for Flexible Pipe API 17B

3 Mechanical description of flexible pipe

In this part the mechanical behavior of the non-bonded flexible pipe will be discussed. The loads on the cross section can be separated to axisymmetric loads and bending loads. To simplify the problem, we can assume the behavior of the pipe can be separated to uncoupled axisymmetric and bending behavior respectively. This chapter mainly based on the theory from Bflex theory manual [6] and handbook of flexible pipe [4].

This can be illustrated from figure below:

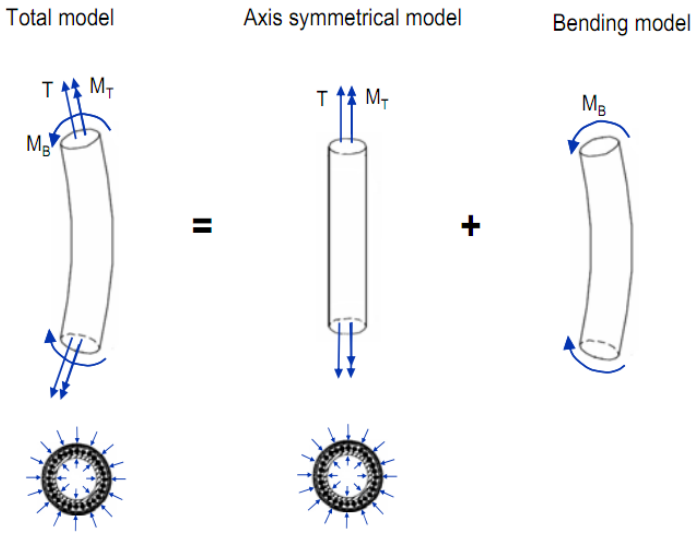

Figure 3-1 mechanical behavior of flexible pipe [7]

To better understand the mechanical behavior of the flexible pipes, it is crucial to clarify which layers and stress components will contribute. Normally, the stress components include 3 normal components σ_{11}, σ_{22}, σ_{33}, and 3 shear stress components σ_{13}, σ_{23}, σ_{12}. Details are shown in Figure 3-2.

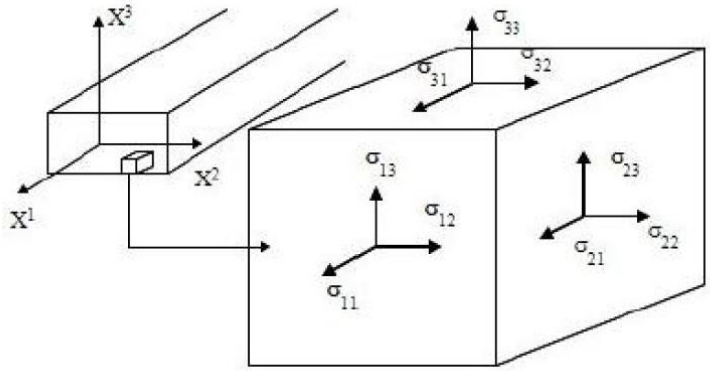

Figure 3-2 general components of stress [8]

The carcass do not carry pressure due to its corrugated structure; the plastic layers behave hydrostatic and the contact pressure is to be transformed directly to the next steel layer. The loads mainly governed by the steel layers. So in this thesis the main study focus is on the tensile armour layer.

3.1 Kinematics of helix

In the flexible pipe, the steel layers are governing the structural strength, the steel layers are constructed with multiple flat tendons which are assumed to set stress free in helical configurations, as shown in Figure 3-3.

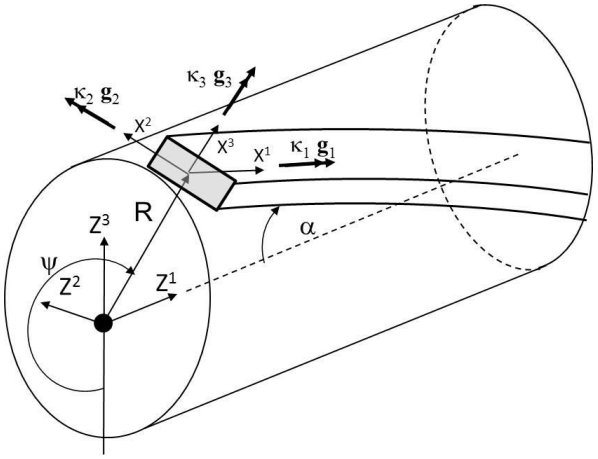

Figure 3-3 Initial torsion and curvature quantities [8]

The initial torsion κ_1, initial normal curvature κ_2 and the curvature along the helix κ_3 can be expressed by the lay angle and the helix radius R as:

$$\kappa_1 = \frac{sin\alpha cos\alpha}{R} \tag{3-1}$$

$$\kappa_2 = \frac{sin^2\alpha}{R} \tag{3-2}$$

$$\kappa_3 = 0 \tag{3-3}$$

Where the α is the lay angle.

The long and thin wires can be described by curved beam theory. When considering only the axisymmetric loads, the generated shear force and bending moment would be insignificant. So the wire equilibrium equation can be used:

$$-\kappa_2 Q_1 + \kappa_1 Q_2 + q_3 = 0 \tag{3-4}$$

$$-\kappa_2 M_1 + \kappa_1 M_2 + Q_2 = 0 \tag{3-5}$$

Where Q_i represent the forces along the X^i axes; M_i represent the moments about X^i axes; q_3 is the contact line load in the radial direction. Neglect the M_i and Q_2, we get

$$q_3 = \kappa_2 Q_1 = Q_2 \tag{3-6}$$

In this thesis, the axisymmetric loads mainly caused by longitudinal force and internal pressure; the bending loads mainly caused by the bending angle added on the left end of the pipe. Thesis three kind of loads will be discussed in the flowing part.

3.2 Behaviour due to axisymmetric loads

Longitudinal loading of the flexible pipe can be illustrate as below

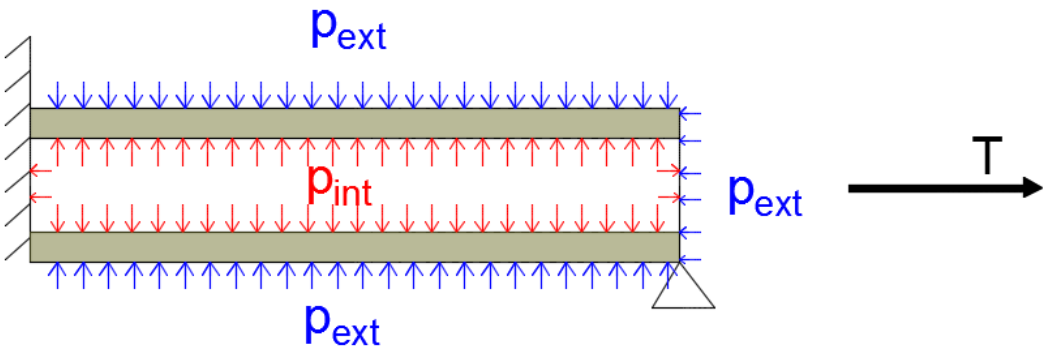

Figure 3-4 axisymmetric loads on flexible pipe

So we can gain the wall tension force of the pipe as below:

$$T_w = T + \pi p_{int} R_{int}^2 - \pi p_{ext} R_{ext}^2 \tag{3-7}$$

Where p_{int} is the internal pressure of the pipe; p_{ext} is the external pressure of the pipe;

R_{int} is the internal radius of the pipe; R_{ext} is the external radius of the pipe;

T is the total longitudinal force on the pipe;

T_w is the longitudianl force on the pipe wall.

For a single wire j of the contributing layer, the forces are shown as figure below:

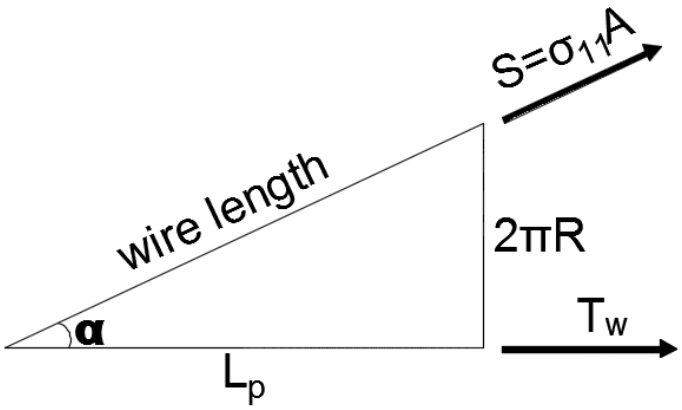

Figure 3-5 forces on a single wire of steel layer

$$T_{wj} = \sigma_{11j} A_j cos\alpha_j \tag{3-8}$$

Then, for all the steel layers, the pure axial equilibrium as below:

$$\sum_{j=1}^{N_a} n_j \sigma_{11j} A_j cos\alpha_j = T_w = T + \pi p_{int} R_{int}^2 - \pi p_{ext} R_{ext}^2 \quad (3\text{-}9)$$

where: N_a is the number of the total contributing layers, T_w is the true wall tension force, n_j is the number of wires in layer j, $\sigma_{11j}$is the axial stress in the layer, A_j is the area of the cross section, T is the effective tension, p_{int} is the internal pressure and p_{ext} is the external pressure. Normally, the lay angle of the pressure spiral wire is close to 90 degree, which means $\alpha_j = 0$, so the main axial load is taken by the tensile armour layer.

The stresses in the tensile armour can be calculated by the wall tension force over the effective tendon area

$$\sigma_t = \frac{T_w}{nA_t cos\alpha} = \frac{T_w}{2\pi R t_{tot} F_f cos^2\alpha} \quad (3\text{-}10)$$

Where n is the total number of tensile armour wires, A_t is the area of the wire, t_{tot} is the thickness including both layers, F_f is the fill factor.

The axial strain in the helix can be obtained by calculate the sum of the longitudinal stain of the of the cross section center and the radial motion of each layer.

Stain by standard beam quantities at the cross-section centre:

$$\epsilon_{11c} = cos^2\alpha\epsilon_p + Rsin\alpha cos\alpha\tau_p \quad (3\text{-}11)$$

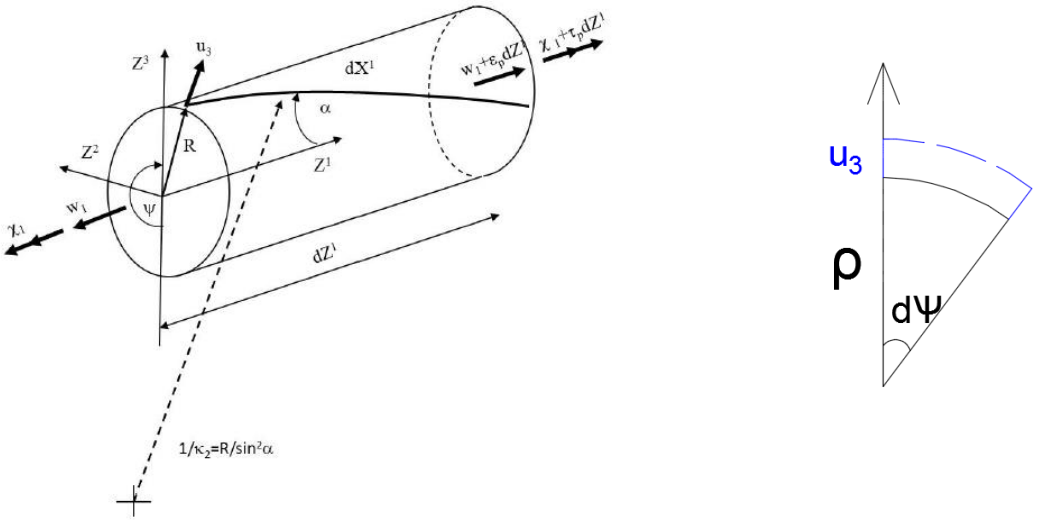

Figure 3-6 kinematic quantities for axisymmetric deformation (left) radius deformation (right)

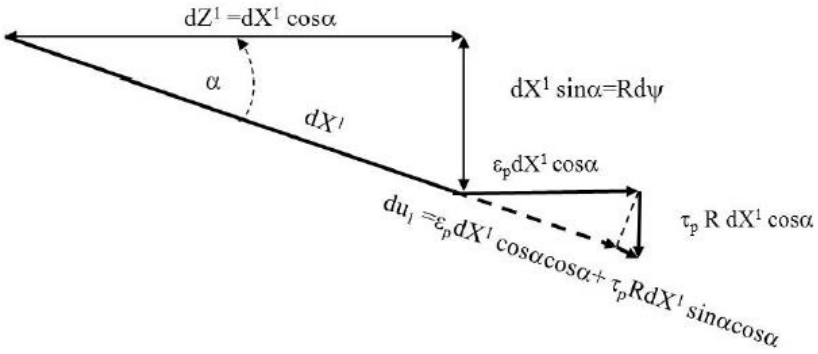

Figure 3-7 infinitesimal segment strain [8]

$$\rho = 1/\kappa_{\,2} = \frac{R}{sin^2\alpha} \tag{3-12}$$

The stain due to radial motion u_3 of the layer:

$$\epsilon_{11R} = \varepsilon = \frac{u_3}{\rho} = \frac{sin^2\alpha}{R}u_3 \tag{3-13}$$

So the axial strain in the helix describe as

$$\epsilon_{11} = \epsilon_{11c} + \epsilon_{11R} = cos^2\alpha\epsilon_p + Rsin\alpha cos\alpha\tau_p + \frac{sin^2\alpha}{R}u_3 \tag{3-14}$$

Assuming no torsion coupling ($\tau_p = 0$), then the axial stiffness of the two layered pipe can be obtained by using energy principles:

$$EA = nEA_t cos\alpha(cos^2\alpha - \upsilon_a sin^2\alpha) \tag{3-15}$$

$\upsilon_a\ is$ the apparent Poisson's ratio defined by the relation between axial straining and radial contraction $\upsilon_a = -\frac{u_3}{R\epsilon_p}$.

3.3 Behaviour in bending

The bending behavior of non-bonded flexibles is more complicated to analyze than the axisymmetric load condition. [11]

3.3.1 Moment curvature behavior (PIPE52 model)

At the beginning, the flexible pipe perform as a rigid pipe according to Navier's hypothesis under increased bending. Under the plane surfaces remaining plane assumption.

Axial force Q_1 along the wire direction before slip

$$Q1 = EA\varepsilon \tag{3-16}$$

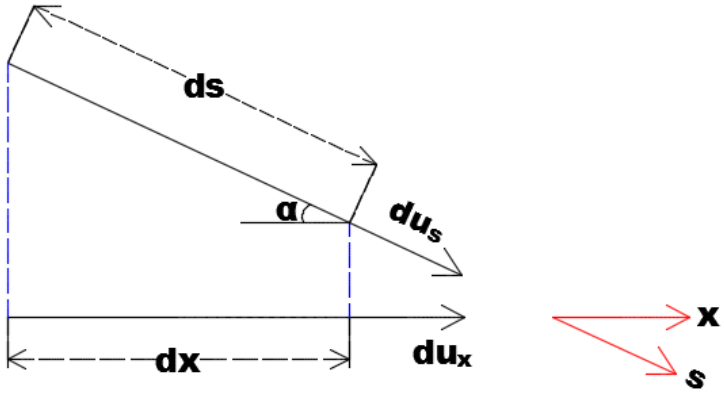

Figure 3-8 helix axial strain

$$\varepsilon = \frac{du_s}{ds} = \frac{du_x cos\alpha}{\frac{dx}{cos\alpha}} = \frac{du_x}{dx} cos^2\alpha \tag{3-17}$$

From above equations, we get

$$Q1 = EA\frac{du_x}{dx} cos^2\alpha \tag{3-18}$$

$$\frac{du_x}{dx} = -Rcos\psi\beta_2 \tag{3-19}$$

Combine above, we get

$$Q1 = -EAcos^2\alpha Rcos\psi\beta_2 \tag{3-20}$$

The associated shear force $q_1$per unit length along the wire needed to fulfill the plane surfaces remain plane condition, and it can be obtained by differentiating the above equation with respect to the length coordinate X_1 and applying the relation $\psi = \frac{sin^2\alpha}{R} X^1$:

$$q_1 = \mathrm{EA}cos^2\alpha sin\alpha sin\psi\beta_2 \tag{3-21}$$

The maximum shear stress q_{1c} is found at the pipe meutral xis of bending as for standard beam theory:

$$q_{1c} = \mu(q_3^I + q_3^{I+1}) \tag{3-22}$$

Where μ is the friction coefficient; q_3^I refers to the inner surface contact force and q_3^{I+1} refers to the outer surface contact force.

Then the critical curvature is found as:

$$\beta_{2c} = \frac{\mu(q_3^I + q_3^{I+1})}{\mathrm{EA}cos^2\alpha sin\alpha} \tag{3-23}$$

The stress at the outer fibre of the pipe at this stage is:

$$\mathrm{S}^{11}(\psi = \pi) = \frac{\mathrm{Q1}}{A} = \mathrm{E}cos^2\alpha R\beta_{2C} = \frac{\mu(q_3^I + q_3^{I+1})\mathrm{R}}{\mathrm{A}sin\alpha} \tag{3-24}$$

An arbitrary cross-section can be divided into two zones as shown in figure below:

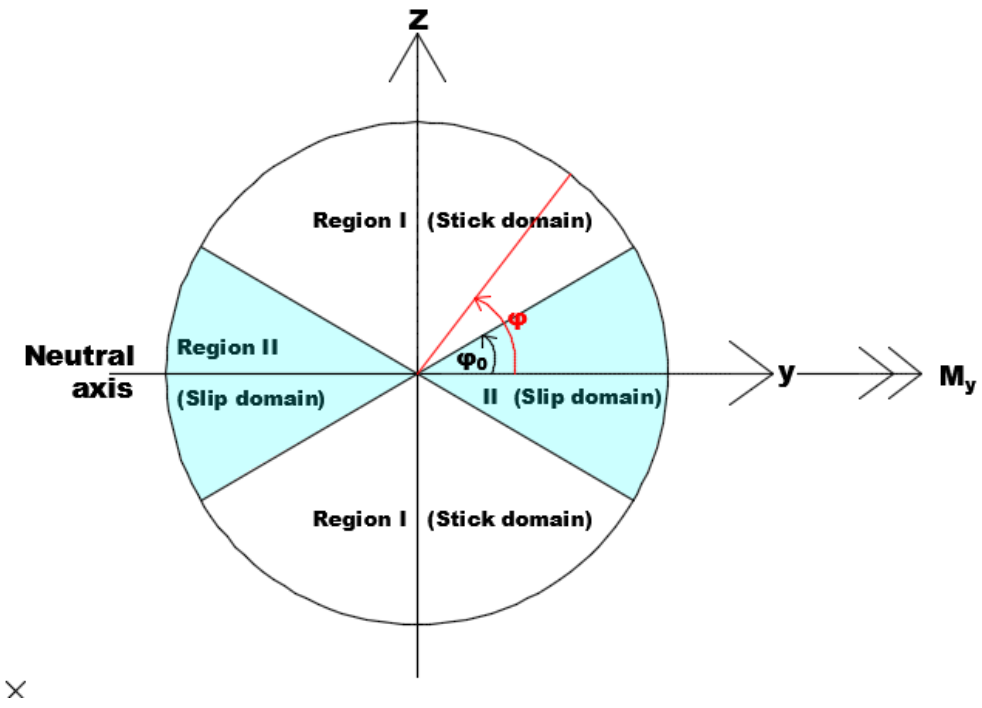

Figure 3-9 cross-section slip zone

One zone is slip region and the other one will be the stick region. Considering one quarter of the cross-section at the tensile side (the upper right part in figure 3.7), the transition between these two regions can be defined by the angle ψ_0:

$$\psi_0 = cos^{-1}(\frac{\beta_{2c}}{\beta_2}) \tag{3-25}$$

β_2 represents the actual curvature of the cross-section at any stage beyond slip.

The stress distribution along region II can be expressed by

$$\sigma_{11}(\psi) = \frac{\mu(q_3^I + q_3^{I+1})\mathrm{R}}{\mathrm{A}sin\alpha}\psi \tag{3-26}$$

The stress distribution in region I can be expressed by

$$\sigma_{11}(\psi) = Ecos^2\alpha R\beta_2(sin\psi - sin\psi_0) + \frac{\mu(q_3^I + q_3^{I+1})\mathrm{R}}{\mathrm{A}sin\alpha}\psi_0 \tag{3-27}$$

when $\psi_0 = \psi_0 = \frac{\pi}{2}$, full slip happens. The stress reaches its full value:

$$\sigma_{11} = \frac{\pi}{2}\frac{\mu(q_3^I + q_3^{I+1})\mathrm{R}}{\mathrm{A}sin\alpha} \tag{3-28}$$

Considering the layer as a thin shell layer with thickness t, then the associated bending moment can be found by integration.

The start slip bending moment from ech layer is found as:

$$M_c = \frac{R^2\mu(q_3^I + q_3^{I+1})\mathrm{n}}{2tan\alpha} = F_f\frac{\pi R^3\cos^2\alpha\mu(q_3^I + q_3^{I+1})}{bsin\alpha} \tag{3-29}$$

The full slip bending moment from the same layer can be found as

$$M_f = \frac{2R^2\mu(q_3^I + q_3^{I+1})\mathrm{n}}{\pi tan\alpha} = F_f\frac{4R^3\cos^2\alpha\mu(q_3^I + q_3^{I+1})}{bsin\alpha} \tag{3-30}$$

We can see that the difference between these two moments are a factor π/4,

$$M_c = \frac{\pi}{4} M_f \tag{3-31}$$

Then the moment curvature diagram which represents the friction contribution to the moment curavture relation from each tensile armour layer can be constructured, details see Figure 3-10.

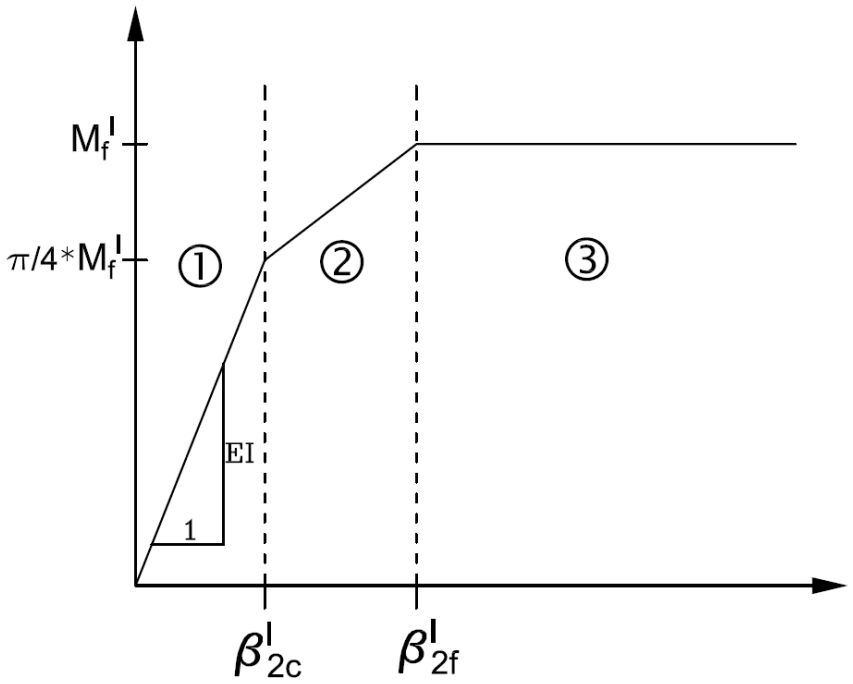

Figure 3-10 moment curvature relation from each layer

In the non-bonded flexible pipe, the contact pressure vary from layer to layer, therefore each layer has an individual moment curvature diagram which include a sum of three-liner relations.

3.3.2 Shear deformation model (HSHEAR352)

Normally, the tensile steel layers are supported by thick plastic layers, shear deformation may occur. The assumption of plane surface remains plane can no longer be used. The shear stress between the wire and the antiwear layer will be governed by the inherent shear deformations and the tape material shear modulus.

For the element HSHEAR352 in bflex2010, only considering axial displacements between the core and each wire, the internal work contribution from each tendon can be written as:

$$W_i = \int_0^l \mathrm{EA}(\beta, 1 + u_{1p,1}) + \mathrm{c}\beta\delta\beta + \mathrm{G}I_1\, w_{1p}\delta w_1 + EI_2 w_{2p}\delta w_2 + EI_3 w_{3p}\delta w_3 dX^1 \quad (3\text{-}32)$$

Where,

$\beta = u_1 - u_{1p}$ is the relative displacement between tendon and core along the helical path, details refer to Figure 3-11.

w_{ip} represent the prescribed torsion and curvature quantities if plane surfaces remained plane and the wire strain, torsion and curvature being described by the loxodromic curve quantities.

C is the non-linear shear stiffness parameter determined by the stick-slip behaviour between layers, value is 0 in the slip domain.

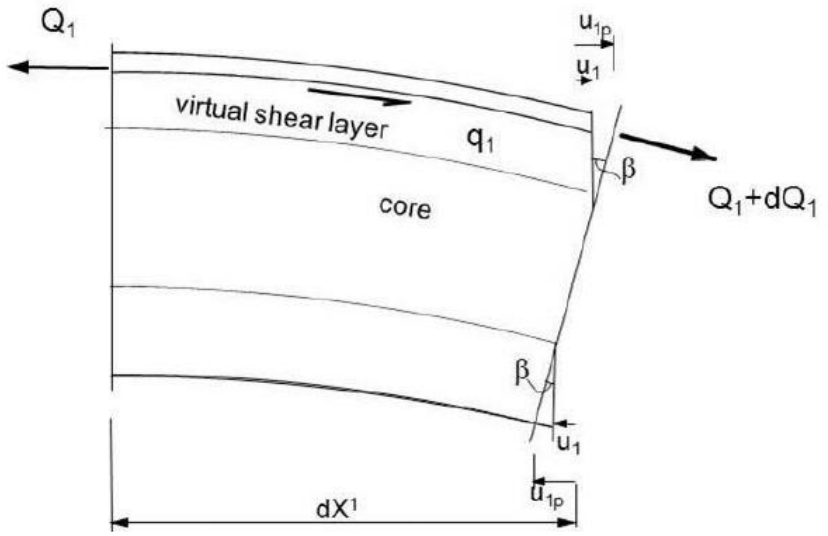

Figure 3-11 shear interaction model [6]

4 Methodology

4.1 Non-linear Finite Element Method

Flexible pipe has the characteristics of low bending stiffness, large deformation and multiple layer construction. So the analysis of the flexible pipes is high nonlinearities. The most dominate nonlinear effects are Geometry Non-linearity, Material Non-linearity and Boundary Non-linearity [9].

• Geometry Non-linearity

The flexible pipe will experience large deformation when the length of the pipe is very long. The deflections of the structure are large compared with the original dimensions of the structure, and the stiffness and loads will change as the structure deforms.

• Material Non-linearity

Material behaviour is based on the current deformation state and possibly the past history deformation, and other constitutive variables may also have some influences. This property is mainly shown in the structures which undergo non-linear elasticity, plasticity, viscoelasticity, creep or inelastic rate effects, and is usually related to the Young's Modulus.

• Boundary Non-linearity

During the analysis of the structure, the boundary conditions may change in the contact area. These nonlinearities include force boundary condition and displacement boundary condition nonlinearities.

Pressure loads of fluid are the most important engineering application concern, including hydrostatic loads on submerged or container structures, aerodynamic and hydrodynamic loads.

4.2 Principle of virtual displacement

4.3 Static Solution Procedure

The static solution procedure is based on user defined load control with Newton-Raphson equilibrium iteration at each load step. For details about calculation refer to [9].

The total static equilibrium can be expressed as

$$\boldsymbol{R}_{int} = \boldsymbol{R}_e \tag{4.1}$$

$$\boldsymbol{R}_{int} = \sum_i \left(\boldsymbol{a}^i\right)^T \boldsymbol{S}^i \tag{4.2}$$

$$\boldsymbol{K}_i(\boldsymbol{r})d\boldsymbol{r} = d\boldsymbol{R} \tag{4.3}$$

$\boldsymbol{R}_{int}$ − The resultant internal structural reaction force vector

$\boldsymbol{R}_e$ − External load force vector

Iterative methods (Newton-Raphson method)

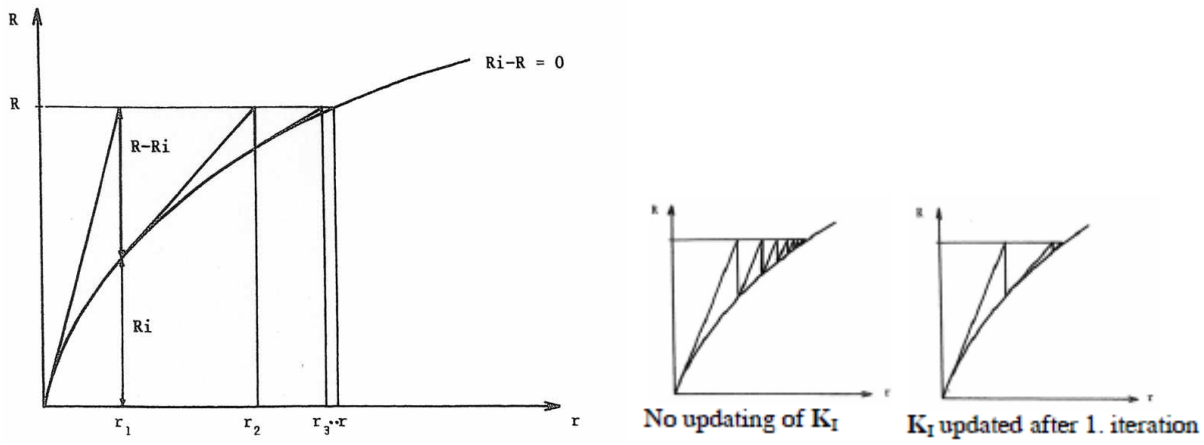

Figure 4-1 Newton-Raphson iterative method and two modified method

$$\boldsymbol{r}_{n+1} = \boldsymbol{r}_n - \boldsymbol{K}_I^{-1}(\boldsymbol{r}_n)(\boldsymbol{R}_{int} - \boldsymbol{R}) \tag{4.4}$$

This method requires that $\mathbf{K}_I$ is established and $\boldsymbol{r}_{n+1}$ solved in each step. This is time confusion. Two modified method are shown in Figure above, one is with no $\mathbf{K}_I$ updating and the other one is to update $\mathbf{K}_I$ after the first iteration.

4.4 BFLEX2010 program

The BFLEX2010 computer program is developed by MARINTEK, it is developed for stress and fatigue analysis of flexible pipes taking into account longitudinal effects which can be significant in some regions of a flexible pipe. This may be due to constraints at the termination, friction effects in bending stiffener or bellmouth region etc. Models for both the tensile and pressure armour are included.

BFLEX2010 consists of several program modules [10]:

- The XPOST graphical user interface for result presentation can be applied to results viewing of both the BFLEX2010 and the local model generated by BFLEX2010POST.

-The BFLEX2010 module, reading and controlling all input data, and performing stress analysis of the tensile armour.

-The BFLEX2010post module, enabling post processing, which includes the PFLEX module, BOUNDARY module, LIFETIME module and BPOST module.

1. The PFLEX module is used for performing pressure spiral bending stress analysis.
2. The BOUNDARY module is used for performing transverse cross-sectional stress analysis
3. The LIFETIME module is used for performing fatigue analysis.
4. The BPOST module, for results postprocessing from the local results database to ASCII files that can be plotted by the plotting program Matrixplot.

4.5 Cross Section（ITCODE 0 &ITCODE 31）

In this thesis two kinds of cross section- ITCODE 0 and ITCODE 31- are used for modeling the structures and analyzing the stress. In BFLEX2010, cross sections are constructed by elements. For ITCODE0, the core is defined by element PIPE52, while both the inner and outer tensile layers are defined by element HSHEAR352. For ITCODE31, all layers are modeled by element PIPE52. For both of the two cross sections, the bending stiffener is modeled by element PIPE52, the contact relation between the flexible pipe and bending stiffener is defined by element CONT130. For the cases with gap between the end-fitting and bending stiffener, element PIPE31 is used to represent the rigid connection between the end-fitting and end of the bending stiffener.

4.5.1 PIPE52

The PIPE52 element is the elastic / elastoplastic pipe element, which handles the core and resultant moment based model for the armour layers. PIPE52 is used for modeling the axisymmetric and bending contribution of the flexible pipe. Another function for it is to model the bending stiffener.

4.5.2 HSHEAR352

The HSHEAR352 element is the elastic helix tensile armour element, which is constituted by four nodes- two centroid nodes and two helix nodes. Normally, the centroid nodes are defined in nodal coordinates while the helix nodes required to be defined by polar coordinates. This element enabling the helix longitudinal slip behaviour. Details are shown as below:

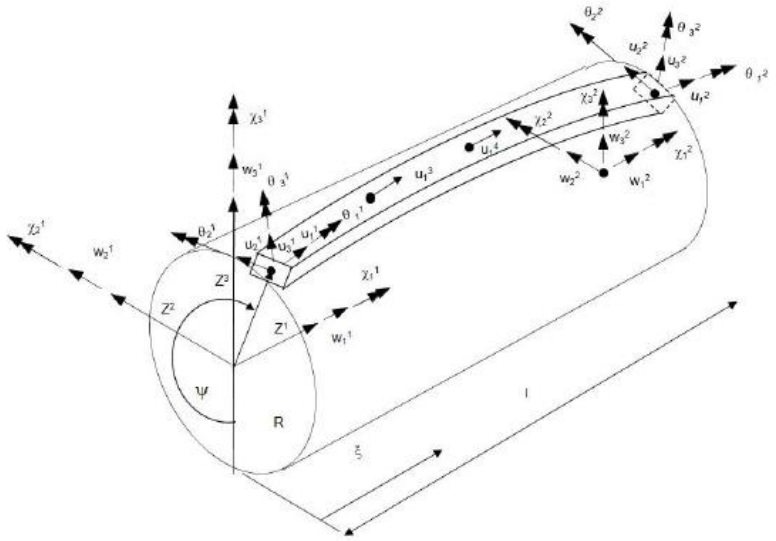

Figure 4-2 HSHEAR352 element [6]

4.5.3 CONT130

CONT130 is non-structural element which is used in two pipe node systems to present the relation between the bending stiffener and pipe interaction.

4.5.4 PIPE31

PIPE31 is elastic pipe element which is using the elastic material model.

Under the plain stress assumption, the Hook's law is used,

$$\begin{bmatrix} \sigma_{11} \\ \sigma_{22} \\ \tau \end{bmatrix} = \frac{E}{1-\nu^2} \begin{bmatrix} 1 & \nu & 0 \\ \nu & 1 & 0 \\ 0 & 0 & \frac{1-\nu^2}{2(1+\nu)} \end{bmatrix} \begin{bmatrix} \varepsilon_{11} \\ \varepsilon_{22} \\ \gamma \end{bmatrix} \tag{4-5}$$

Utilize the fact that the hoop stress is known using shell theory for further simplification. No degree of freedom is related to the hoop effect.

5 Modeling

Two types of models with different cross sections are used for analysis in this thesis: ITCODE 0 and ITCODE 31. Original model refers to the model with no gap between the end fitting and bending stiffener; modified model refers to the model with 0.25, 0.5, 0.75, 1.5 and 3pitch length gap.

5.1 Model description

This model describes a 10 meter length non-bonded flexible riser with a 5 meter length bending stiffener. This model is used to analyze the effects of the gap length between the end fitting and bending stiffener, and to quantify the gap length impact on the fatigue behavior of the flexible pipes.

5.2 Layer and element type

Flexible pipe

For both itcode 0 and itcode 31 models, the flexible pipe is defined by three main layers, which includes core, tenslayer1 and tenslayer2. The core layer includes all the other layers except the tensile armour layers, while the tenslayer1 and tenslayer2 represent the inner and outer tensile armour layer, respectively. For both itcode 0 and itcode 31, the element type used to describe core layer is pipe 52. While the tensile armour layers are defined differently, for itcode 0, they are defined by element hshear 352. For itcode 31, they are defined by element pipe 52.

Bending stiffener and contact

The bending stiffener is established by pipe52 element. To describe the contact between the flexible pipe and the bending stiffener, cont130 element is used. Pipe 31 element is used to model the rigid connection between the end fitting and the bending stiffener.

Table 5-1 Finite element modeling description of both cross section

Layer name		Element type ITCODE 0	Element type ITCODE 31	Description
mypipe	core	pipe52		Core element group except tensile armour layers
	tenslayer1	hshear352	pipe52	Inner tensile armour layer
	tenslayer2	hshear352	pipe52	Outer tensile armour layer
mybendstiffener	bendstiffener	pipe52		Bending stiffener
bscontmat1	bscontact	cont130		Contact between the bending stiffener and core
stiffmat	outerpipe	pipe31		Rigid connection between end fitting and bending stiffener

5.3 Pipe coordinate and geometry

5.3.1 For the original model (0 gap length)

For the core layer, 201 nodes are defined in the global system and 200 elements are established. For the tensile armour layers, 16 tendons are modeled around the cross section for each layer. The nodes and elements are defined for establishing the tensile armour layers are different in model itcode 0 and itcode 31.

The tensile armour layers of ITCODE 0

Firstly, in the polar coordinate 201 nodes are defined along a helix with 10,000mm total height. Commands refer to Nocoor Polar in appendix A.

For the inner tensile layer (tenslayer1), the helix pitch angle is calculated according to the given *theta* value:

$$L_{p_1} = \frac{theta_1/2\pi}{L_0} = \frac{62.1/2\pi}{10000} = 1011.79 \tag{5-1}$$

$$\alpha_1 = \arctan\left(\frac{2\pi R_1}{L_{p_1}}\right) = \arctan\left(\frac{2\pi * 135.1}{1011.79}\right) = 0.69806 \tag{5-2}$$

There are 16 tendons on the cross section of each layer, so these 201 nodes repeated 16 times, and 16 helixes are defined.

$$\text{dtheta} = \frac{2\pi}{16} = 0.392 \tag{5-3}$$

To define the elements of tenslayer1, four nodes are used to build up each element, two from the global node system and the other two are from the polar node system. Commands refer to ELcon tenslayer1 in Appendix A. For example, for the first element No.1001, two nodes No.1&2 are from the global node system and the other two No.1001&1002 are from the polar node system. Along the helix direction, there are 200 elements in total; along the translation direction, there are 16 helixes in total. So for the last element (No.1016) along the cross section, the number of the two nodes on the polar coordinate can be calculated as (n is the number of the helixes)

$$n_{3_1} = 201 * (\mathrm{n} - 1) + 1001 = 4016 \tag{5-4}$$

For the outer tensile armour layer (tenslayer2), similar calculations are performed as inner tensile layer (tenslayer1). Relevant parameters are

$$L_{p_2} = \frac{theta_2/2\pi}{L_0} = \frac{59.42/2\pi}{10000} = 1057.42 \tag{5-5}$$

$$\alpha_2 = \arctan\left(\frac{2\pi R_2}{L_{p_2}}\right) = \arctan\left(\frac{2\pi * 141.2}{1057.42}\right) = 0.69808 \tag{5-6}$$

$$n_{3_2} = 201 * (\mathrm{n} - 1) + 20001 = 23016 \tag{5-7}$$

L_0 is the total pipe length

Tenslayer 1 means the inner tensile armour layer; tenslayer 2 means the outer tensile layer

R is the radius of the layer cross-section

α is the pitch angle of the helix of the tensile layer

L_p is the pitch length

Subscribe 1 means inner tensile layer, subscribe 2 means outer tensile layer

The tensile armour layers of ITCODE 31

For model itcode 31, the tensile layers are modeled with the same element type (pipe 52) as the core layer. So the modeling method is same as for the core element method. Commands refer to Nocoor Coordinates and Elcon tenslayer1 in appendix B.

5.3.2 Modified model

The gap lengths of the modified models are calculated according to the pitch length of the inner layer (tenslayer1). All the important parameters are shown in Table 5-2

Table 5-2 calculated parameters for all models

Model	$L_0[mm]$	Tenslayer	$R[mm]$	α [rad]	$L_p[mm]$	θ_1[rad]	θ_0[rad]
Original (0 pitch gap)	10000	1	135.1	-0.69806	-1011.79	-62.100	0
		2	141.2	0.69808	1057.42	59.420	0
0.25 pitch gap	10252.95	1	135.1	-0.69806	-1011.79	-63.671	-1.571
		2	141.2	0.69808	1057.42	60.923	1.503
0.5 pitch gap	10505.89	1	135.1	-0.69806	-1011.79	-65.242	-3.142
		2	141.2	0.69808	1057.42	62.426	3.006
0.75 pitch gap	10758.84	1	135.1	-0.69806	-1011.79	-66.812	-4.712
		2	141.2	0.69808	1057.42	63.929	4.509
1.5 pitch gap	11517.68	1	135.1	-0.69806	-1011.79	-71.525	-9.425
		2	141.2	0.69808	1057.42	68.438	9.018
3 pitch gap	13035.36	1	135.1	-0.69806	-1011.79	-80.950	-18.850
		2	141.2	0.69808	1057.42	77.456	18.036

Here, $\theta_1$is the radian corresponding to the whole pipe length along the helix and $\theta_0$is the radian corresponding to the gap length along the helix, calculated as below

$$\theta_1 = 2\pi \frac{L_0}{L_p} \tag{5-8}$$

$$\theta_0 = 2\pi \frac{L_0 - 1000}{L_p} \tag{5-9}$$

Calculation methods for other parameters refer to chapter 5.3.1.

5.4 Cross section input description and geometry

Table 5-3 details of cross section

No.	Layer	Material	Thickness[mm]	Lay angle[˚]
1	Carcass [CARC]	steel	7.2	88.062
2	[THER]	plastic	3	-
3	[THER]	plastic	6	-
4	[THER]	plastic	3	-
5	Pressure [ZETA]	steel	10	88.868
6	[THER]	plastic	2.5	-
7	Tensile [TENS]	steel	3.6	-40
8	[THER]	plastic	2.5	-
9	Tensile [TENS]	steel	3.6	40
10	[THER]	plastic	1.3	-
11	[THER]	plastic	2.5	-
12	[THER]	plastic	10	-

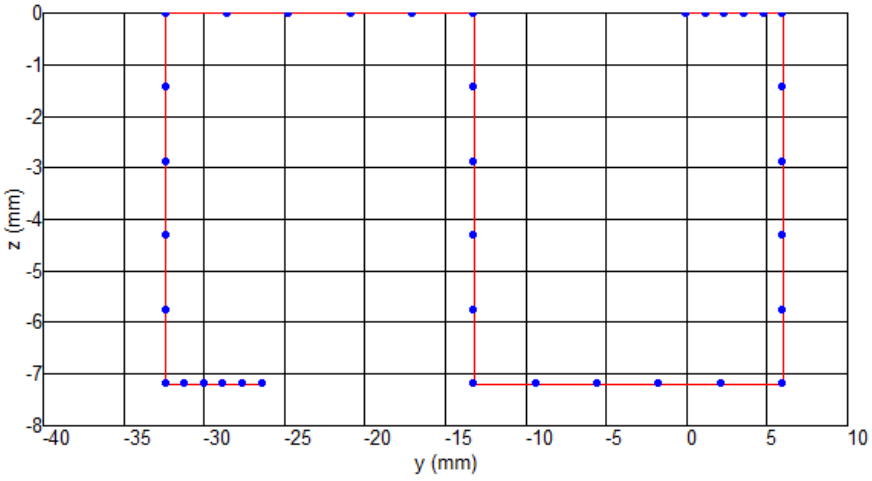

Figure 5-1 Carcass layer single tendon cross section geometry

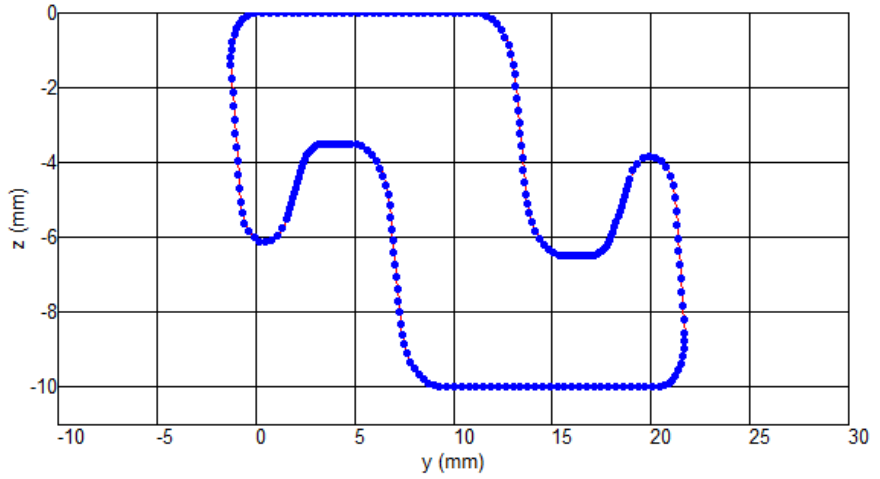

Figure 5-2 Pressure layer single tendon cross section geometry

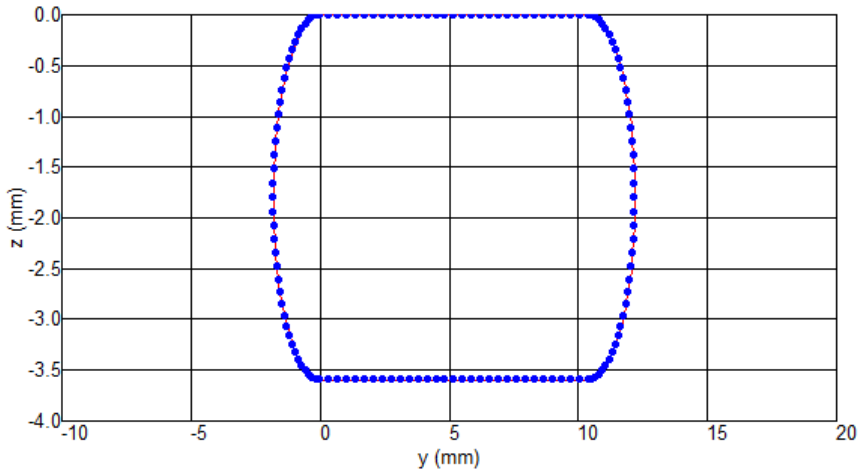

Figure 5-3 Tensile layer single tendon cross section geometry

5.5 Bending stiffener and contact interactions

bending stiffener

The bending stiffener is defined by 101 nodes from No. 501 to No.601 in the global coordinate system. Accordingly, 100 elements are defined from element No.501 to No.600. The contact interactions between the bending stiffener and the flexible pipe are included by introducing the contact element- cont130. 100 elements are defined to connect global nodes (node 1 to 100) and bending stiffener elements (element 501 to 600) numbering from 601 to 700. Commends refers to ELCON bscontact & CONTINT bscontact in appendix A/B.

Connected pipe (outerpipe)

For the models with a gap between the end fitting and bending stiffener, the pipe connected the end fitting and bending stiffener is modeled as a rigid pipe with element type pipe 31. Commends refer to Elcon outerpipe in appendix A/B. The material property is defined by commend MATERIAL stiffmat. The connecting pipe (outerpipe) has outer radius 110mm and thickness 10mm. We should note that these values just give a visible figure, they do not have physical meaning.

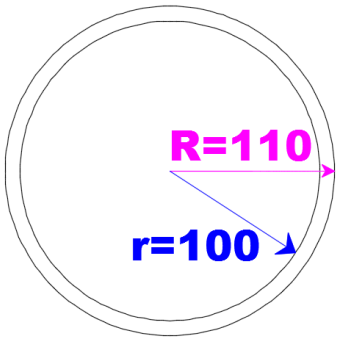

Figure 5-4 cross section of connected pipe

Axial stiffness:

$$\mathrm{EA} = \mathrm{E}(\pi \mathrm{R}^2 - \pi \mathrm{r}^2) = 200GPa * \pi(110^2 - 100^2)\mathrm{mm}^2 = 1.32 * 10^9 N \quad (5\text{-}10)$$

Bending stiffness:

$$\mathrm{I}_y = \mathrm{I}_z = \frac{\pi[(2\mathrm{R})^4 - (2\mathrm{r})^4]}{64} = \frac{\pi[(2 * 110)^4 - (2 * 100)^4]}{64} mm^4 = 3.645 * 10^7 mm^4 \quad (5\text{-}11)$$

$$\mathrm{EI}_y = \mathrm{EI}_z = 200GPa * 3.645 * 10^7 mm^4 = 2 * 10^5 Nmm^2 \quad (5\text{-}12)$$

Where

E: Young's Modulus

A: area of the cross section

R: radius of the outer circle

r: radius of the inner circle

I_y: the area moment of inertia of the cross-section about the y axis

I_z: the area moment of inertia of the cross-section about the z axis

EI_y: the bending stiffness of the cross-section about the y axis

EI_z: the bending stiffness of the cross-section about the z axis

However, the calculated bending stiffness according to the cross section geometer is too small to represent rigid connection. To guarantee strong enough bending stiffness, here we multiply 10^{10} to the calculated bending stiffness, so we use $2*10^{15}$ Nmm^2 as the bending stiffness in the model.

To get the torsion stiffness, we calculated the relation between the torsion stiffness and the bending stiffness:

$$I_t = \frac{\pi\,[(2R)^4 - (2r)^4]}{32} = 2\,I_y \tag{5-13}$$

$$G = 80GPa = 0.4E \tag{5-14}$$

$$GI_t = 0.4E * 2\,I_y = 0.8EI_y = 0.8 * 2 * 10^{15}Nmm^2 = 1.6 * 10^{15}Nmm \tag{5-15}$$

G: modulus of rigidity

I_t: the torsion constant for the section.

GI_t: the torsional rigidity.

5.6 Boundary condition

ITCODE 0

1. For the core layer, node 1 at the left end only have one freedom in direction 5(rotation around y axis), the other five directions are fixed. The node at the right end of the core is fixed in the y and z directions.
2. For the bending stiffener of the original model, node 501 same as node 1, only have one freedom in direction 5(rotation around y axis), the other five directions are fixed.
   For the bending stiffener of the modified model, since the end node 501 and the end node 1 of the core are rigid connected, the boundary conditions of node 501 are defined as fixed only in 2 and 6 directions (no movement in y direction and no rotation around z axis).
3. For both of the tensile layers, due to the property of the element hshear352, all the nodes of the tendons at both ends are fixed in x direction.

ITCODE 31

The tensile layers are defined with the same global nodes as the core layer. When defined the boundary condition for global node 1, then the boundary conditions for both the core and tensile layers are defined. Fix the global node1 in five directions only rotation around y axis is allowed. The boundary conditions for the bending stiffener and the right end of the pipe are the same as ITCODE 0.

5.7 Load application (original model)

In this thesis, gravity and external pressure loads are neglected. Three types of load histories are applied on the models. Constant internal pressure load (20MPa) is applied along the whole pipe. The horizontal concentrated load is applied at the end of the core of the end node. Two concentrated load conditions are applied respectively: low longitudinal force - 0.1MN and high longitudinal force - 0.5MN. Cyclic prescribed angle displacement for the original model is applied at the left end node of the core (node number 1) and the bending stiffener (load number 501), which refers to the end fitting point. For the modified models, cyclic prescribed angle displacements refer to chapter 5.8.

In BFLEX2010, load history is linearly interpolated between two points. The load histories are shown in the table below:

Table 5-4 Cyclic prescribed angle displacement of the original model-history 100

Time(s)	Load factor(angle degree)
0	0
2	0
102	3
302	-3
402	0

Table 5-5 Horizontal concentrated load (elongation load)-history 200
Constant internal pressure load -history 500

Time(s)	Load factor
0	0
1	1
402	1

5.8 Uniform load conditions

To analyze the effect of the gap length, initial load conditions should be uniformed, so that all the results can be comparable. In this thesis, one of the most important loads is the cyclic bending moment which is applied at the left end of the pipe. For all the cases, the largest bending moment at the left end of the bending stiffener should be the same.

In Bflex modeling, the bending moment is applied by adding cyclic prescribed angle displacement at the left end of the pipe. To guarantee node 501 (the end node of the bending stiffener) has the same largest moment during the load history, simulations are performed to get the corresponding bending angle.

5.8.1 Low longitudinal force - 0.1MN

The results of the corresponding bending angle are shown in the table and figure below:

Table 5-6 Comparison of moment and angle curve under 0.1MN

Gap length	0 pitch length		0.25 pitch length		0.5 pitch length		0.75 pitch length	
Unit	Angle amplitude [degree]	Moment [KNm]	Angle amplitude [degree]	Moment [KNm]	Angle amplitude [degree]	Moment [KNm]	Angle amplitude [degree]	Moment [KNm]
ITCODE0	3	46.293	2.9	46.412	2.8	46.563	2.7	46.686
ITCODE31	3	46.72	2.9	46.885	2.8	46.874	2.7	46.692

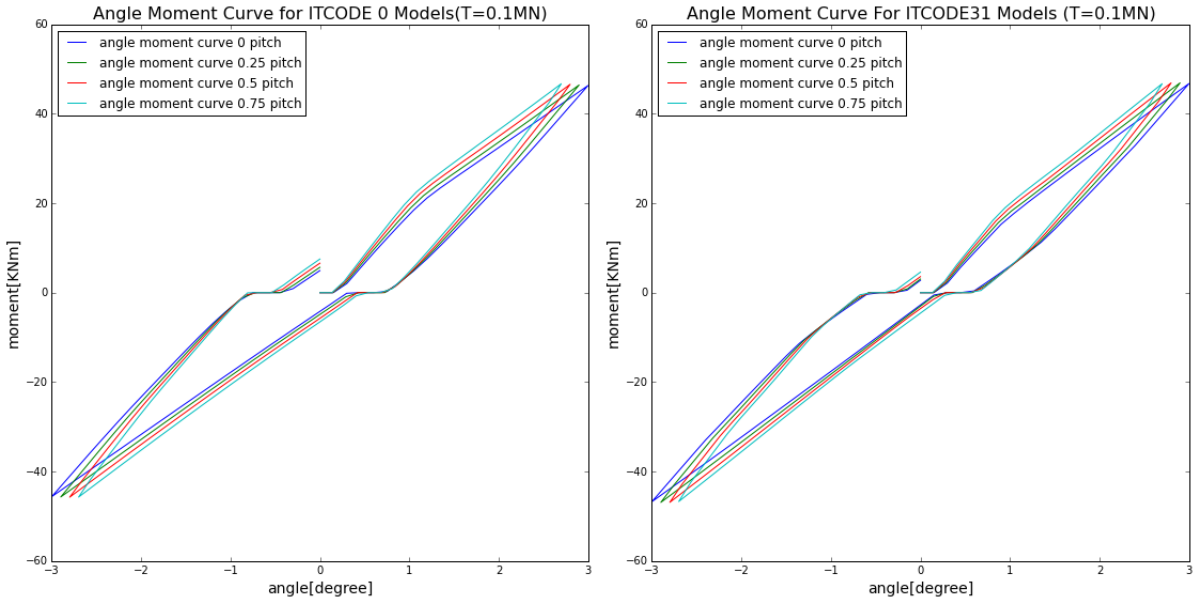

Figure 5-5 Angle and Moment curve for ITCODE 0 &ITCODE 31 models (T=0.1MN)

The angle-moment curvatures of both ITCODE 0 and ITCODE 31 have shown the same trend as the gap length growing. To keep the same bending moment at the end of the bending stiffener, the prescribed angle amplitude at the end of the pipe is decreasing. So the prescribed angle amplitude 3, 2.9, 2.8, 2.7 degree are applied on the cases 0, 0.25, 0.5 and 0.75 pitch, respectively.

5.8.2 High longitudinal force - 0.5MN

The prescribed angle amplitude 3, 2.85, 2.73, 2.64, 2.4, 2.07degree are applied on the cases 0, 0.25, 0.5, 0.75, 1.5 and 3, respectively. The results of the corresponding bending angle amplitude are shown in the table and figure below:

Table 5-7 Comparison of moment and angle curve under 0.5MN

Gap length	0 pitch length		0.25 pitch length		0.5 pitch length	
Unit	Angle amplitude [degree]	Moment [KNm]	Angle amplitude [degree]	Moment [KNm]	Angle amplitude [degree]	Moment [KNm]
ITCODE0	3	103.975	2.85	103.92	2.72	103.781
ITCODE31	3	105.668	2.85	105.305	2.73	105.197
Gap length	0.75 pitch length		1.5 pitch length		3 pitch length	
Unit	Angle amplitude [degree]	Moment [KNm]	Angle amplitude [degree]	Moment [KNm]	Angle amplitude [degree]	Moment [KNm]
ITCODE0	2.62	104.192	2.33	103.632	1.64	103.754
ITCODE31	2.64	105.6	2.4	105.456	2.07	105.31

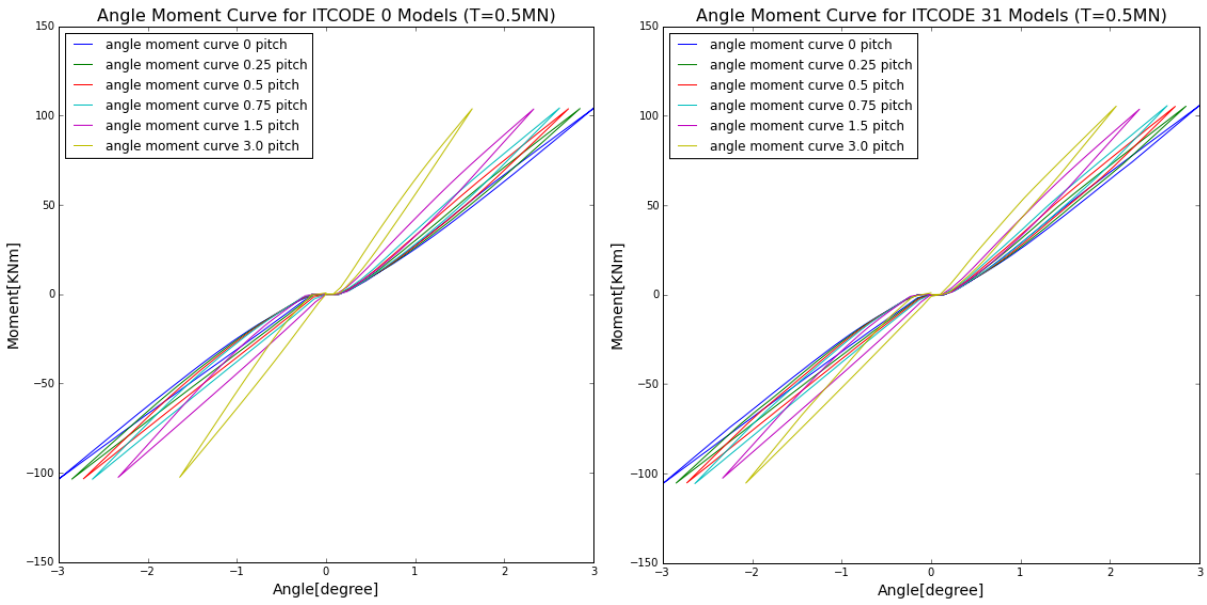

Figure 5-6 Angle and Moment curve (T=0.5MN)

5.9 Model simplification

The model with the boundary condition and the load history described above can be simplified as the figure below:

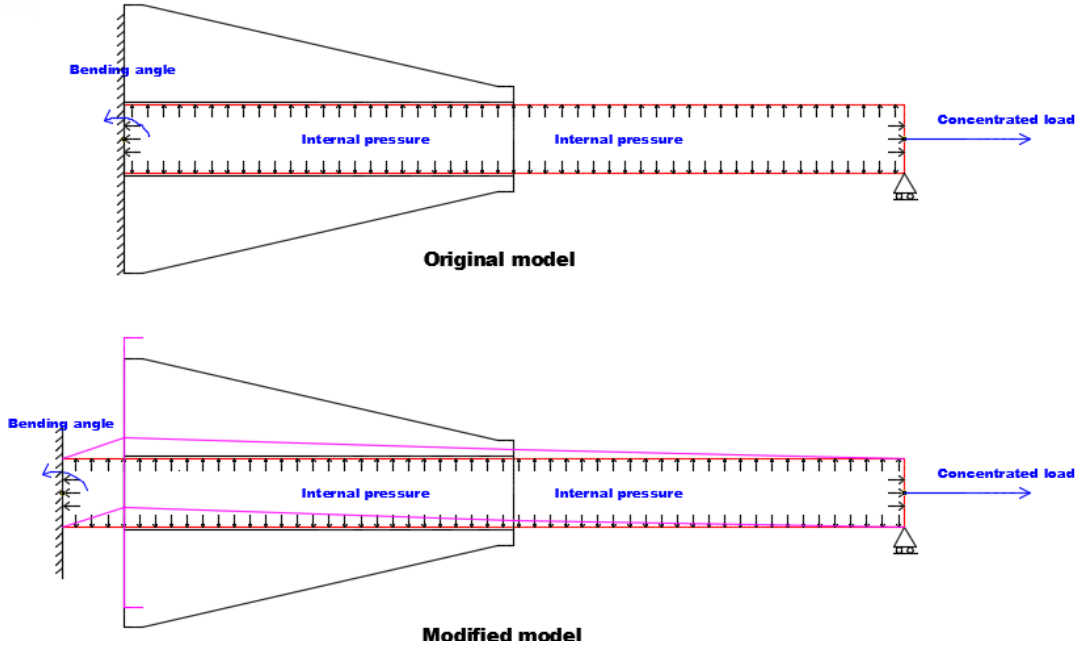

Figure 5-7 Couplings, loads and boundary conditions

6 Stress analysis and fatigue calculation

In this section, four cases of each cross section (ITCODE0 and ITCODE31) are compared in terms of local stress components and maximum fatigue damages. First step is to find out the node where reaches the maximum fatigue damage. Then, get the stress component ranges in the cases and compare them.

6.1 Fatigue analysis

Fatigue may happen when the structures are exposed to cyclic loads. In most cases, the load is smaller than the yield stress of the material, the damage cased per cycle is quite insignificant. Fatigue damage is a cyclic damage accumulation process.

6.1.1 SN curve

Normally, fatigue data is presented in a stress-life diagram-SN diagram. The relation between stress range $\Delta\sigma$ and number of cycles to failure N is represented on the diagram. SN curve is gained based on huge numbers of experimental data from fatigue testing [11].

In the finite life region, the fatigue data may be represented by an SN curve of the equation:

$$\mathrm{N}(\Delta S)^m = A \quad (A\ is\ constant) \tag{6-1}$$

Transform the equation form to log-log form, a straight line is gain.

$$\log\Delta S \quad = -\frac{1}{m} logN + \frac{1}{m} logA \tag{6-2}$$

N: The number of cycles to failure

ΔS: Stress range

m: the negative inverse slope of the SN curve

A typical SN curve is shown as below:

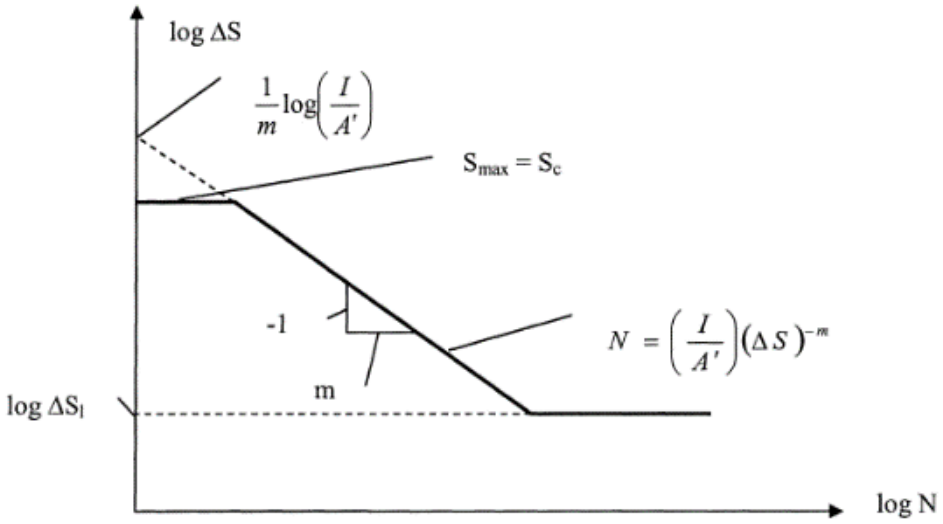

Figure 6-1 typical SN curve [11]

6.1.2 Fatigue calculation in Bflex2010

In bflex2010, there are two approach to calculate fatigue damage. The details of the processes are shown in the figure below, blue arrows refer to the method that calculate the fatigue damage directly from BFLEX2010POST with the command FAPLOT; the yellow arrows refer to the other method that calculate the fatigue damage using LIFETIME module. In this thesis, the first method is used. For more details about fatigue refer to BFLEX user manual.

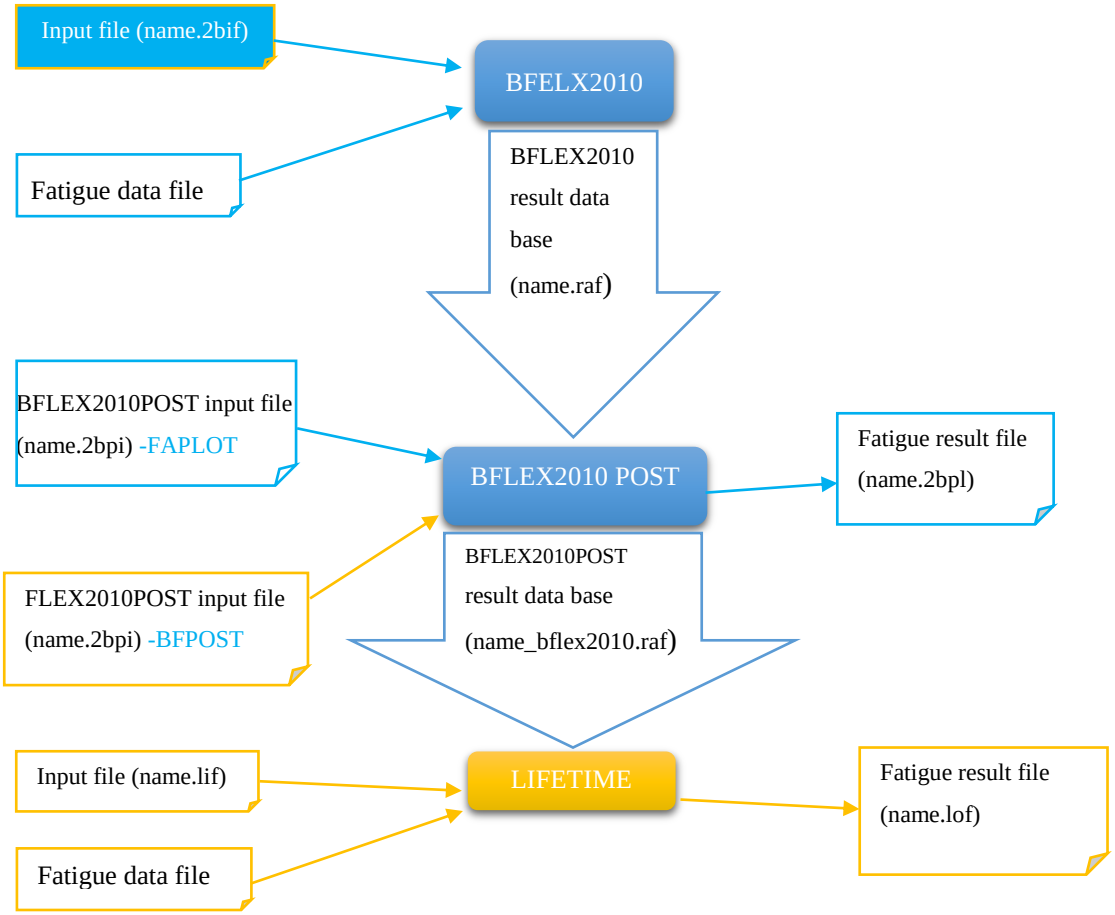

6.1.3 Fatigue data input

One specific fatigue data file is used in all the cases which means all the cases use the same SN curve. The applied fatigue data and the corresponding SN curve are shown below:

NFDPO1	R1	IGERB1	INTCO1	SCF1	SIGUTS	POINT	SRANGE	NCYFAL
2	0.1	0	1	1	1000	1	10	1e11
						2	1170	7e4

NFDPO1= 2 means two points in the fatigue S-N diagram.

R1=0.1 means $R = \frac{\sigma_{min}}{\sigma_{max}} = 0.1$ for the S-N diagram.

IGERB1 is used to define which method to use for taking the mean stress into account for longitudinal failure mode. Applied 0 means no mean stress is taken into account.

INTCO1=1 is to set both the stress and N in log scale for interpolation in S-N diagram

SCF1=1 means the stress concentration factor is s1.

SIGUTS=1000 means Ultimate stress is 1000MPa.

POINT is to define the number of the point. Here two points: point 1 and point 2 are defined.

SRANGE is used to define the stress range (in increasing order), starting with the minimum threshold value (unit: MPa).

NCYFAL is to define the corresponding number of cycles to failure.

For more details refer to [10].

6.2 Maximum fatigue damage results

In this part, fatigue analysis is performed in Bflex2010 based on the SN diagram approach.

In order to find out the effect to the maximum fatigue damage due to the different load conditions, two kinds of load conditions are analyzed, which are the low longitudinal force 0.1MN and the high longitudinal force 0.5MN. Moreover, to find out the effect of the gap length, different cases (0, 0.25, 0.5 and 0.75 pitch length) are analyzed under these two conditions. For the high load condition, two more cases (1.5 and 3 pitch length) are modeled and simulated to further analyze the maximum damage trend due to the gap length increasing.

6.2.1 Low longitudinal force - 0.1MN

The maximum fatigue damage and the corresponding damage locations from each case under 0.1 MN tension force are shown as below:

Table 6-1the maximum fatigue damage under longitudinal forces 0.1MN

Cross Section	**ITCODE 0**		**ITCODE 31**	
Gap (pitch length)	Damage location	Maximum damage	Damage location	Maximum damage
0	Left end	4.4588e-8	Right outside bending stiffener	3.8947e-8
0.25	Right outside bending stiffener	4.0845e-8	Right outside bending stiffener	3.8947e-8
0.5	Right outside bending stiffener	4.0869e-8	Right outside bending stiffener	3.8947e-8
0.75	Right outside bending stiffener	4.0678e-8	Right outside bending stiffener	3.8946e-8

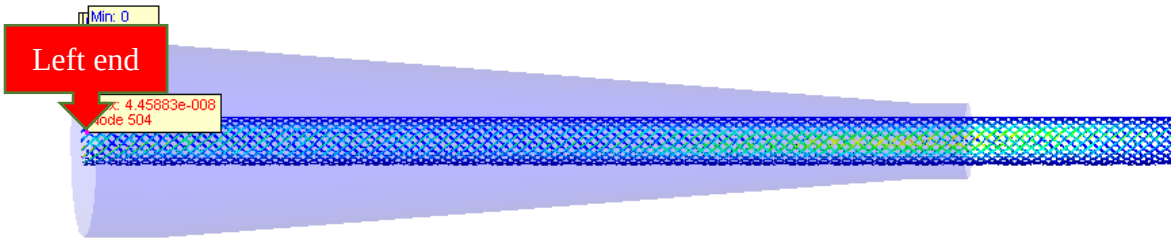

Figure 6-2 The position of maximum damage of case 0 (ITCODE 0)

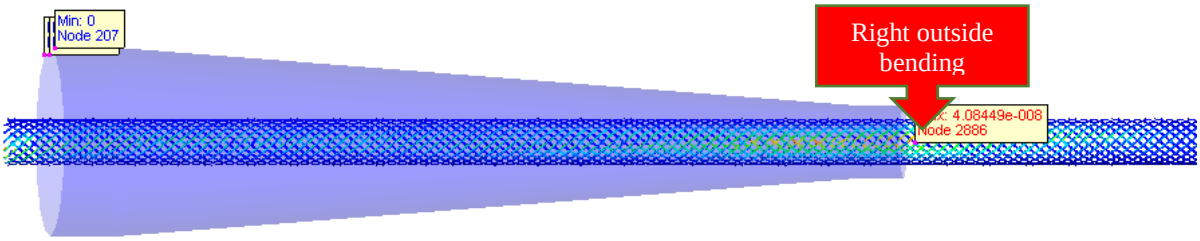

Figure 6-3 The position of maximum damage of case 0.25, 0.5, 0.75 (ITCODE 0)

Only the case of cross-section ITCODE0 without any gap (case 0) got the maximum damage at the left end of the pipe, details are shown in Figure 6-2. All the other cases got the maximum damage right outside the bending stiffener, the position is shown in Figure 6-3.

The maximum fatigue damage and corresponding gap length curves are shown below:

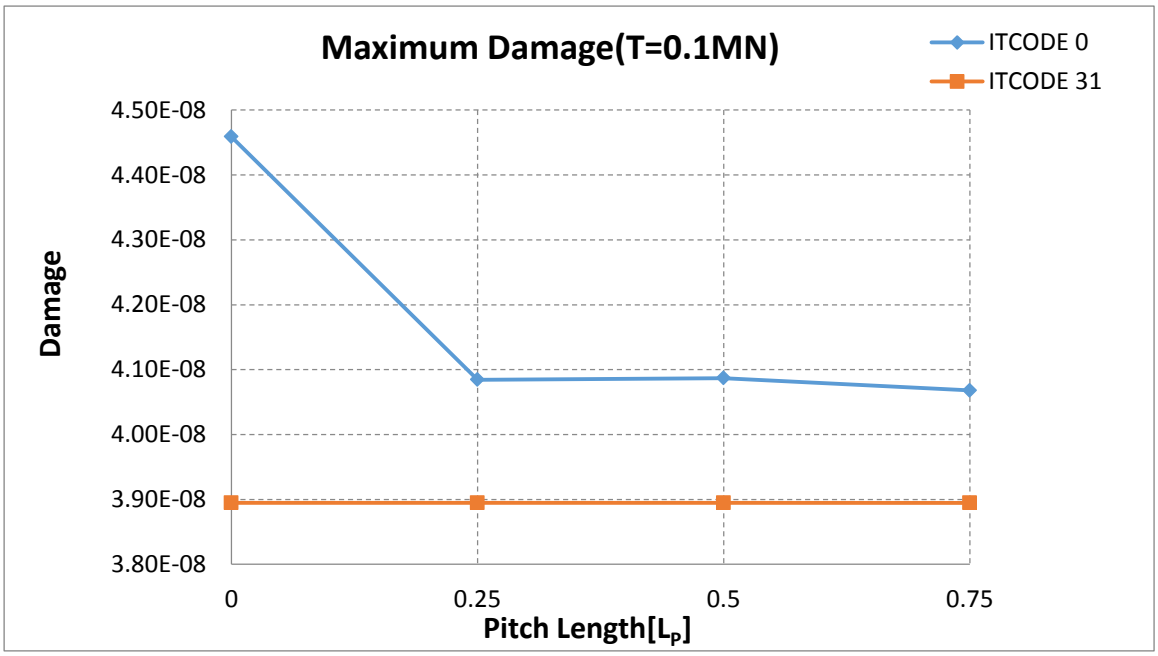

Figure 6-4 Maximum fatigue damages comparison under low tension force 0.1MN

For the models with cross section ITCODE 0, from Figure 6-4 we can see that the maximum damage values are very close with each other except the case with 0 gap. The 0 gap case has a much larger damage value than the other three cases.

For cross section ITCODE 31, all the maximum damage happened outside the right end of the bending stiffener. And the values have no significant difference. So we can conclude that the gap length has no significant effects for the maximum fatigue damage under this condition.

Compare ITCODE 0 and ITCODE 31, for the models with the same gap length, the case of ITCODE 0 always results a larger maximum damage.

6.2.2 High longitudinal force – 0.5MN

The maximum fatigue damage and the corresponding location from each case under 0.5 MN tension force are shown as Table 6-2:

Table 6-2 the maximum fatigue damage under longitudinal forces 0.5MN

Cross section	**ITCODE 0**		**ITCODE 31**	
Gap length (pitch)	Damage location	Maximum damage	Damage location	Maximum damage
0	Left end	$3.34433e^{-7}$	Left end	$10.1407e^{-8}$
0.25	Left end	$3.12211e^{-7}$	Left end	$9.12436e^{-8}$
0.5	Left end	$2.57995e^{-7}$	Left end	$7.98877e^{-8}$
0.75	Left end	$1.69072e^{-7}$	Left end	$7.1342e^{-8}$
1.5	Inside bending stiffener	$9.84287e^{-8}$	Inside bending stiffener	$7.05049e^{-8}$
3	Inside bending stiffener	$9.73958e^{-8}$	Inside bending stiffener	$6.99241e^{-8}$

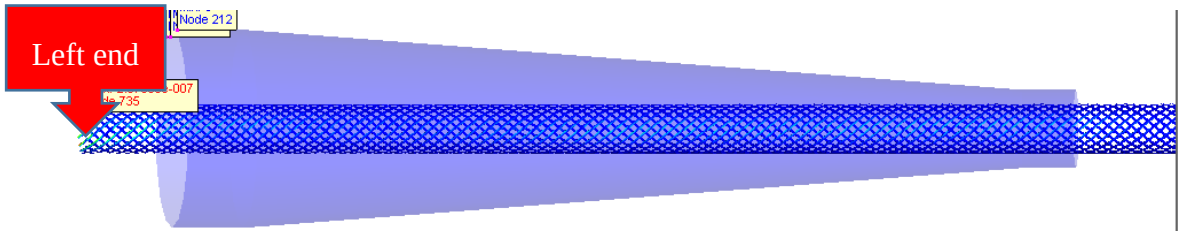

Figure 6-5 The position of maximum damage of case 0, 0.25, 0.5, 0.75 pitch gap

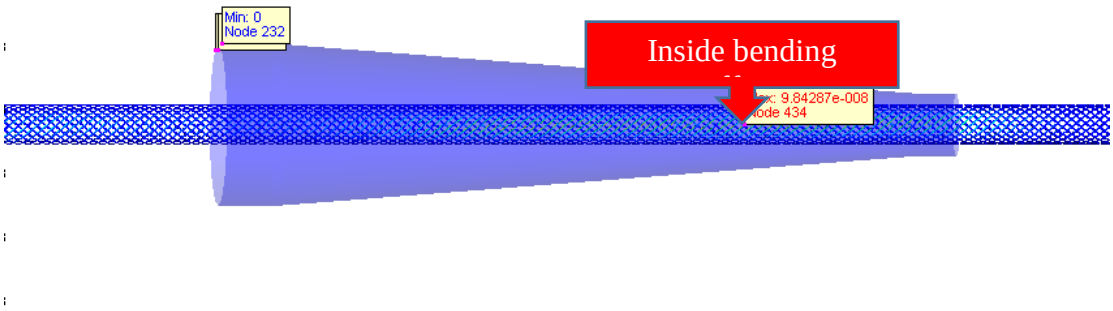

Figure 6-6 The position of maximum damage of case 1.5, 3.0 pitch gap

After increased the tension force to 0.5MN, the cases with 0, 0.25, 0.5 and 0.75 pitch gap length of both the two cross-sections got the maximum damage at the left end of the pipe, details are shown in Figure 6-5. However, the new cases with large gap length (1.5 and 3.0 pitch) got the maximum damage right inside the bending stiffener, see Figure 6-6.

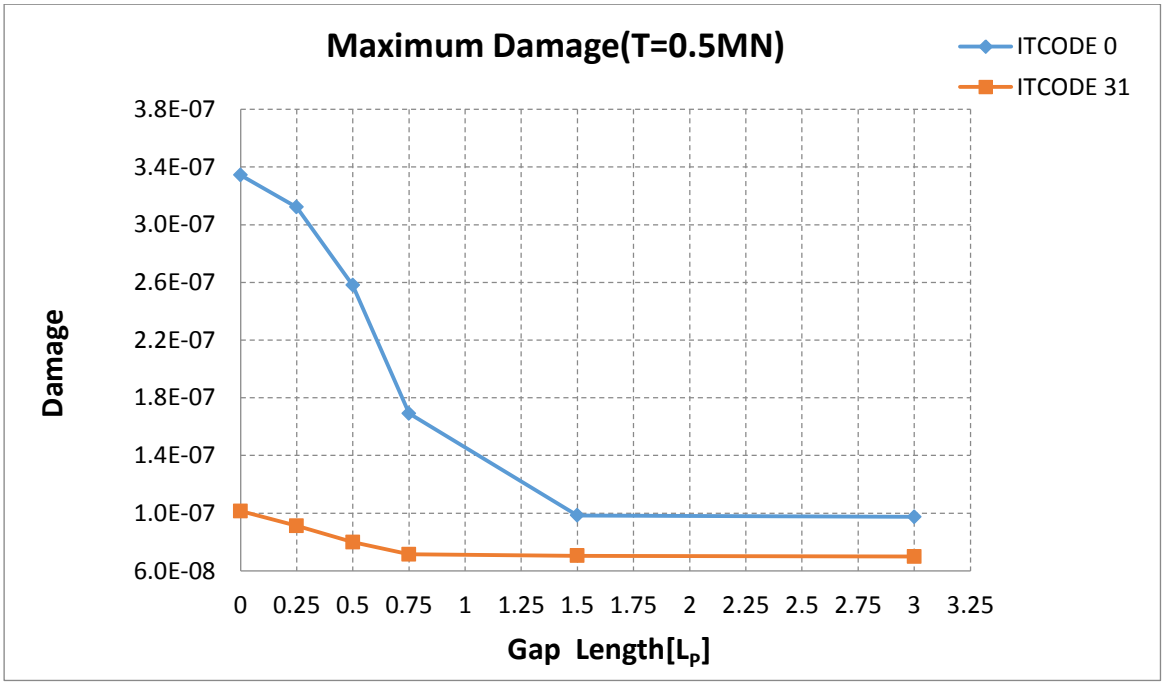

Figure 6-7 Maximum fatigue damage for all the cases under the tension force 0.5MN

For ITCODE 0, in Figure 6-7, we can see that the maximum damage for the cases from 0 pitch to 0.75 pitch have dramatically decreased (almost linear decrease) from $3.34433e^{-7}$ to $1.69072e^{-7}$, which decreased almost 50% of the original value. From case 0.75 pitch to 1.5 pitch, the damaged value decreased to $9.84287e^{-8}$ (42% of the value in 0.75 case), the line

connected these two points has a much smoother slope than previous lines. However, from case 1.5 pitch to 3.0 pitch, it shows a flat line which means that the damage value have no significant decline anymore.

Therefore, we can conclude that for a certain distance (1.5 pitch length in this case), increasing the gap length can contribute to decreasing the maximum fatigue damage for the pipe. However, after the gap reach a certain length, continue increasing the gap length cannot significantly decrease the maximum damage anymore.

For ITCODE 31, from case 0 to 0.75, only a small decrease of the maximum damage from $10.1407e^{-8}$ to $7.1342e^{-8}$, about 29.55% of the original value. Moreover, from case 0.75 to 3, the line in Figure 6-7 shows almost a straight flat line, which means that the damage value are almost the same in these cases.

Compare ITCODE 0 and ITCODE 31, for the models with the same gap length, the case of ITCODE 0, same as the low longitudinal force condition, always represents a larger maximum damage value. The difference of the damage values between these two cross-sections are extremely large when the gap lengths are short (0 to 0.75 pitch length). After the gap length increased to 1.5 pitch length, the maximum damage from the two cross-sections shows a slight and constant difference.

6.2.3 Discussion

Different load conditions cause different damage locations and damage values.

Under low longitudinal force, the gap length does not have significant effect on the maximum damage for both ITCODE31 and ITCODE0.

Under high longitudinal force, for ITCODE0, increase the gap length in a certain distance can decrease the fatigue damage dramatically. After that, fatigue damage cannot be significantly influenced anymore. Therefore, find the most efficient gap length will be very beneficial. For ITCODE 31, maximum damage slightly decrease as the gap length increased until a certain length, after that the damage do not change anymore. In short, ITCODE 31 cannot precisely represent the effect of changing the gap length.

6.3 Stress Analysis of the maximum fatigue damage

In this part, stress analysis is performed at the points where maximum fatigue occur, to figure out the reason of the maximum damage changing trend.

6.3.1 Local stress components description

Tensile layers are the core components for this thesis to discuss, and the local stress components of tensile layer tendon are shown in the figure below.

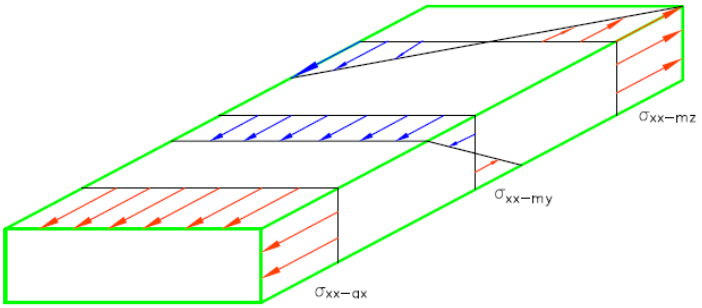

Figure 6-8 local stress components of tensile layer tendon [12]

σ_{xx-ax}: local axial stress of the tendon, which is mainly caused by longitudinal tension force and internal pressure.

σ_{xx-my}: local normal curvature stress of the tendon due to the bending about the weak axis.

σ_{xx-mz}: local transverse curvature stress of the tendon due to the bending about the strong axis.

$\Delta\sigma_{xx}$: local longitudinal stress of the tendon, which is the total stress along the tendon length direction. It can be calculated as below,

$$\Delta\sigma_{xx} = \sigma_{xx-ax} + \sigma_{xx-my} + \sigma_{xx-mz}$$

6.3.2 Description of the analysis location

In Bflex2010 software, each element is divided into three sections along the element length. The stress components and fatigue damages are integrated in each node of the 3 sections.

In cross-section ITCODE0, the tensile layers are modeled with rectangular cross section tendon. Each tendon element is composed by three sections with 4 nodes on each section.

In cross-section ITCODE31, the tensile layers are modeled with circular cross section element. Each element is composed by three sections with 16 nodes in sequence along each cross section. Details see from Figure 6-9.

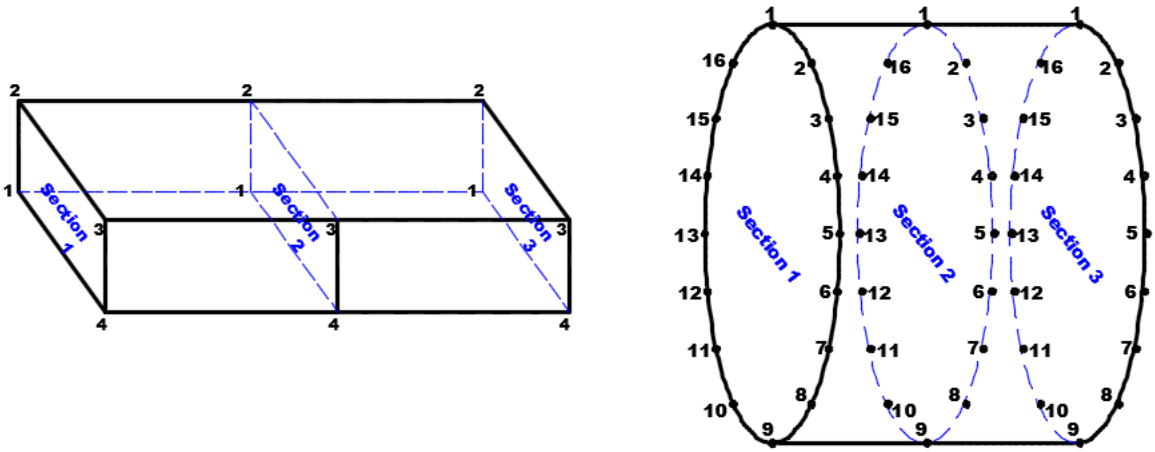

Figure 6-9 Rectangular (ITCODE0) and circular (ITCODE31) element section and point location.

6.3.3 Low longitudinal force - 0.1MN

For ITCODE 0, the stress range of the locations where got the maximum fatigue damage under 0.1MN tension force are shown in Table 6-3. The variation trend of the individual stress range and maximum damage with the increasing gap length are shown in Figure 6-10, the integrated relation of all the stress components and the maximum damage are shown in Figure 6-11.

Table 6-3 stress range of the point where got the maximum damage -ITCODE 0

Gap (pitch length)	Element number	Section	Point	$\Delta\sigma_{xx}$	$\Delta\sigma_{ax}$	$\Delta\sigma_{my}$	$\Delta\sigma_{mz}$	Maximum damage
0	1002	1	2	187.328	168.353	1.922659	17.05214	$4.45883e^{-8}$
0.25	2709	1	2	165.216	163.464	7.01827	1.841331	$4.08449e^{-8}$
0.5	2776	1	3	164.797	163.498	7.42554	5.72821	$4.08692e^{-8}$
0.75	2861	1	3	162.784	162.455	6.76143	1.771977	$4.06779e^{-8}$

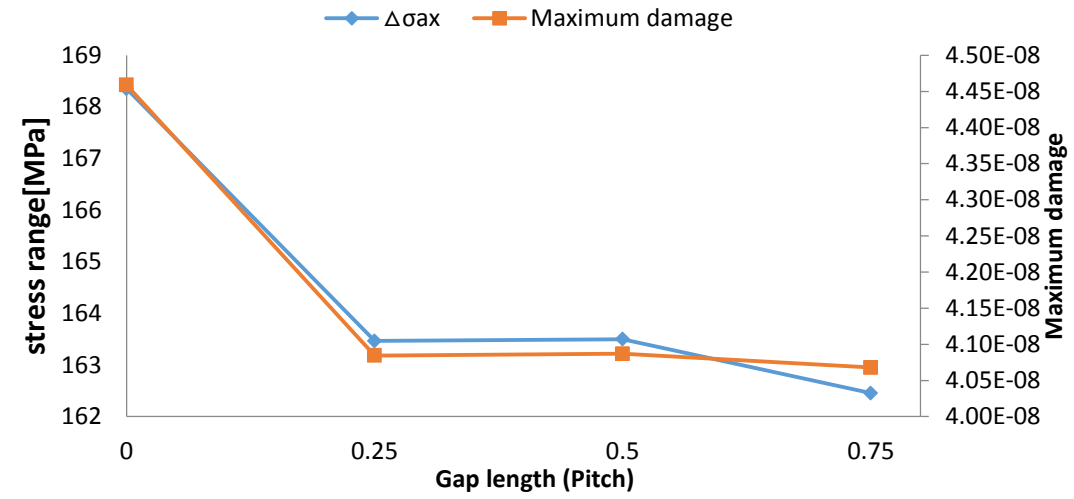
Δσax
Maximum damage
169
168
167
166
165
164
163
162
stress range[MPa]
4.50E-08
4.45E-08
4.40E-08
4.35E-08
4.30E-08
4.25E-08
4.20E-08
4.15E-08
4.10E-08
4.05E-08
4.00E-08
Maximum damage
0
0.25
0.5
0.75
Gap length (Pitch)

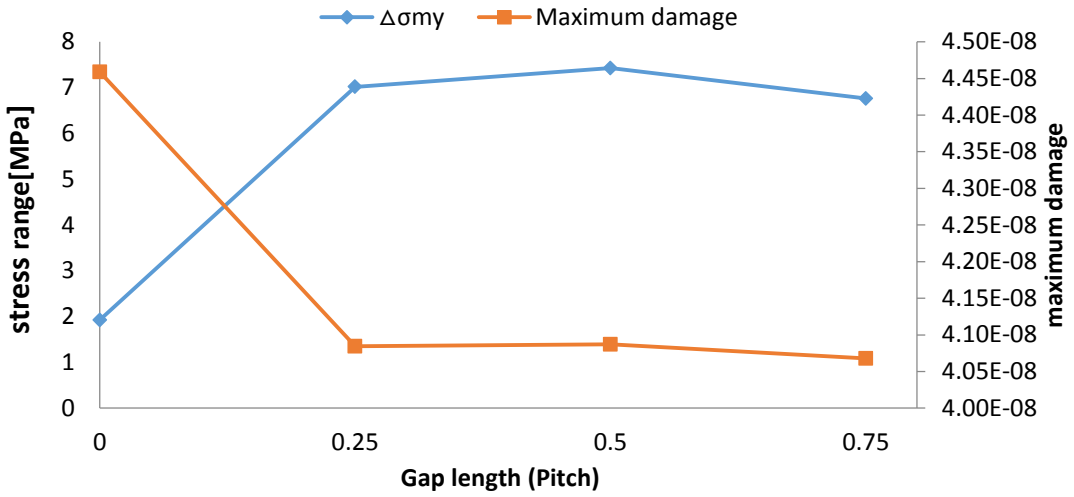
Δσmy
Maximum damage
8
7
6
5
4
3
2
1
0
stress range[MPa]
4.50E-08
4.45E-08
4.40E-08
4.35E-08
4.30E-08
4.25E-08
4.20E-08
4.15E-08
4.10E-08
4.05E-08
4.00E-08
maximum damage
0
0.25
0.5
0.75
Gap length (Pitch)

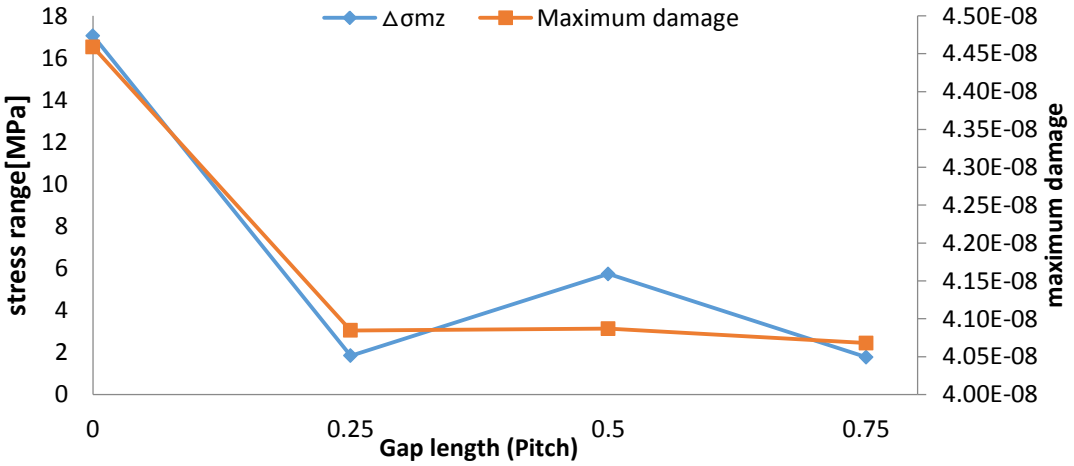
Δσmz
Maximum damage
18
16
14
12
10
8
6
4
2
0
stress range[MPa]
4.50E-08
4.45E-08
4.40E-08
4.35E-08
4.30E-08
4.25E-08
4.20E-08
4.15E-08
4.10E-08
4.05E-08
4.00E-08
maximum damage
0
0.25
0.5
0.75
Gap length (Pitch)

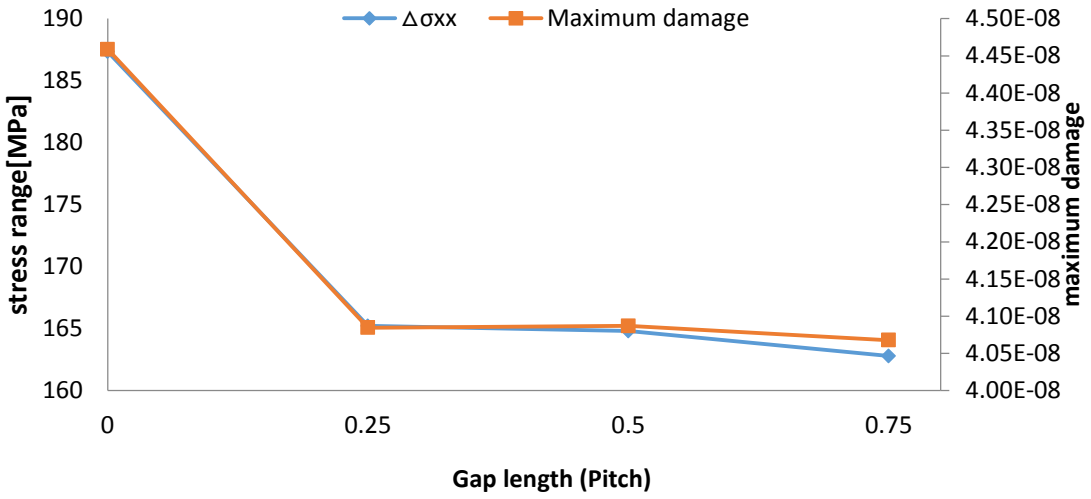

Figure 6-10 relation between the individual stress range and the maximum damage of ITCODE0

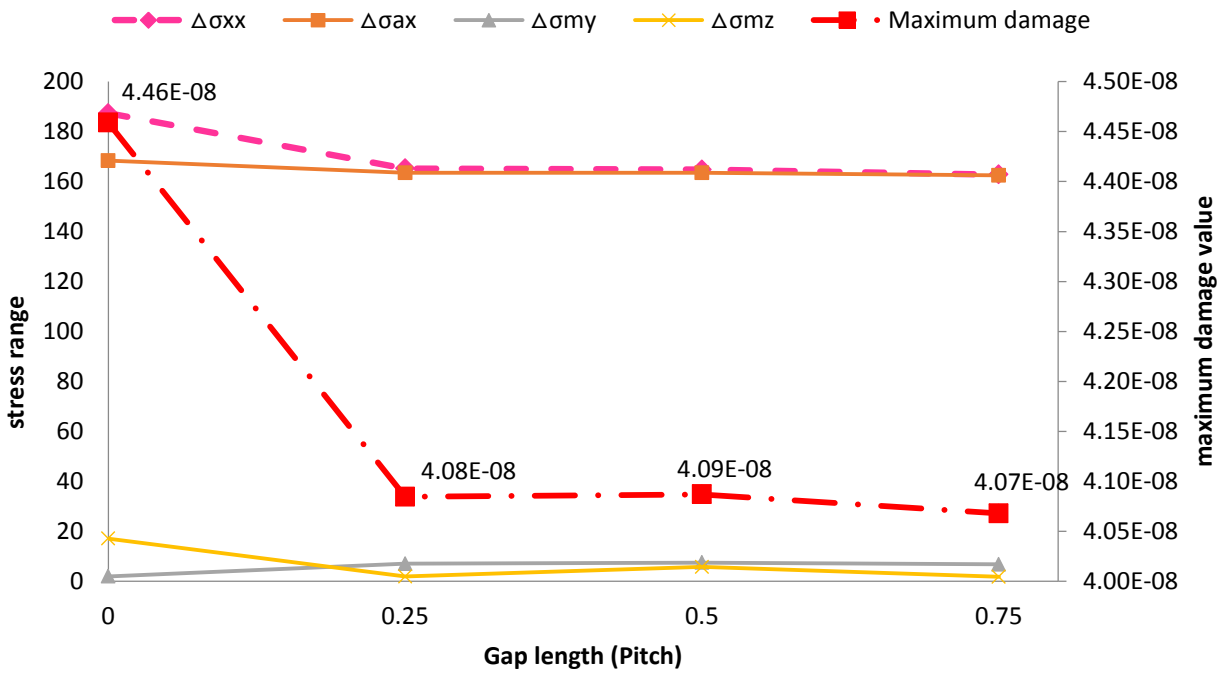

Figure 6-11 stress range of the point where got the maximum damage of ITCODE 0

From Figure 6-11, we can see a sudden drop in the maximum damage value from case 0 to 0.25, and all the stress components have a sudden drop too. This is mainly because the damage location of case 0 is far away from the other cases, details are shown in Figure 6-5. $\Delta\sigma_{xx}$ is mainly following the trend of $\Delta\sigma_{ax}$, which means σ_{ax} has a relatively large

amplitude and plays a controlling role among all the stress components. Compare case 0.25, 0.5 and 0.75, we cannot see any remarkable difference of the maximum damage.

For ITCODE31, the stress range of the location where got the maximum fatigue damage under 0.1MN tension force are shown as Table 6-4

Table 6-4 stress range of the point where got the maximum damage - ITCODE 31

Gap (pitch length)	Element number	Section	Point	$\Delta\sigma_{ax}$	$\Delta\sigma_{my}$	$\Delta\sigma_{mz}$	Maximum damage
0	1100	1	5	160.872	9.44839	0.370619	3.89466e-8
0.25	1105	1	5	160.872	9.29412	0.383044	3.89467e-8
0.5	1110	1	5	160.872	9.12623	0.394321	3.89466e-8
0.75	1115	1	5	160.871	8.94326	0.404249	3.89464e-8

From the element number, we can observe that all these damage happen at the same location along the pipe. Compare different gap length cases in Figure 6-12, the stress ranges and the maximum damage show no significant fluctuation. We can conclude that under this situation, the gap length has no significant effect for the stress range and fatigue damage for cross section ITCODE31.

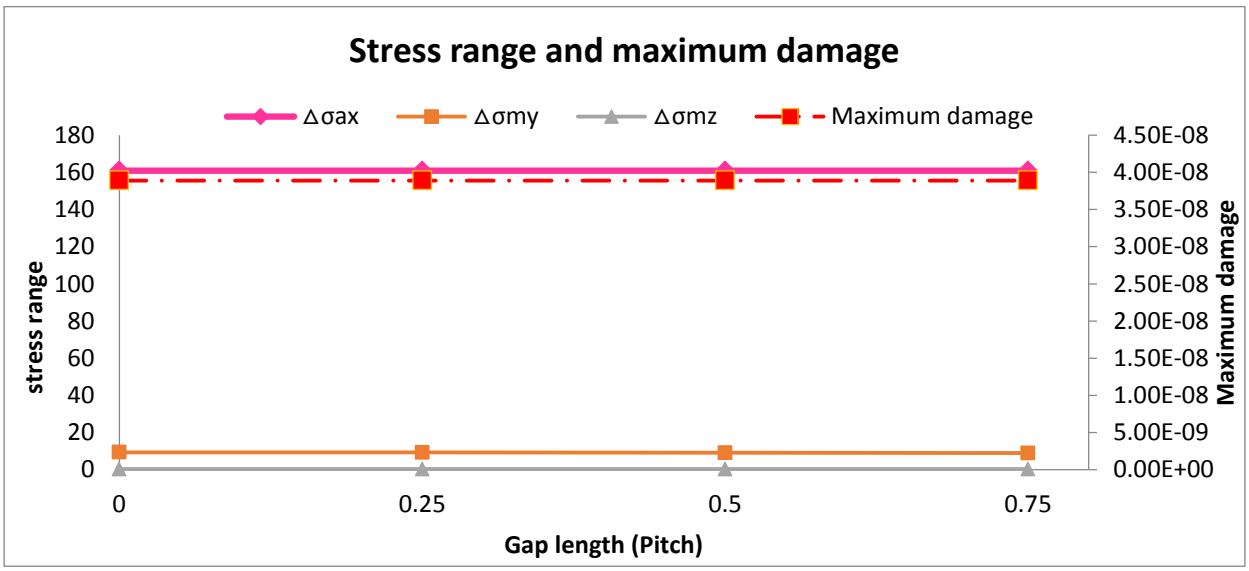

Figure 6-12 stress range of the point where got the maximum damage under 0.1MN tensile force-ITCODE 31

6.3.4 High longitudinal force - 0.5MN

For ITCODE 0, the stress range of the locations where got the maximum fatigue damage under 0.5MN tension force is shown in Table 6-5. And the variation trend of the stress range and maximum damage with the increasing gap length are shown in Figure 6-14.

Table 6-5 stress range of the point where got the maximum damage -ITCODE 0

Gap Length (pitch)	**Element number**	**Section**	**Point**	**Θ[°]**	**$\Delta\sigma_{ax}$ [MPa]**	**$\Delta\sigma_{my}$ [MPa]**	**$\Delta\sigma_{mz}$ [MPa]**	**$\Delta\sigma_{xx}$ [MPa]**	**Maximum damage**
0	1003	1	2	45	331.337	4.549	106.83	442.716	3.34433e-7
0.25	1003	1	2	45	324.375	3.571	82.902	341.468	3.12211e-7
0.5	1003	1	2	45	306.096	2.775	62.230	312.521	2.57995e-7
0.75	1002	1	2	22.5	263.468	3.289	30.613	265.702	1.69072e-7
1.5	2601	3	3	0	219.674	3.378	1.696	219.841	9.84287e-8
3	3089	3	3	0	218.897	3.113	1.858	218.979	9.73958e-8

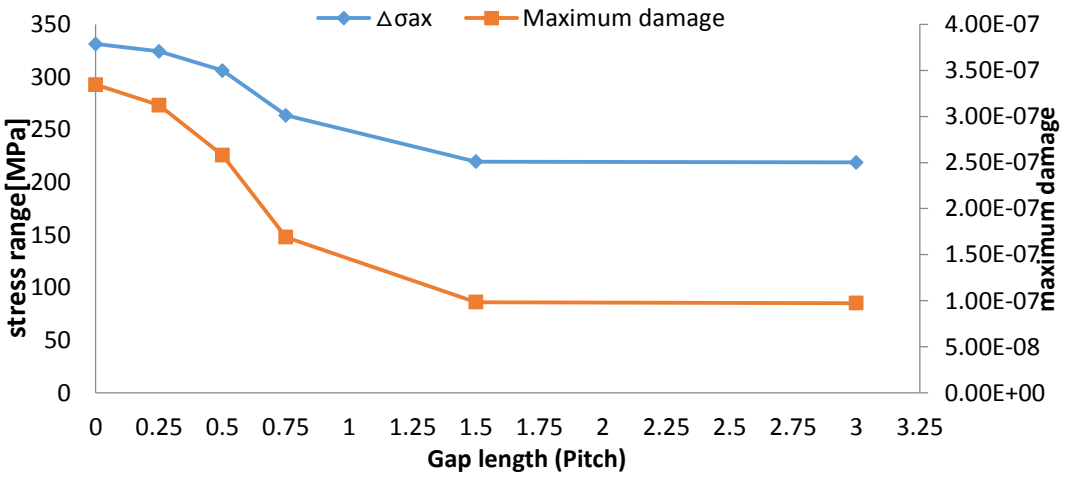

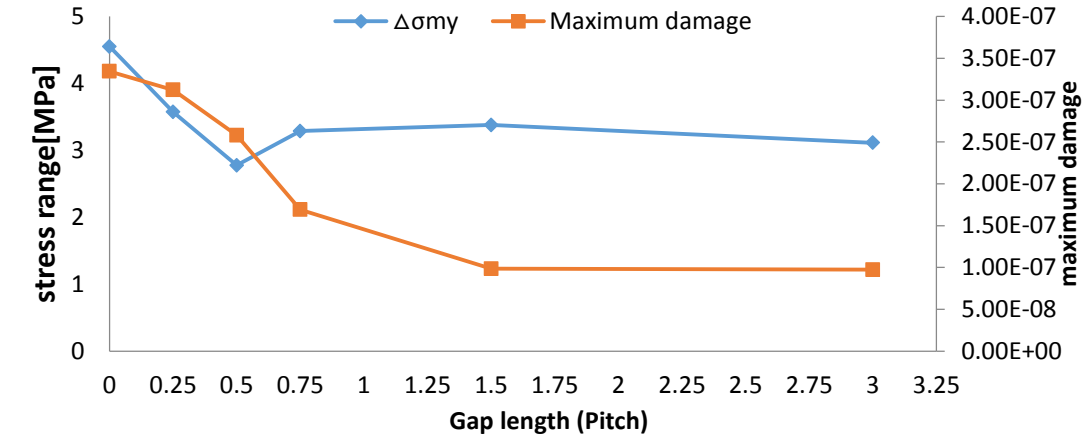

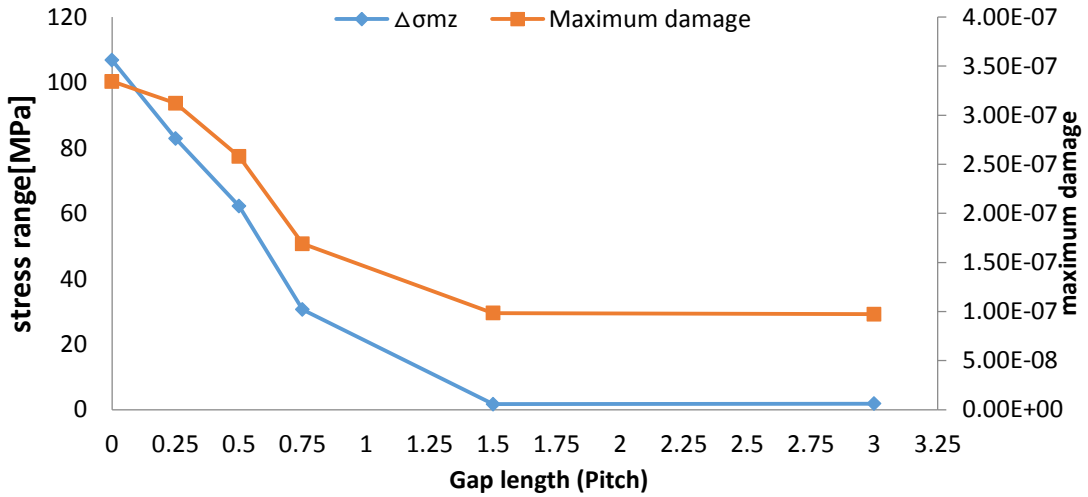

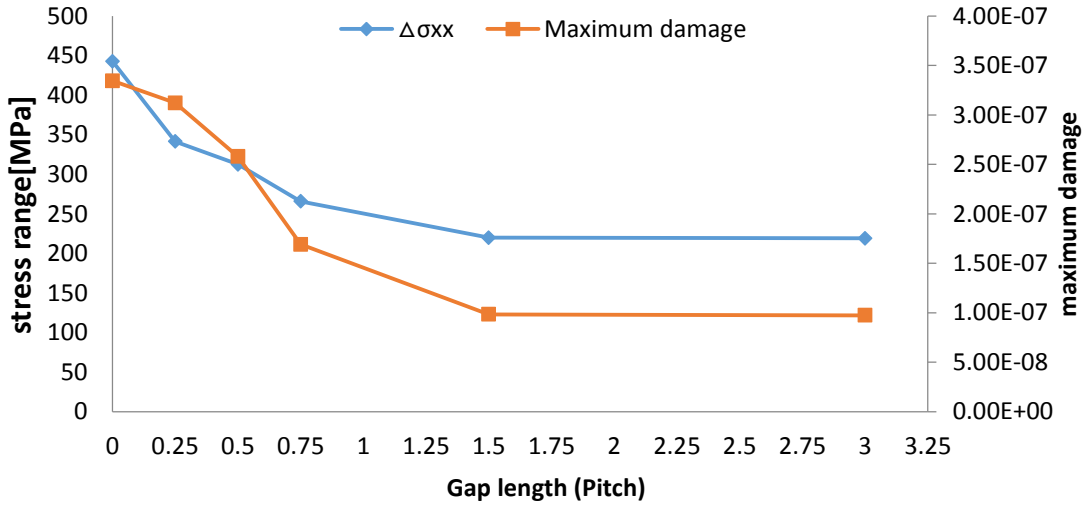

Figure 6-13 relation between the individual stress range and the maximum damage under0.5MN tensile force-ITCODE 0

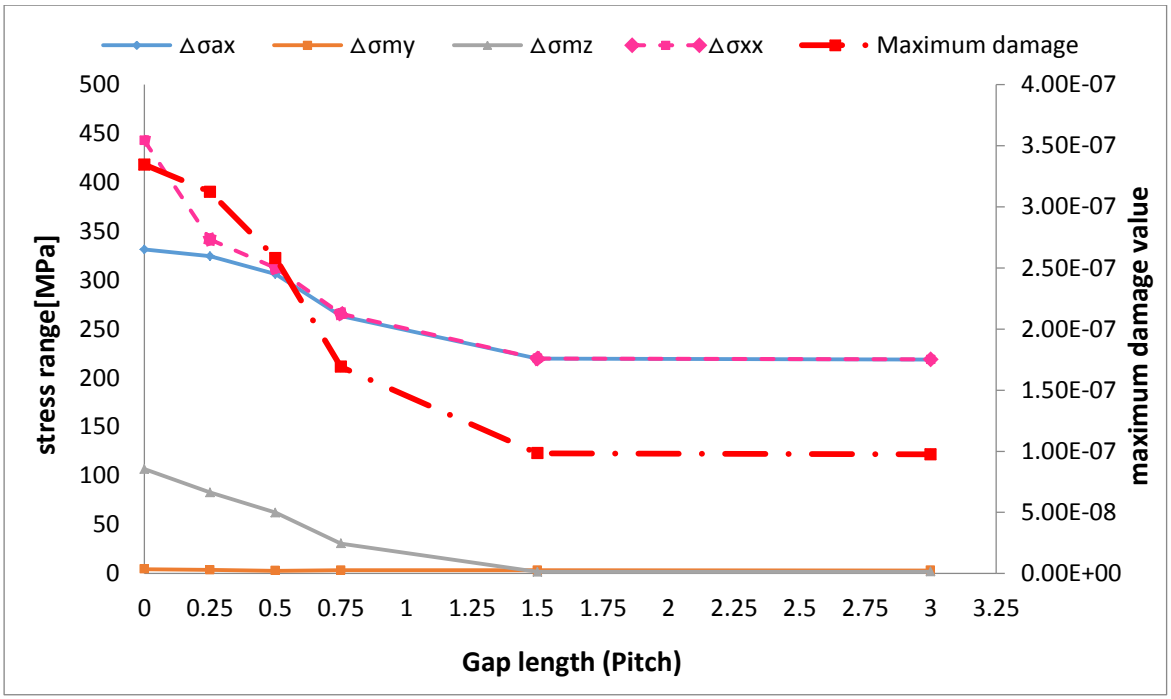

Figure 6-14 stress range of the point where got the maximum damage under0.5MN tensile force-ITCODE 0

From Table 6-5, we can see that case 0, 0.25 and 0.5 get the maximum damage at the same location with the same shift angle of 45 ˚. For case 0.75, the angle shift to 22.5 ˚, this is the reason why $\Delta\sigma_{my}$ has a sudden increase in Figure 6-13. As the gap length increases from 0 to 1.5, $\Delta\sigma_{ax}$ decreses about 100Mpa, after that $\Delta\sigma_{ax}$ keeps almost constant.

As we can see from Figure 6-14, as the gap length increases, $\Delta\sigma_{my}$ keeps a very small value (negligible) in all the cases, while $\Delta\sigma_{mz}$ decreases in a certain gap length (1.5 pitch in this case). From this phenomenon we can consider that, increasing the gap length has no significant effect on $\Delta\sigma_{my}$, moreover, $\Delta\sigma_{my}$ do not have any important effect on the fatigue damage under this condition. So the variation trend in the fatigue damage is mainly caused by the combination of $\Delta\sigma_{ax}$ and $\Delta\sigma_{mz}$.

ITCODE 31

Table 6-6 stress range of the point where got the maximum damage - ITCODE 31

Gap (pitch length)	Element number	Section	Point	Θ [˚]	$\Delta\sigma_{ax}$ [MPa]	$\Delta\sigma_{my}$ [MPa]	$\Delta\sigma_{mz}$ [MPa]	Maximum damage
0	1002	1	13	0	221.886	8.52769	0.006443	$1.0141e^{-7}$
0.25	1002	1	13	0	214.511	7.1075	0.005328	$9.1244e^{-8}$
0.5	1003	1	13	0	204.796	5.22967	0.006817	$7.9824e^{-8}$
0.75	1004	1	13	0	197.251	3.77358	0.006960	$7.1444e^{-8}$
1.5	1103	1	5	180	185.955	1.56726	0.001999	$7.0505e^{-8}$
3	1133	1	5	180	195.831	3.46739	0.261129	$6.9924e^{-8}$

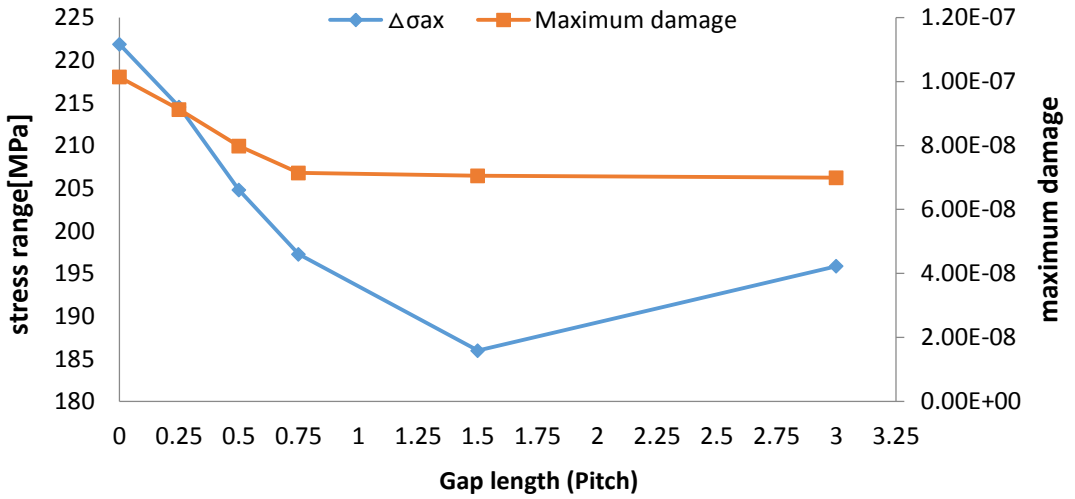

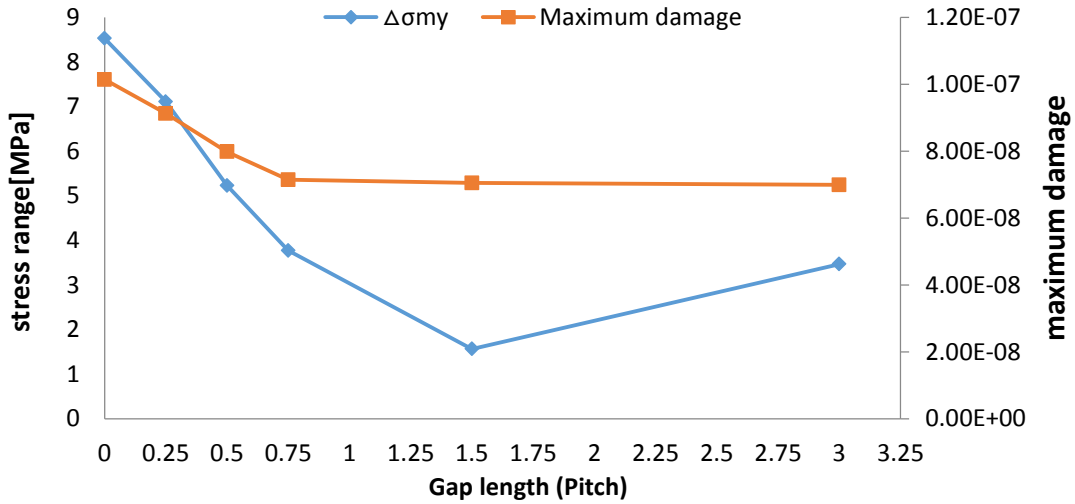

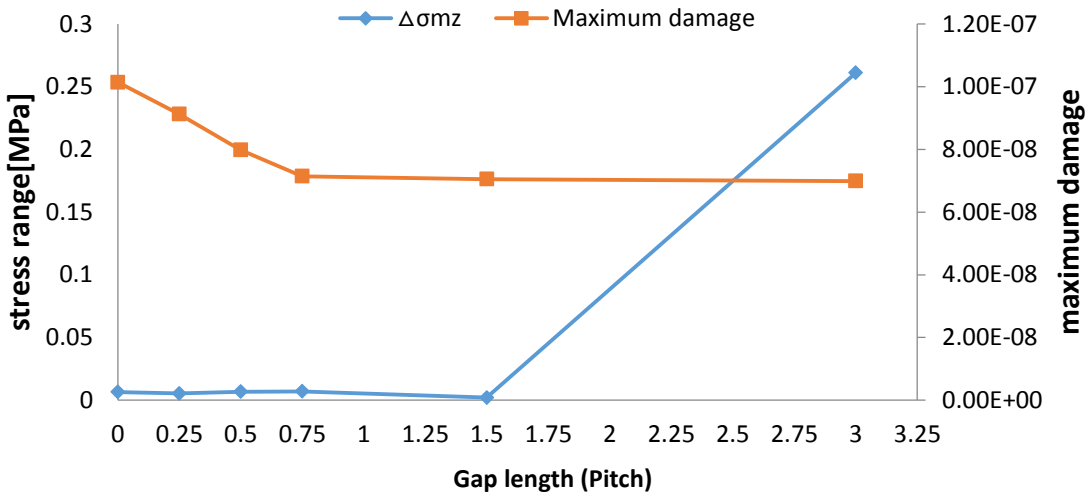

Figure 6-15 relation between the individual stress range and the maximum damage under0.5MN tensile force-ITCODE31

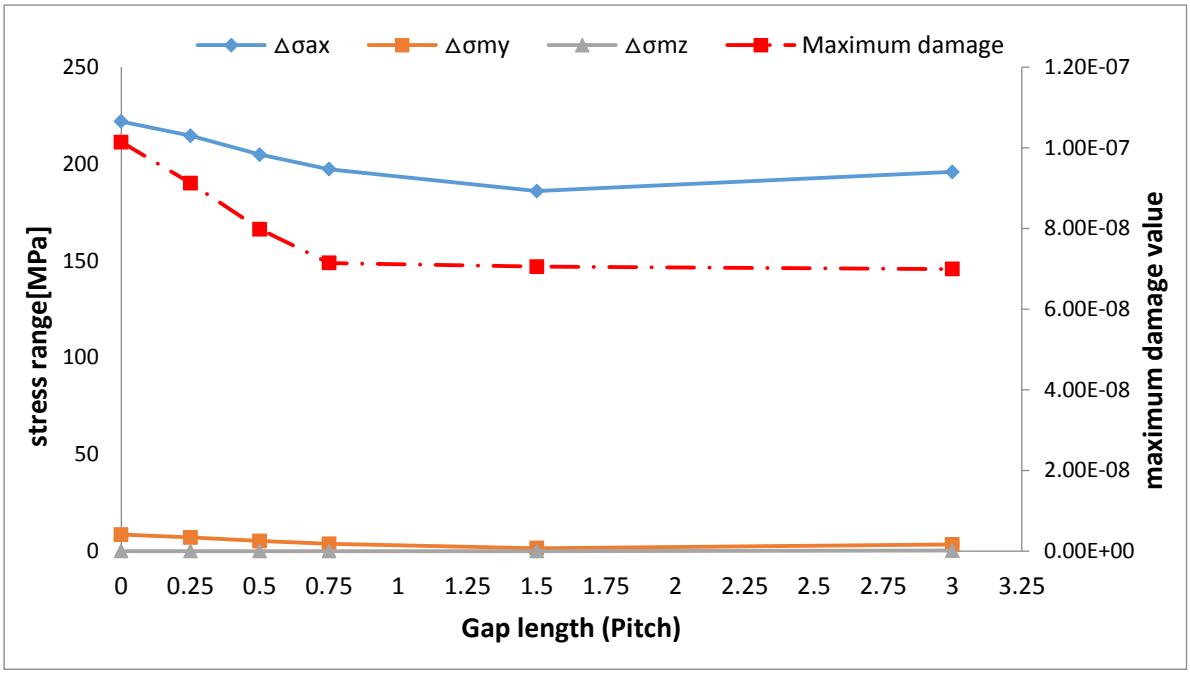

Figure 6-16 stress range of the point where got the maximum damage under 0.5MN tension force -ITCODE 31

From Table 6-6, we can see that case 0, 0.25, 0.5 and 0.75 get the maximum damage at the same location with no shift angle. The shift of element is mainly due to end effects. For case 1.5 and 3, the angle shift to 180 ˚. Though there is an increase of $\Delta\sigma_{mz}$ from case 1.5, the total increased value is very small and negligible. As the gap length increase from 0 to 1.5pitch, $\Delta\sigma_{ax}$ decreases about 40Mpa. This value is much smaller than ITCODE0.

As we can see from Figure 6-16, as the gap length increasing, $\Delta\sigma_{mz}$ keeps almost zero and $\Delta\sigma_{my}$ also represents the negligible value in all the cases. For $\Delta\sigma_{my}$, there is a decreasing from case 0 to 0.65 with a small margin about 2MPa. $\Delta\sigma_{ax}$ decreases with the same trend as ITCODE 0, while the decreased value is much smaller than the one in ITCODE0.

6.3.5 Discussion

Under low longitudinal force, the gap length does not have remarkable effect for the stress amplitude for both ITCODE31 and ITCODE0. While for ITCODE0, when the damage location is far away from the other cases, the stress amplitude will be quite different from others too.

Under high longitudinal force, the location of the maximum damage always changes not only in the longitudinal direction but also in the cross-sectional direction. Compare the two cross-sections, the cases of ITCODE0 always represent larger axial stress σ_{ax} and larger amplitude $\Delta\sigma_{ax}$ as the gap length increases. For the case0, 0.25, 0.5 and 0.75, which got the maximum damage at the left end of the pipe, one difference of the damage location is that ITCODE31 have no shift angle while ITCODE0 shift an angle of 45 ˚or 22.5 ˚. This is mainly because ITCODE0 take into account of the shear force caused by the plastic layers while ITCODE31 does not.

6.4 Stress history in three locations

The fatigue damage is mainly decided by the stress range, so in this part, to better understand the stress along the flexible pipe, stress history in three fixed locations are analyzed. The first point is on the left end of the pipe where always get the maximum fatigue damage. The second point is the start point of the bending stiffener with the same shift angle as location 1. The third point is the position where case 1.5 and case 3 pitch get the largest fatigue damage, 3500mm away from the left end of the bending stiffener. Details can be seen from figure below:

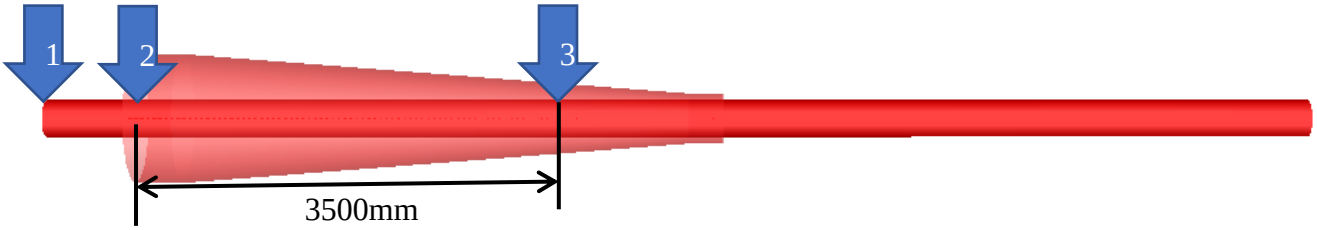

Figure 6-17 the three locations of the studied stress history

6.4.1 Left end of the pipe (Location 1)

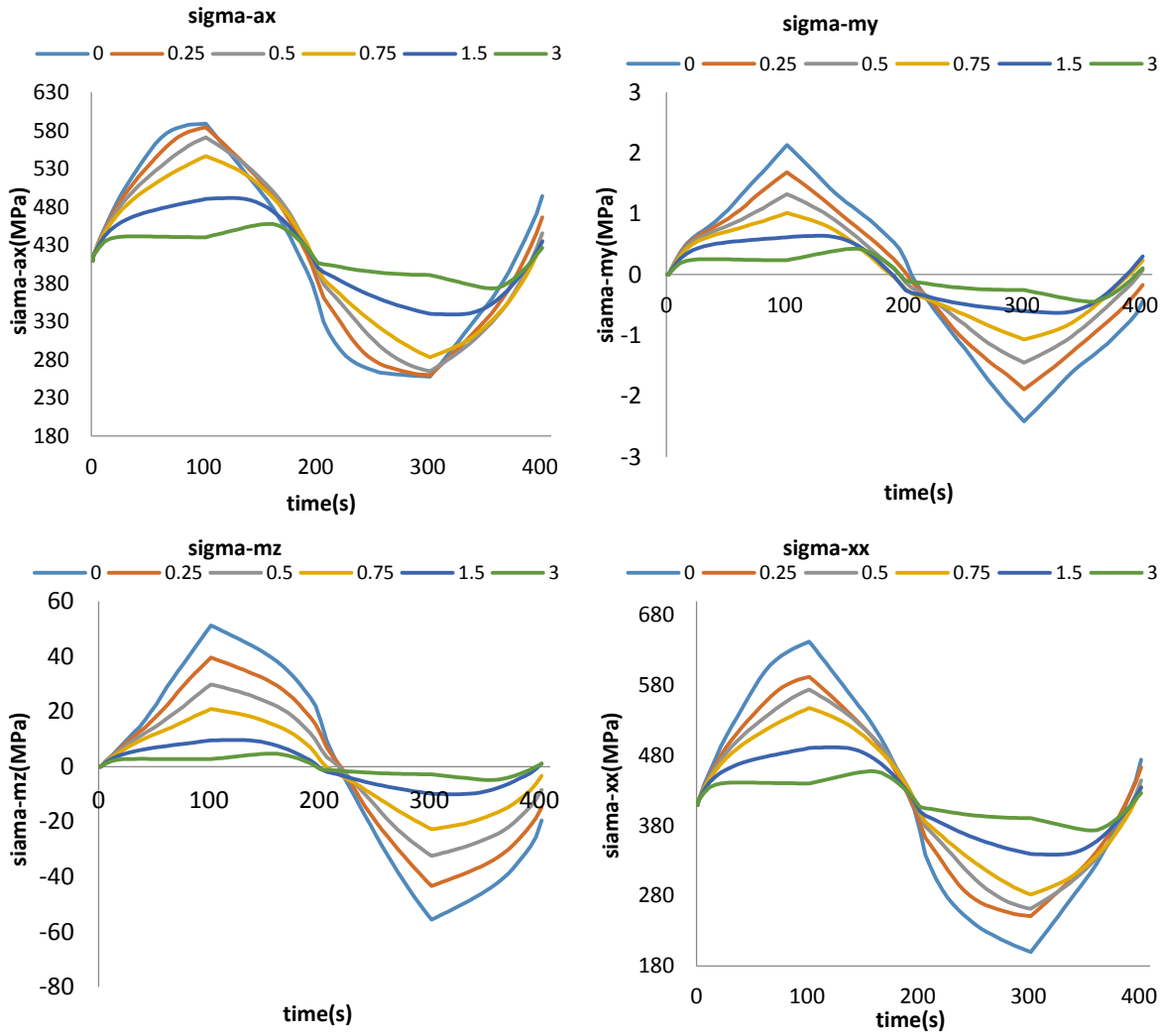

Figure 6-18 Location 1 stress history (element 1003, section 1, node 2) itcode0

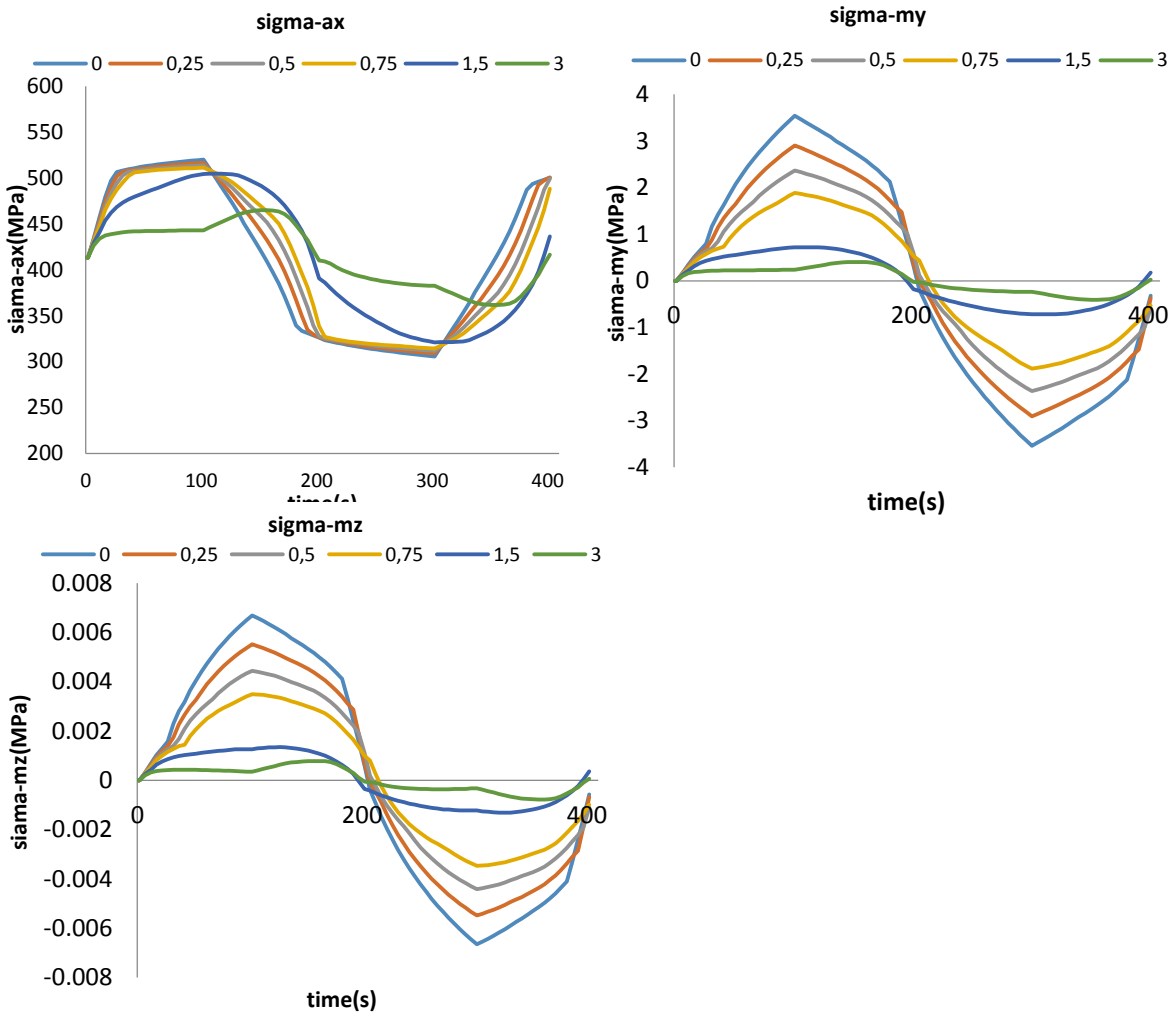

Figure 6-19 Location 1 stress history (element 1004, section 1, node 13) itcode31

For ITCODE0, from Figure 6-18, we can see that as the gap length increases, all the stress components decreases correspondingly. From gap 0 to gap 0.75, the decreasing amplitude is nearly constant. We can conclude that as the gap length increases, the stress on the left end will decreases accordingly. Therefore, when the gap length is big enough, the maximum damage will not occur at this location anymore.

For ITCODE31, to neglect the end effect, the fourth element along the longitudinal direction has been taken into consideration. The stress amplitude histories are very similar with ITCODE 0, the only difference from ITCODE0 is $\Delta\sigma_{mz}$ history. we can see that $\Delta\sigma_{mz}$ is almost zero for ITCODE31.

In short, at the end of the pipe, increasing the gap length will lead to the decreasing of the stress amplitude, and the increasing range is almost constant, no convergence will occur.

6.4.2 Left end of the bending stiffener (location 2)

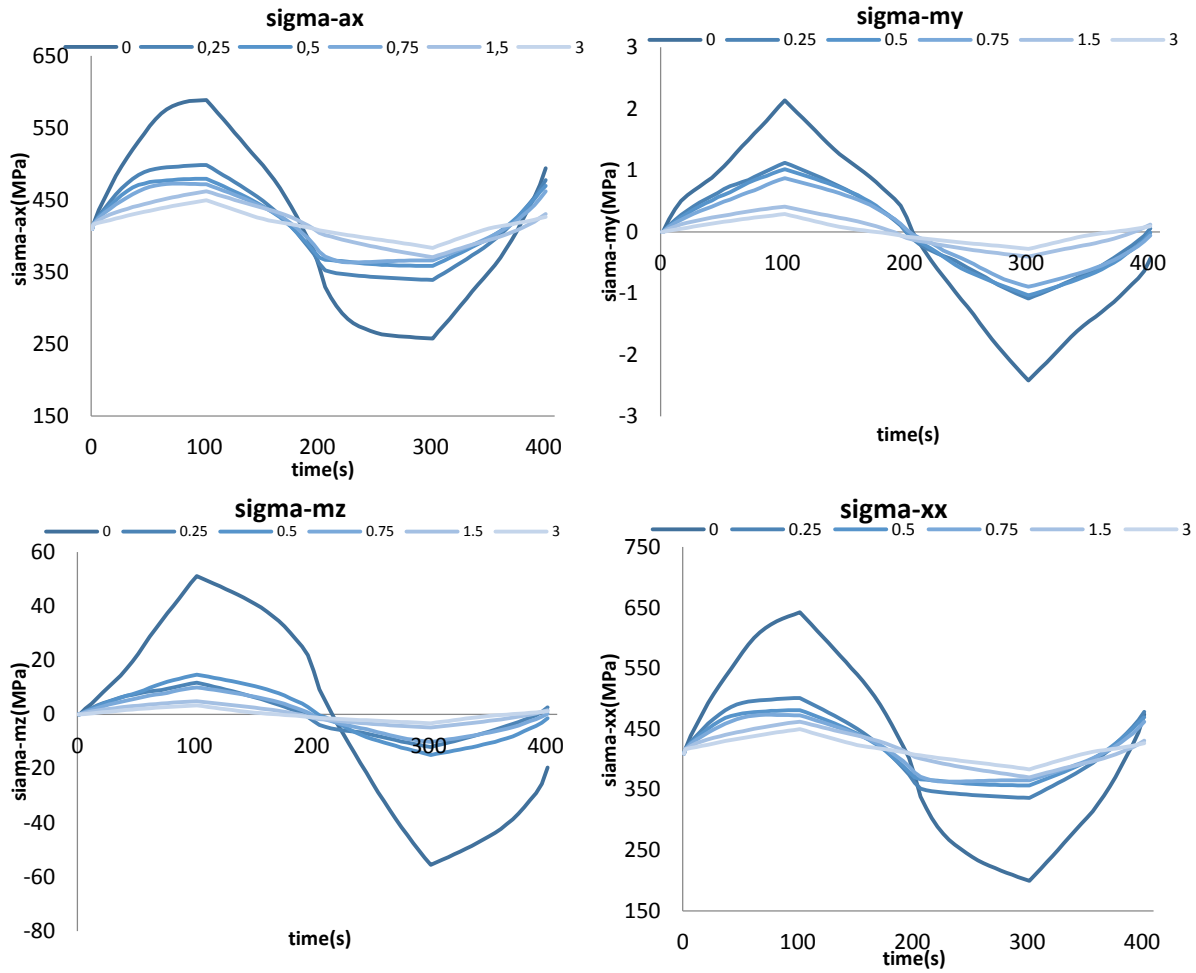

Figure 6-20 stress history of location 2(θ=45°) -ITCODE0

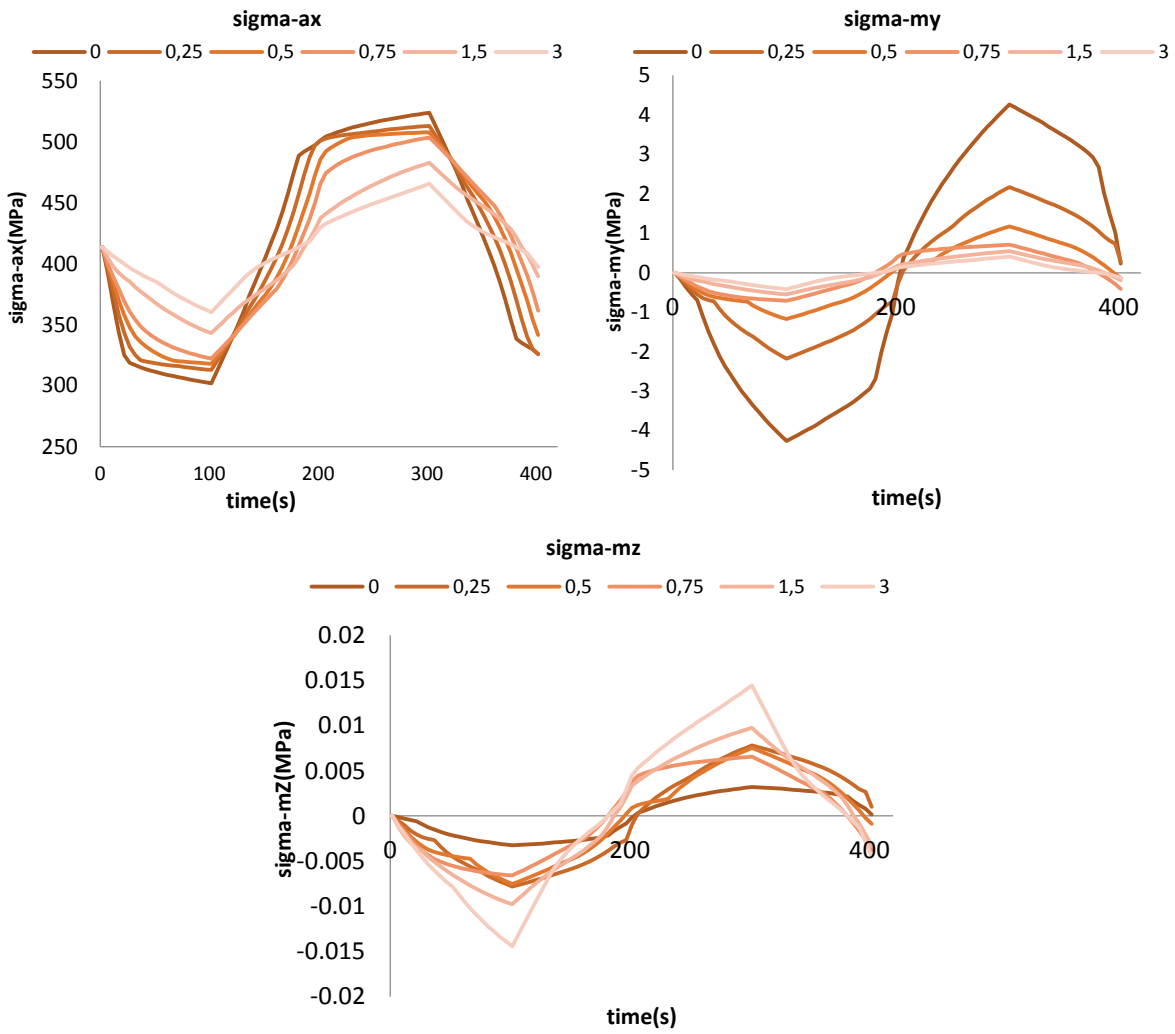

Figure 6-21 stress history of location 2 –ITCODE31

At this location, from

Figure 6-20, we can see that for ITCODE0 the amplitude of all these stress components decreases as the gap length increases. However, the decreasing range is gradually reducing. So when the gap length increases to a certain length, continue increasing gap length will have no significant effect on decreasing the stress components. Apparently, $\Delta\sigma_{ax}$ plays a controlling role among all the stress components. $\Delta\sigma_{mz}$ has some effect on the total stress $\Delta\sigma_{xx}$, while $\Delta\sigma_{my}$ is very small.

In Figure 6-21, similar stress history relations are shown. Different from ITCODE0, the stress amplitude value $\Delta\sigma_{mz}$ is almost zero. The decreasing value of $\Delta\sigma_{ax}$ seems constant, no convergence trend is shown.

We can conclude that as the gap length increases, the stress amplitude will decrease correspondingly. While the decreasing range will reducing gradually, and it will convergence when the gap length grows to a certain length.

6.4.3 3500mm from the left end of the bending stiffener(location 3)

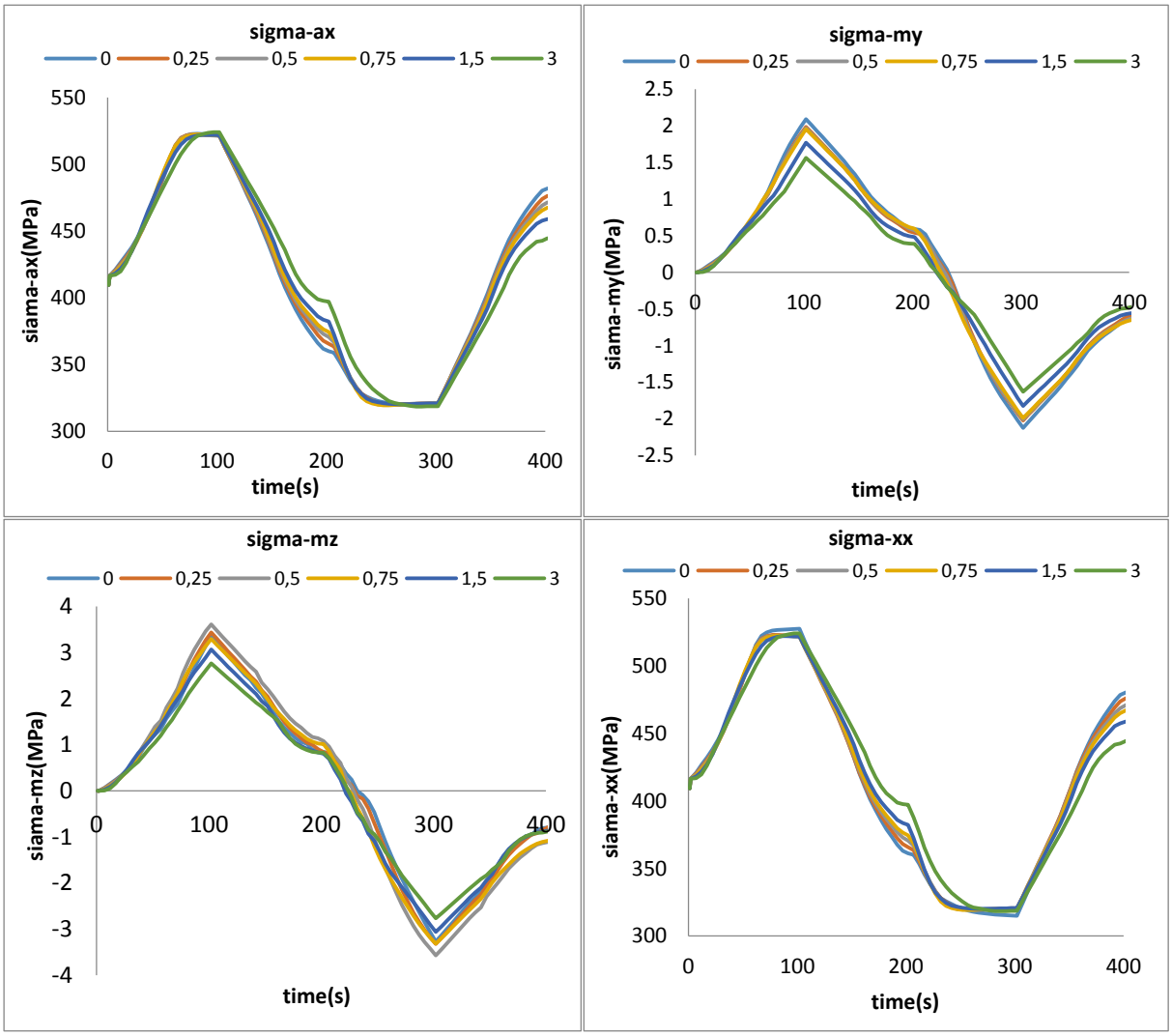

Figure 6-22 3500mm from the left end of the bending stiffener(θ=0°)-ITCODE0

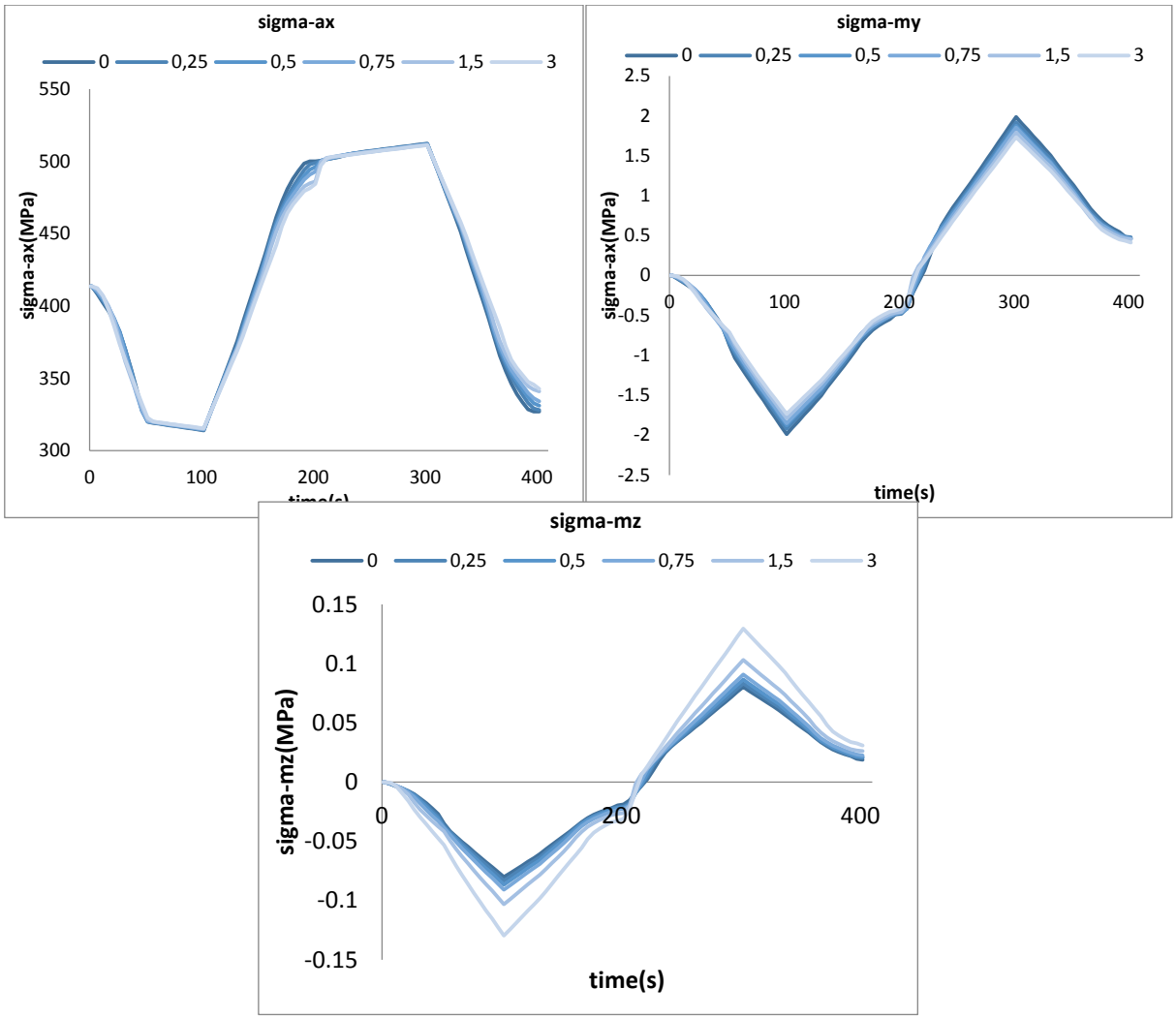

Figure 6-23 3500mm from the left end of the bending stiffener(θ=0°)-ITCODE31

From figure above, for both the two cross-sections, we can see that inside the bending stiffener the maximum and minimum value of σ_{ax} do not have any significant change with the gap length increasing, in other words, the amplitude keeps constant. While for σ_{my}, the amplitude decrease as the gap length increase, but the amplitude nearly the same when the gap is between 0.25pitch to 0.75pitch, which means the gap length don't have significant effect in this range. The only difference between these two cross-sections is the amplitude of σ_{mz}, in ITCODE0 the amplitude is about 4Mpa, while in ITCODE31 this value is about 0.2Mpa which is negligible.

We can conclude that the gap length has no remarkable influence for the stress amplitude inside the bending stiffener.

6.5 Global Curvature

In this part, the global curvatures from load step 102 (the step got the maximum bending moment) from each case are analyzed.

6.5.1 Low longitudinal force - 0.1MN

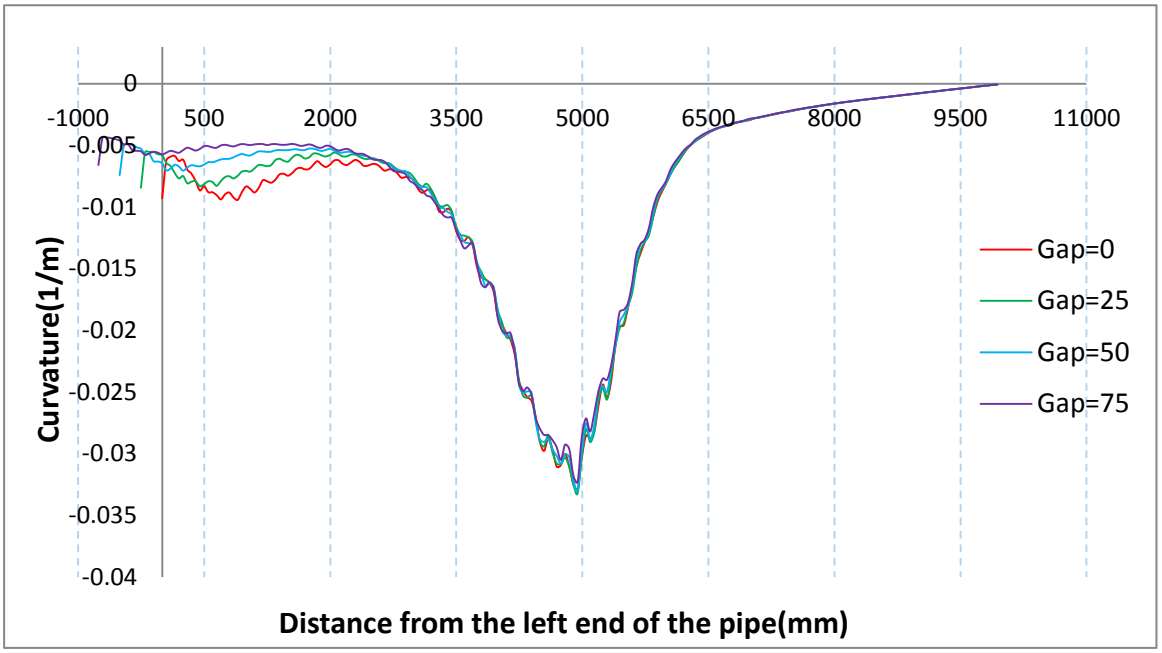

Figure 6-24 Global curvature of itcode 0 under T=0.1MN (load step102)

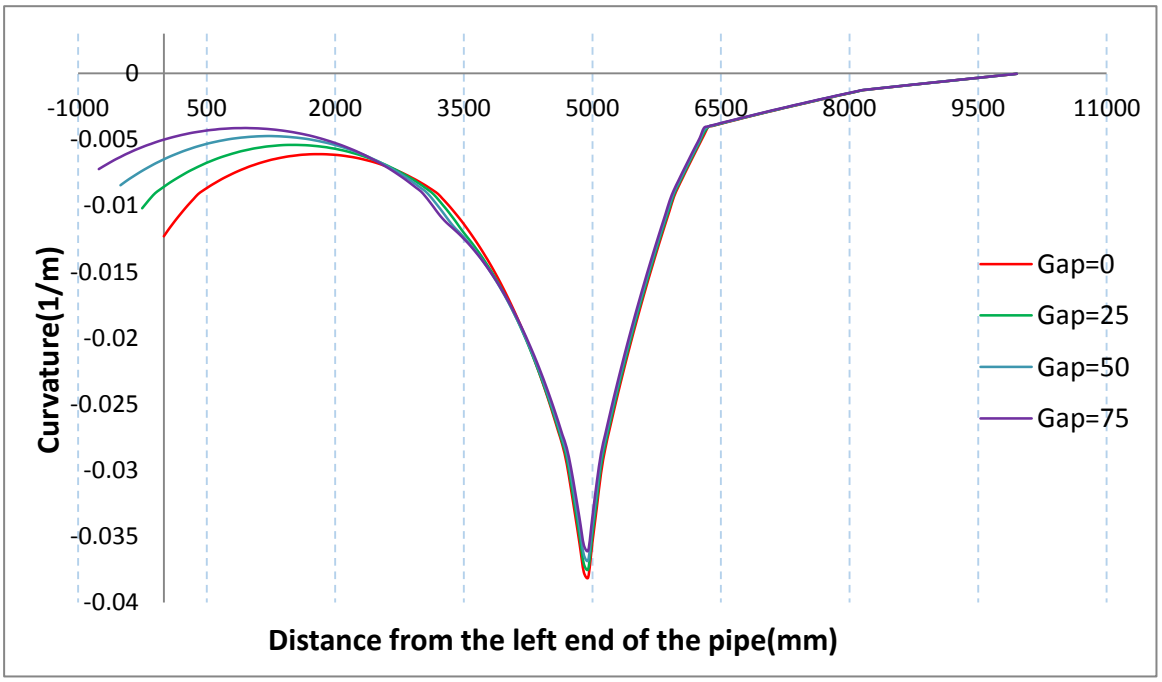

Figure 6-25 Global curvature of itcode 31 under T=0.1MN (load step102)

Compare Figure 6-24 and Figure 6-25, we can see that, in all these cases, the largest curvature happens close to the 5000mm where is the end of the bending stiffener. And the maximum curvature value is very large. This can be the direct reason why the maximum damage happened right outside the bending stiffener. The large curvature represents that the bending stiffener was not functional under this load conditions. Further optimization of the bending stiffener should be performed. Additionally, we can see that as the gap length increasing, the maximum curvature decreasing slightly.

6.5.2 High longitudinal force – 0.5MN

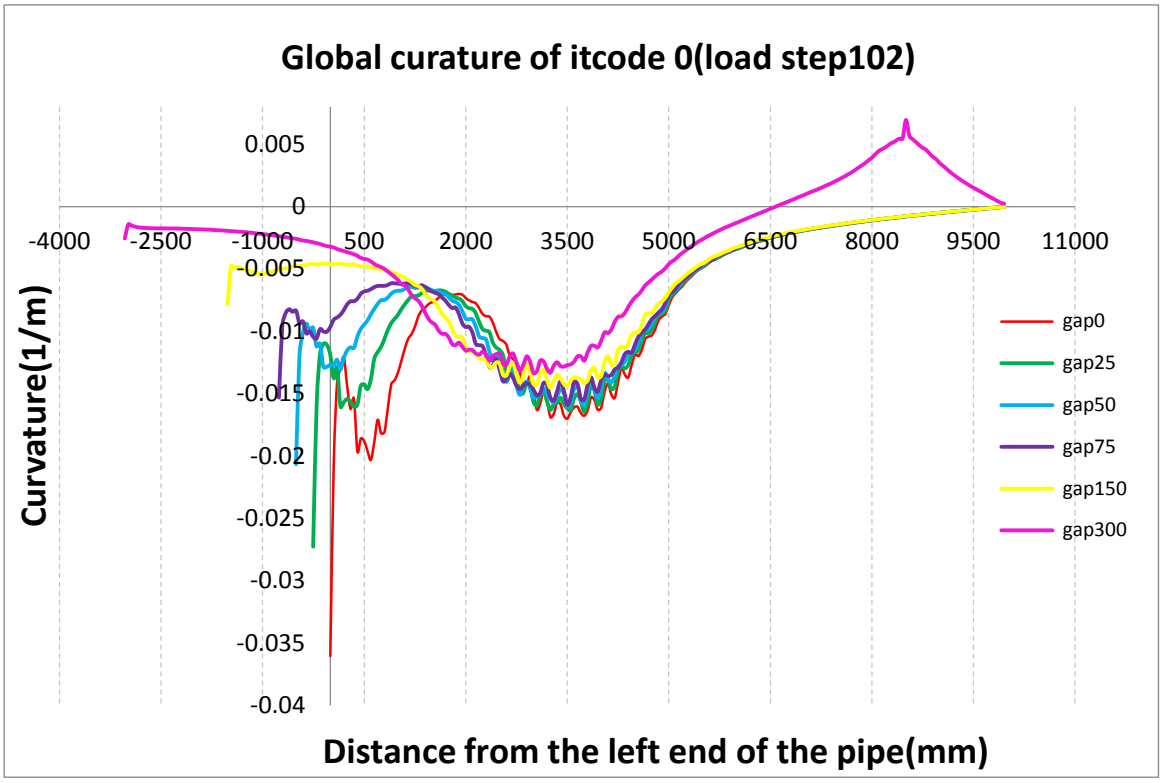

Figure 6-26 Global curature of itcode 0 under T=0.5MN (load step102)

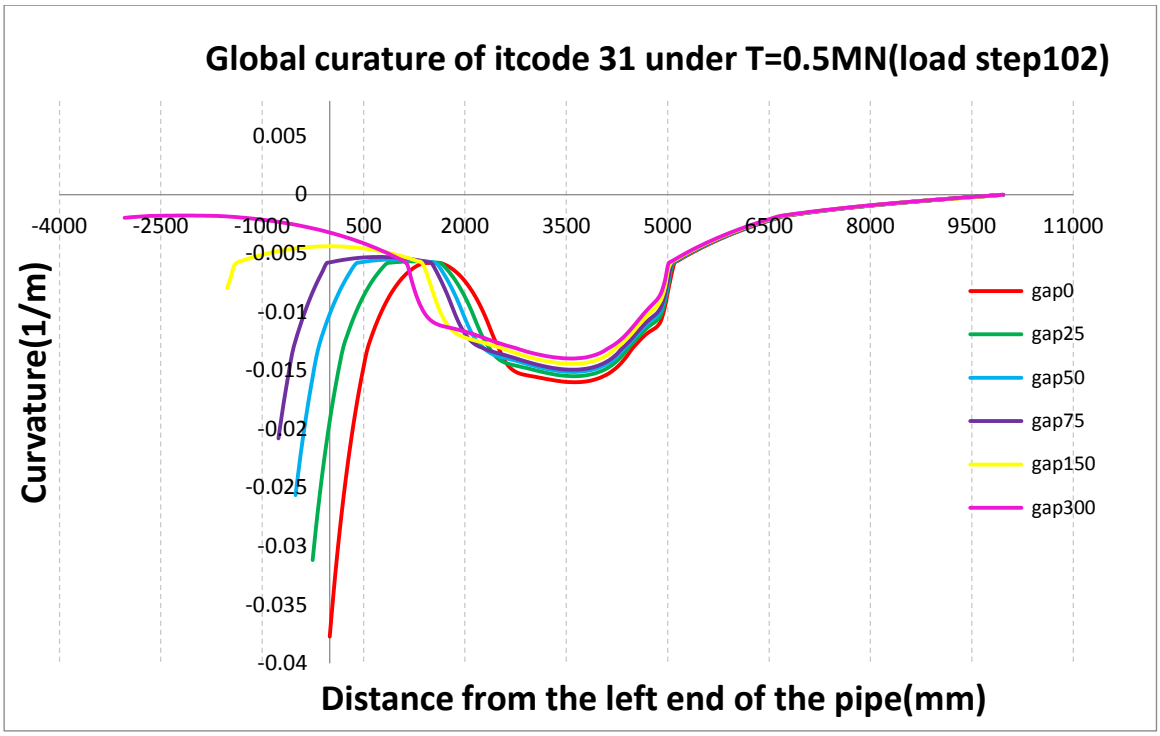

Figure 6-27 Global curature of itcode 0 under T=0.5MN (load step102)

As we can see from Figure 6-26 and Figure 6-27, for case 0, 0.25, 0.5 and 0.75, the largest curvatures no longer appear at 5000mm location, they move to the left end of the pipe instead. This can be the explaining of the maximum damage locations move to the left end. For both of the two new cases with large gap length, the curvature at the left end decreased dramatically, even smaller than the one appear inside the bending stiffener. This is the reason why the maximum fatigue damage appears inside the bending stiffener.

6.6 Friction Sensitivity Study

In this part, friction sensitive study is performed to analyze the effect of the friction factor. Normally, the friction factor of the flexible pipe is from 1.0 to 2.0. The previous models are modeled with factor 1.0, so in this part, two more friction factor values are analyzed, which are 1.5 and 2.0.

6.6.1 Friction study based on the maximum fatigue damage locations

The analysis results based on the maximum fatigue damage are shown as the following:

Table 6-7 maximum damage, stress under 0.5MN tension force, friction factor is 0.15

Gap length	**Position**	$\Delta\sigma_{xx}$	$\Delta\sigma_{ax}$	$\Delta\sigma_{my}$	$\Delta\sigma_{mz}$	**Maximum damage**
0	left	534.021	445.765	3.8413	84.4147	8.09E-07
0.25	left	400.003	390.709	4.62213	42.3958	5.46E-07
0.5	left	341.171	337.85	3.5544	30.037	3.54E-07
0.75	middle	310.379	310.101	3.50445	0.80444	2.75E-07
1.5	middle	299.809	299.705	3.14773	0.1361241	2.48E-07
3	middle	288.726	288.661	2.85492	1.094017	2.22E-07

Table 6-8 maximum damage, stress under 0.5MN tension force, friction factor is 0.2

Gap length	**Position**	$\Delta\sigma_{xx}$	$\Delta\sigma_{ax}$	$\Delta\sigma_{my}$	$\Delta\sigma_{mz}$	**Maximum damage**
0	left	540.205	488.816	5.23532	46.1527	1.06E-06
0.25	left	412.072	404.461	4.25687	34.2447	6.05E-07
0.5	middle	347.006	346.671	3.24859	0.344877	3.83E-07
0.75	middle	335.954	335.694	3.10856	0.846444	3.48E-07
1.5	middle	315.618	315.464	2.87084	1.787043	2.89E-07
3	middle	293.002	292.935	2.68291	1.365382	2.32E-07

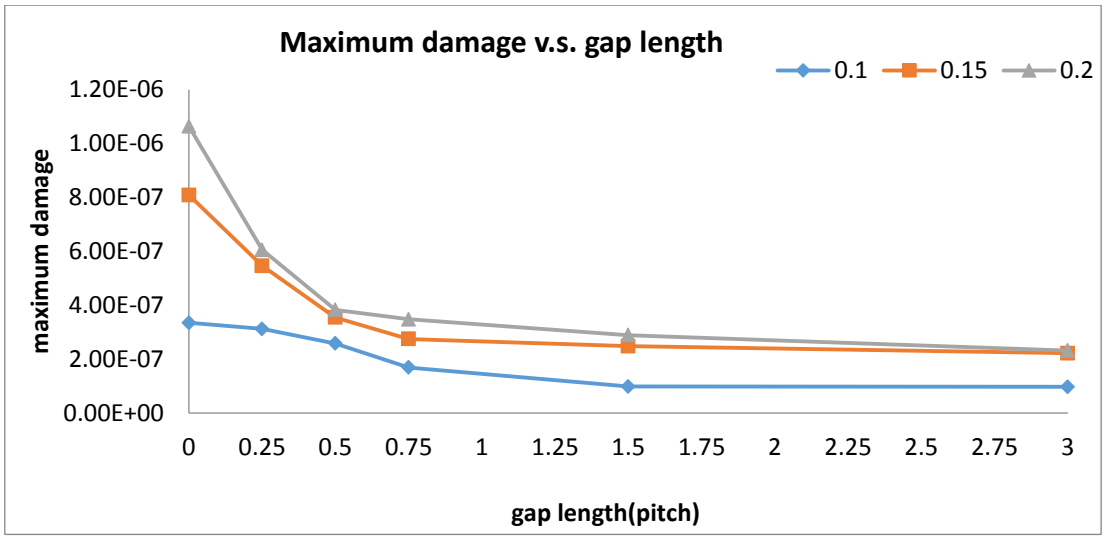

Figure 6-28 maximum damage for different gap lengths under 0.5MN tension force

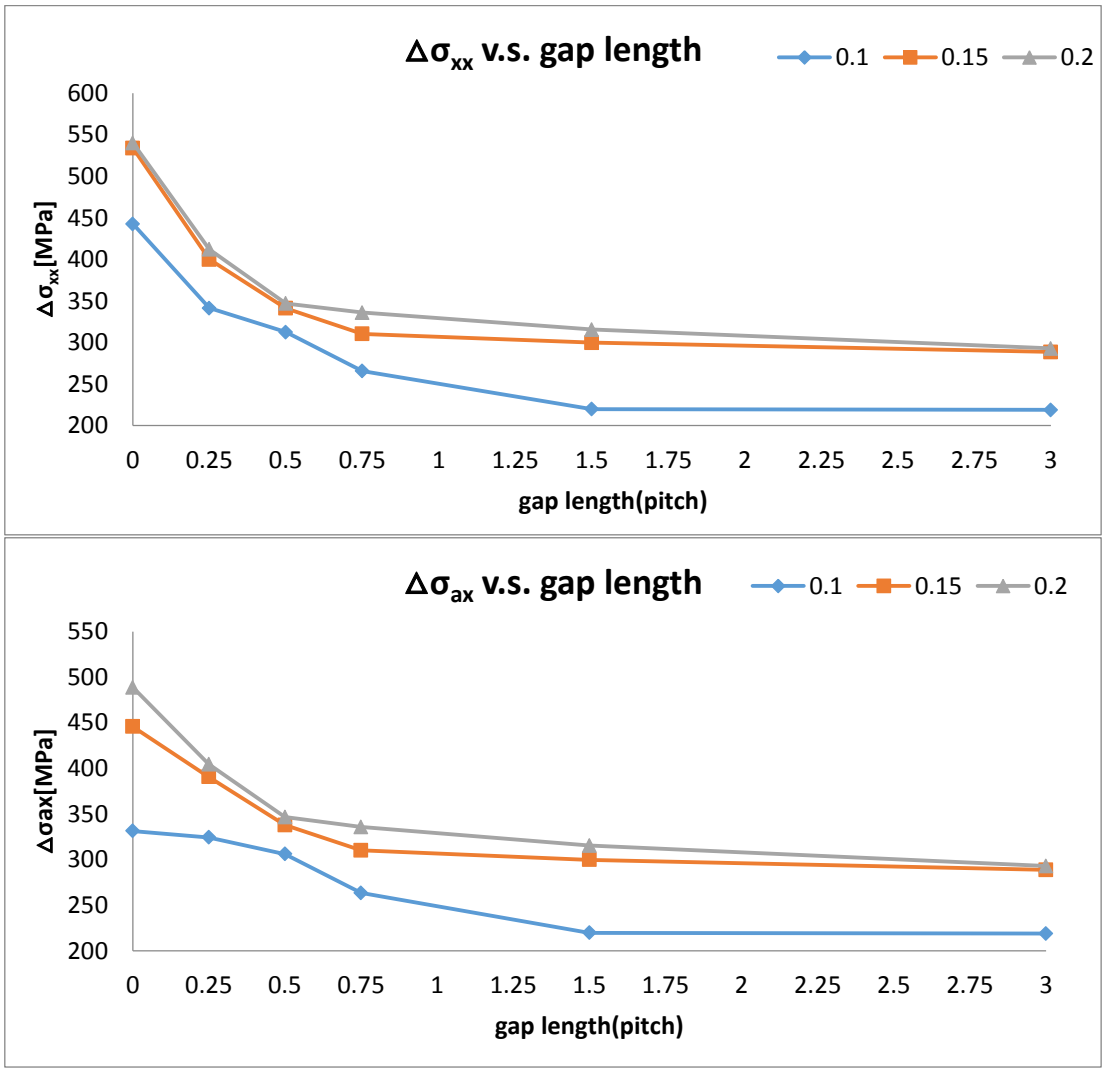

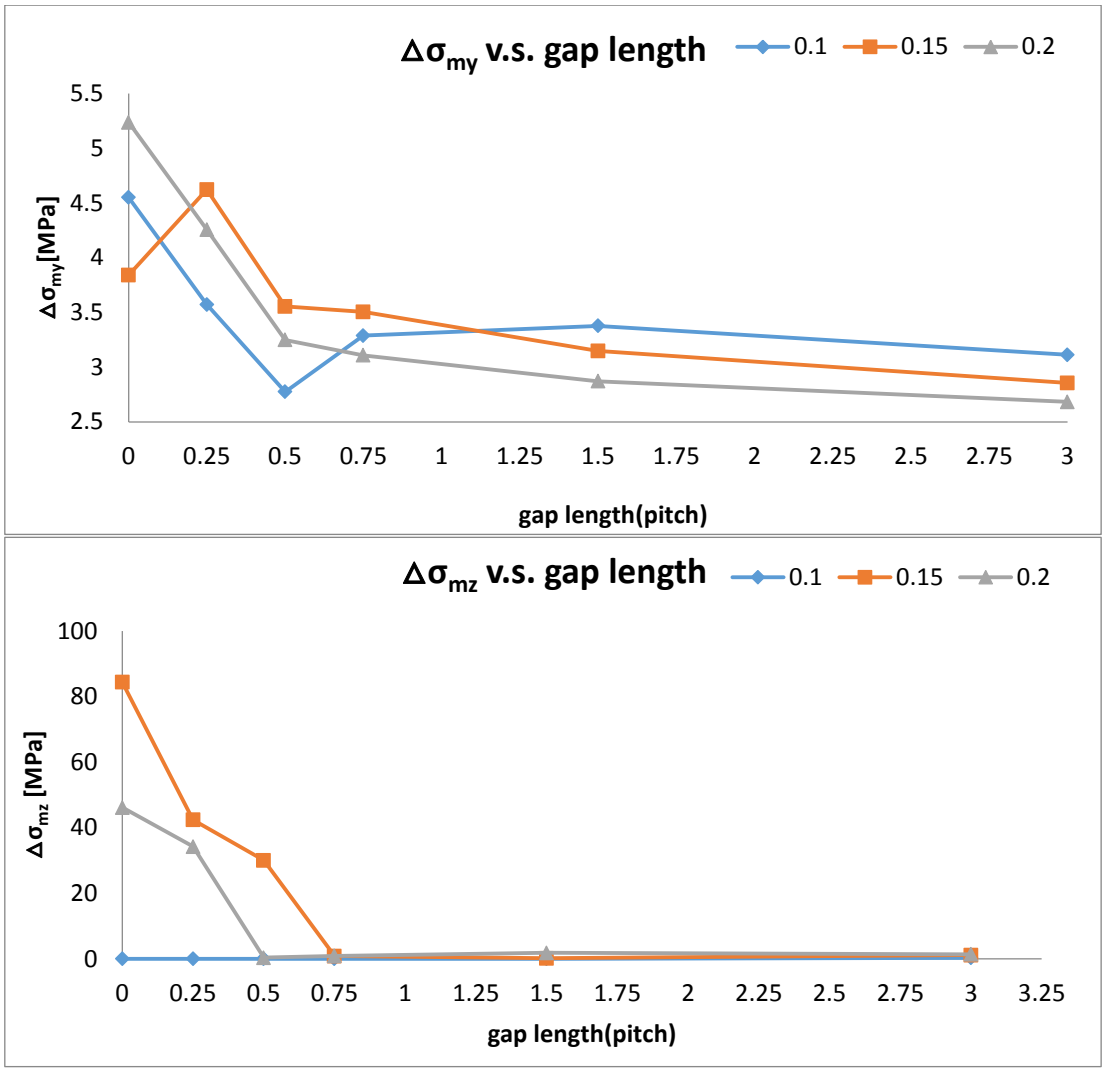

Figure 6-29 stress range for different gap lengths under 0.5MN tension force

From case 0 to case 0.75, in Figure 6-28, we can see the slope increases as the fricion facotor increases. Which means as the friction increases, the damage decreasing speed will increases. However, after the gap length reachs to 0.75 pitch, the maximum damage tend to be constant, then this friction effect in negligible. After the gap length reaches to 1.5 pitch, the friction effect disappear.

From Figure 6-29, we can see that $\Delta\sigma_{ax}$ has the same trend as the maximum damage curve. $\Delta\sigma_{my}$ has big fluctuation, this is because the points we are study is based on the maximum fatigue location, so the physical location on the pipe is changing. $\Delta\sigma_{my}$ and $\Delta\sigma_{mz}$ is sensitive to location. But after the gap length reachs 0.75 pitch, these two stress amplitude tends to be constant.

6.6.2 Friction study based on the same physical locations

Friction based on the same location is studied in this part. The following results were collected from the left end of the bending stiffener(location 2). From the figure below, we can see that the effect of the friction on $\Delta\sigma_{my}$ and $\Delta\sigma_{mz}$ is very small. And after the gap get to 1.5 pitch length, all the stress components shows convergence, the friction factor has no effect anymore.

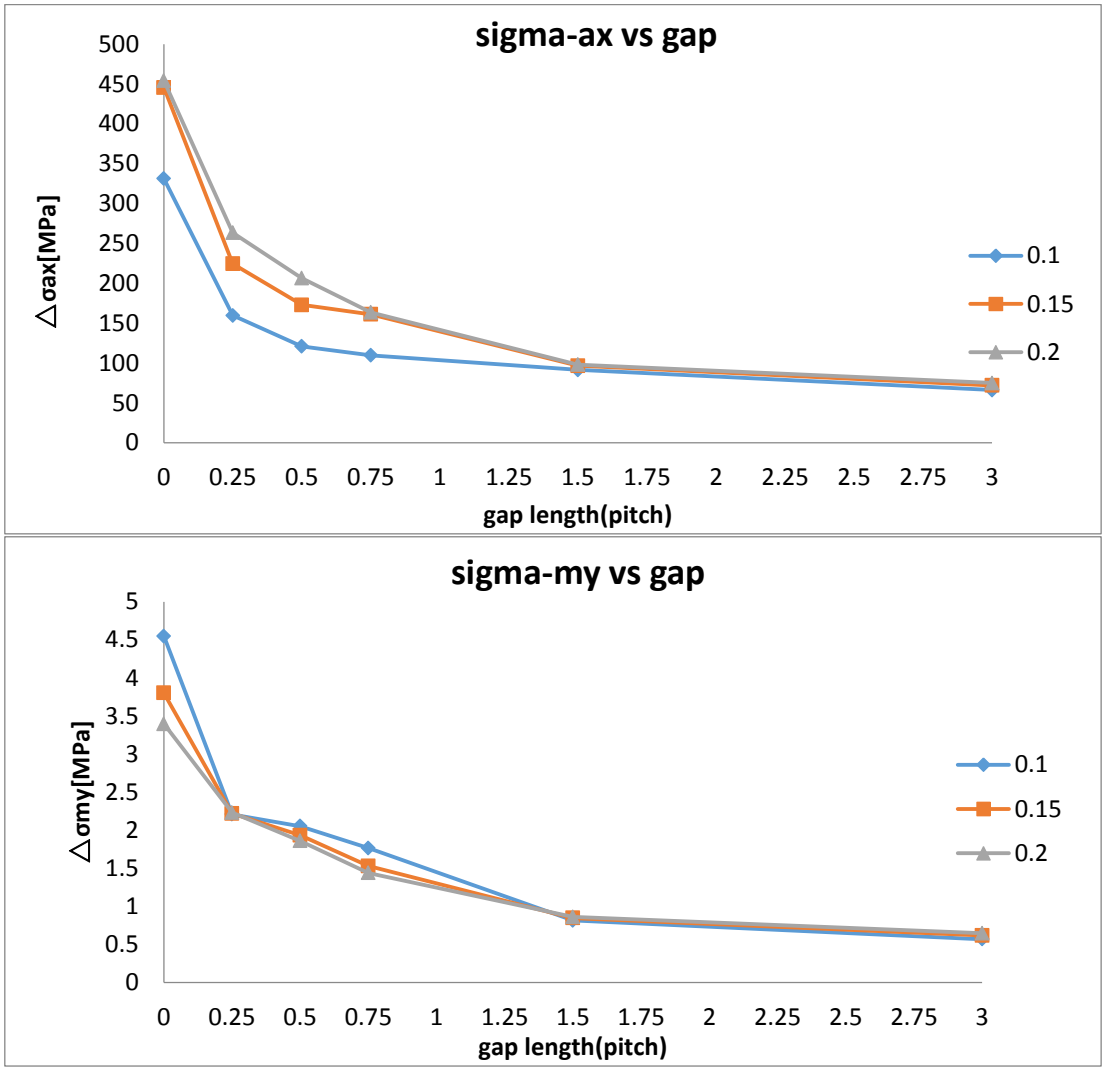

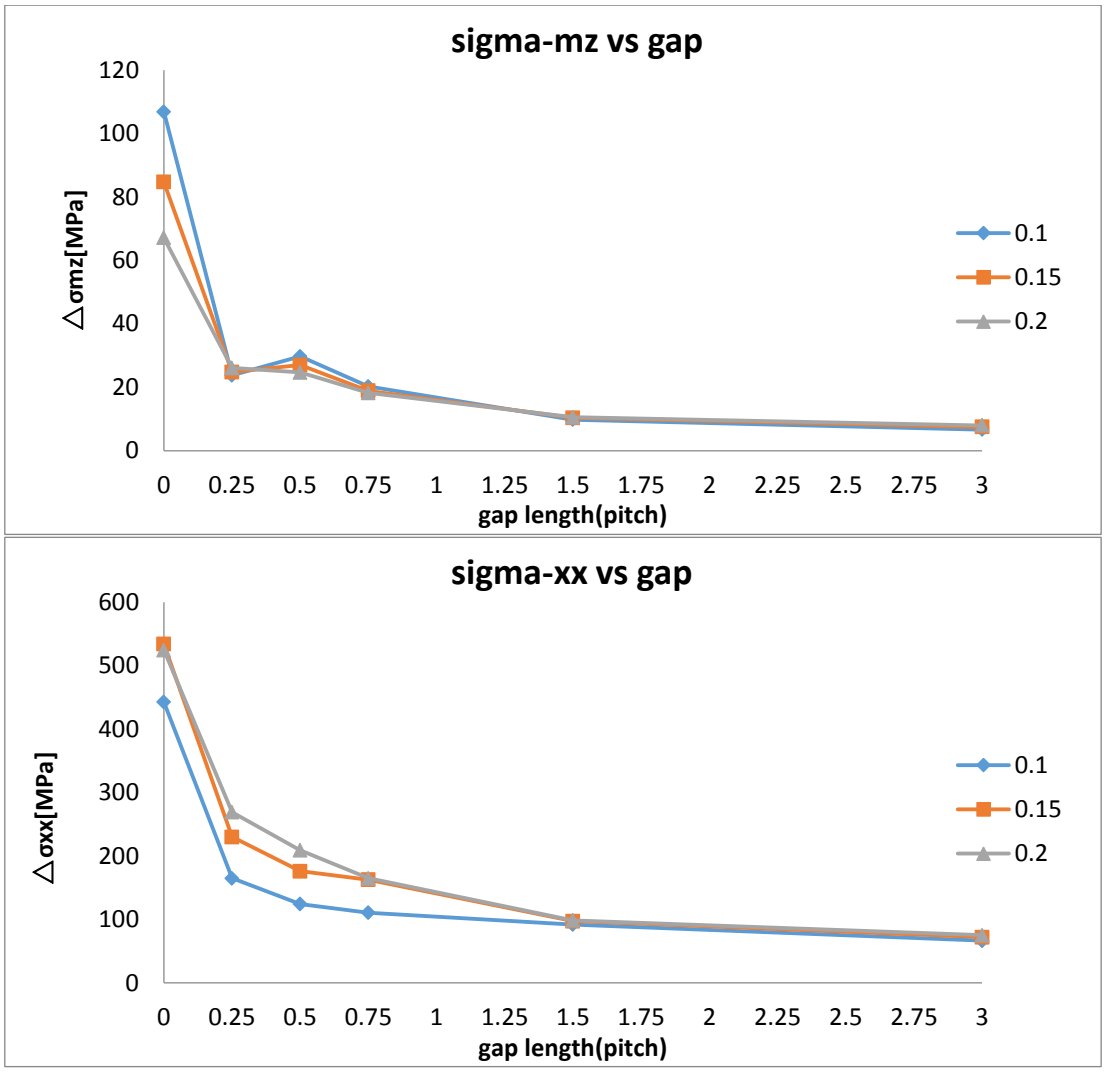

Figure 6-30 stress range on location 2 under 0.5MN tension force

7 Summary

7.1 Conclusions

This thesis is mainly focus on studying how the gap length affects the maximum fatigue damage, including both the damage location and the damage value. Furthermore, how the gap length affects the stress components have been studied.

Models with two kinds of cross-section, ITCODE0 and ITCODE31, are built with gap length of 0, 0.25, 0.5, 0.75 pitch cases, respectively. Analysis is performed mainly on the inner tensile layer where will get the largest fatigue damage and stress components. Two kinds of load conditions are analyzed to study the effect of different load condition- 0.1MN and 0.5MN longitudinal force.

To study the gap length effects accurately, two approaches has been performed. Firstly, analysis was based on studying the maximum damage. After that analysis has been taken based on the fixed physical location.

The flowing conclusions from this project can be drawn:

1. Under different longitudinal load, the maximum fatigue damage value, damage location, stress distribution and amplitude will be all different. Thus, the installation and operation load condition should be clearly specified when designing a new flexible pipe with bending stiffener.
2. Under low longitudinal force
   - Increasing the gap length has no significant effect on the maximum fatigue damage and stress range.
   - The global curvature is very large at the end of the bending stiffener, which means the tension is too small and the bending stiffener cannot be functional.
3. Under high longitudinal force

   When concentrated on studying the maximum fatigue damage, we can get the conclusion:
   - As the gap length increasing, for ITCODE0, the fatigue damage will decreases dramatically. While for ITCODE31, the fatigue damage has only slight trend of decrease. This means that ITCODE 31 cannot precisely represent the effect of the gap

length change. After the gap length reach to a certain length, for both of these two cross-sections, fatigue damage cannot be significantly influenced anymore.

- Friction sensitive study has been performed under this approach, three friction factors (0.1, 0.15 and 0.3) have been analyzed. From case 0 to case 0.75, the decreasing speed of maximum fatigue damage increases as the friction factor increases. While after the gap increases to 0.75 pitch, the effect to the maximum damage becomes very small and negligible.

Second approach is based on studying the fixed physical location along the flexible pipe. Three locations are studied, which are the left end of the pipe, the left end of the bending stiffener and the point 3500mm from the left end of the bending stiffener inside the bending stiffener. Follow conclusions can be drawn:

- At the end of the pipe, increasing the gap length will lead to the decreasing of the stress amplitude, and the increasing range is almost constant, no convergence will occur.
- At the end of the bending stiffener, as the gap length increases, the stress amplitude will decrease correspondingly. While the decreasing range will reducing gradually, and it will convergence when the gap length grows to a certain length.
- Inside the bending stiffener, the gap length has no remarkable influence for the stress amplitude inside the bending stiffener.
- Friction at the left end of the bending stiffener has been studied, we can conclude that after the gap get to 1.5 pitch length, continue improving the friction factor has no effect for any of the stress components.

7.2 Future work

Modeling improvement

The pipe length modeled in this thesis is around 10 meters, while the bending stiffener is 5m. In reality, the pipe length is much longer than 10 meters, this short length can cause some effects on the analysis. To improve modeling, the pipe long should be modeled with a more realistic length in the further work.

Regarding modeling the models which have gap between the end fitting and the bending stiffener, the modeling method used here is to establish the first node/element from the left end, which leads to the element number and node number always changing from case to case.

Therefore, during the stress analysis it is hard to get the element/node number from the same location in all cases. Calculations have to be done to find the right location number. This problem can be solved by modeling the pipe with fixed element/node number from the end of bending stiffener, which means to start model without adding the number from the gap part, and the number for the gap pipe should start with minus value.

Recommendation for future work

From chapter 6.2.2, ITCODE0 under 0.5MN longitudinal force, we get the conclusion that, for a certain gap length, increasing the gap length can contribute to decreasing of the maximum fatigue damage for the pipe. However, after that length, increase of the gap length cannot significantly decrease the maximum damage anymore. In reality, the longer gap length means higher cost of production. Therefore, finding the best gap length is very important. From the analysis results we know this value is between 0.75 and 1.5 pitch length, so more cases with gap length between these values should be performed in the future.

In this thesis, to simplify the analysis, external pressure was neglected. So future work should take the external pressure into account.

Different load conditions should be analyzed. For example, change the internal pressure or change the bending angle at the left end of the bending stiffener and study the effects.

The parameters of the bending stiffener should be studied. For example, change the geometry, length and radius of the bending stiffener and study the effects. Additionally, change the stiffness of the bending stiffener and study the effects.

References

[1] Y. Bai , Q. Bai, Subsea Pipelines and Risers, Elsevier Science Ltd, 2005.

[2] American Petroleum Institute, Specification for bonded Flexible Pipe, API SPECIFICATION 17k, 2014.

[3] American Petroleum Institute, Specification for nonbonded Flexible Pipe, API SPECIFICATION 17J, 2014.

[4] S. Sævik, C. M. Larsen, J. Qvist, D. Fergestad and S. A. Løtveit, Handbook on Design and Operation of Flexible Pipes, Trondheim: MARINTEK / NTNU / 4Subsea, 2014.

[5] American Petroleum Institute, "Recommended Practice for Flexible Pipe API 17B," 2002.

[6] S. Sævik, bflex2010- Theory Manual, Trondheim: MARINTEK, 2013.

[7] N. S. O. S. Geir Skeie, "Efficient Fatigue Analysis of Helix Elements in Umbilicals and Flexible Risers: Theory and Applications," 2012.

[8] S. Sævik, "Lecture notes in offshore pipeline technology," NTNU, 2013.

[9] T. Moan, "Finite Element Modeling and Analysis of Marine Structures," 2003.

[10] S. Sævik, BFLEX 2010 Version 3.1.0 - Beta User Manual, Trondheim: NTNU, 2014.

[11] S. Berge, "Fatigue design of welded structures," Department of Marine Technology,NTNU, Trondheim, 2006.

[12] M. Caire , M. A. Vaz, THE EFFECT OF FLEXIBLE PIPE NON-LINEAR BENDING STIFFNESS BEHAVIOR ON BEND STIFFENER ANALYSIS, California, USA, 2007.

[13] J. L. N. B. V. L.-C. D. C. P. E. T. Perdrizet1, “Stresses in armour layers of flexible pipes comparison of Abaqus models,” , *SIMULIA Customer Conference*, 2011.

Appendix A (ITCODE0 gap0)

```
HEAD BFLEX2010 - model - real nonlin bs -independent nodsys - itcode 0 - 1
#-------------------------------------------------------------------------
# Control data
#               maxit  ndim  isolvr npoint ipri  conr  gacc    iproc
CONTROL    100     3         2      16      1    1.e-5  9.81   STRESSFREE
TIMECO      2.0      1.0  1.0    201.0  STATIC   auto   none     all    50   7    1e-5
TIMECO    402.0    1.0  5.0    201.0  static       auto   NONE    all    20   5    1e-5
#-------------------------------------------------------------------------
# Nocoor input
#                          no       x        y    z
Nocoor Coordinates   1        0        0    0
                          201     10e3    0    0
Nocoor Coordinates 501      0        0    0
                          601     5e3        0    0
#       no          x0    y0   z0   b1   b2   b3    R        node    xcor    theta
Nocoor Polar  0.0   0.0  0.0  0.0  0.0  0.0  135.1    1001     0.0         0
                                                                 1201     10.0e3   -62.1
#           n   ninc    dx      dtheta
Repeat 16   201     0.0     0.392
#       no          x0    y0   z0   b1   b2   b3     R       node     xcor     theta
Nocoor Polar  0.0   0.0  0.0  0.0  0.0  0.0  141.2   20001     0.0        0
                                                                 20201     10.0e3   59.42
#           n      ninc     dx      dtheta
Repeat 16     201      0.0      0.392
Visres Integration 1 Sigma-xx-ax Sigma-xx-my Sigma-xx-mz SIGMA-XX fatigue
#-------------------------------------------------------------------------
# Elcon  input
# The core
# GRO: this info is no longer required
#        group       elty         material  no  n1     n2  n3   n4
Elcon  core        pipe52     mypipe    1   1      2
#       n   elinc  nodinc
Repeat   200   1        1
# The bend stiffener
#               group       elty          crossname       elid        n1    n2  n3   n4
Elcon  bendstiffener pipe52    mybendstiffener 501      501     502
#           n    elinc  nodinc
Repeat  100   1        1
# Tensile Layers
# Tensile Layer 1
#          group       elty    flexcrossname    no      n1   n2     n3     n4
Elcon  tenslayer1 hshear352    mypipe      1001   1     2    1001   1002
                                                                 1016   1     2    4016   4017
#           n   elinc  nodinc
Repeat  200   16      1
#
# Tensile Layer 2
#             group        elty   flexcrossname   no     n1   n2    n3     n4
Elcon  tenslayer2   hshear352   mypipe      20001   1    2   20001  20002
                                                                 20016   1    2   23016  23017
#           n   elinc  nodinc
Repeat  200   16       1
## Contact between bend stiffener and pipe
#
ELCON  bscontact cont130    bscontmat1  601   1  REPEAT 100 1 1
#-------------------------------------------------------------------------
```

```
# Orient input
#
# The core
#                          no        x   y    z
Elorient Coordinates    1          0  1e3  0
                        200        0  1e3  0
#                        no        x    y   z
Elorient Coordinates   501        0   1e3  0
                       600        0   1e3  0
# Tensile Layer 1
#                          no      x y    z
Elorient Coordinates  1001       0  1e3  0
                      1016       0  1e3  0
repeat 200 16 0 0 0
# Tensile Layer 2
#                          no      x y    z
Elorient Coordinates  20001     0  1e3  0
                      20016     0  1e3  0
repeat 200 16 0 0 0
# Contact
Elorient Eulerangle      601    0 0   0
                         700    0 0   0
#       groupn             mname       sname      is1     isn   istx  isty     istz  gt1(MAXIT)   gt2(IGAP)
CONTINT bscontact    core    bendstiffener  501    600    2    5001    2      60                1
#--------------------------------------------------------------------------------
# Definition of flexible pipe cross-section
#                name    type     ifric   disfac forfac geofac  endfac   ID    Timeini  itcode extprlay   ielbfl fimod  dens
CROSSECTION  MYPIPE  FLEXCROSS  1  10000.0  10.0   0.0   -0.001   203.2   2.0      0     12       21     0     1000e-9  3
#nelgr   el1   el2
core tenslayer1 tenslayer2
# CTYPE     TH   matname  FRIC  LAYANG  RNUM   TEMP     nlmat      CCODE CFATFL  AREA        IT          INY         IKS      WIDTH
   CARC    7.20    steel   0.1   88.062    1    0.0      none   C203_3247   NONE  0.00  0.000e+00   0.000e+00   0.000e+00    0.00
   THER    3.00  plastic   0.1    0.000    0    0.0      none       NONE    NONE  0.00  0.000e+00   0.000e+00   0.000e+00    0.00
   THER    6.00  plastic   0.1    0.000    0    0.0      none       NONE    NONE  0.00  0.000e+00   0.000e+00   0.000e+00    0.00
   THER    3.00  plastic   0.1    0.000    0    0.0      none       NONE    NONE  0.00  0.000e+00   0.000e+00   0.000e+00    0.00
   ZETA   10.00    steel   0.1   88.868    1    0.0   nl_steel  Z203_3247   fi09  0.00  0.000e+00   0.000e+00   0.000e+00    0.00
   THER    2.50  plastic   0.1    0.000    0    0.0      none       NONE    NONE  0.00  0.000e+00   0.000e+00   0.000e+00    0.00
   TENS    3.60    steel   0.1  -40.000   44    0.0   nl_steel  T203_3247   fi09  0.00  0.000e+00   0.000e+00   0.000e+00    0.00
   THER    2.50  plastic   0.1    0.000    0    0.0      none       NONE    NONE  0.00  0.000e+00   0.000e+00   0.000e+00    0.00
   TENS    3.60    steel   0.1   40.000   46    0.0   nl_steel  T203_3247   fi09  0.00  0.000e+00   0.000e+00   0.000e+00    0.00
   THER    1.30  plastic   0.1    0.000    0    0.0      none       NONE    NONE  0.00  0.000e+00   0.000e+00   0.000e+00    0.00
   THER    2.50  plastic   0.1    0.000    0    0.0      none       NONE    NONE  0.00  0.000e+00   0.000e+00   0.000e+00    0.00
   THER   10.00  plastic   0.1    0.000    0    0.0      none       NONE    NONE  0.00  0.000e+00   0.000e+00   0.000e+00    0.00#
#CROSS-SECTION BOUNDARY DATA
#          NAME       type  X0  Y0   CCURV    P1        P2      P3       P4      NINTER    ICODE
CROSSGEOM CARC-C203_3247 BFLEX  0   0   S      6.00     180.00     0.0      1.2       5        2
                                            S      7.20      90.00     0.0      1.2       5        0
                                            S     19.20       0.00     0.0      1.2       5        0
                                            S      7.20     270.00     0.0      1.2       5        0
                                            S     19.20       0.00     0.0      1.2       5        0
                                            S      7.20      90.00     0.0      1.2       5        0
                                             S      6.00     180.00     0.0      1.2       5        2
#
CROSSGEOM ZETA-Z203_3247  BFLEX 0  0  CI          90.0000   187.5000  1.2500   0.0000    10       0
                                          S           3.6810    97.5000    0.0000   0.0000    10       0
                                          CI        187.5000  330.0000  1.2500   0.0000    10       2
                                          S           1.6155   240.0000   0.0000   0.0000    10       0
                                          CO        150.0000   90.0000   1.2500   0.0000    10       0
                                          S           1.3770   180.0000   0.0000   0.0000    10       3
```

```
                                        CO      90.0000   10.0000   2.0000   0.0000    10     0
                                         S       3.2435  100.0000   0.0000   0.0000    10     0
                                        CI     190.0000  270.0000   2.0000   0.0000    10     0
                                         S      11.1670  180.0000   0.0000   0.0000    30     1
                                        CI     270.0000  367.5000   1.2500   0.0000    10     0
                                         S       3.6810  277.5000   0.0000   0.0000    10     0
                                        CI       7.5000  150.0000   1.2500   0.0000    10     2
                                         S       1.6155   60.0000   0.0000   0.0000    10     0
                                        CO     330.0000  270.0000   1.2500   0.0000    10     0
                                         S       1.3770    0.0000   0.0000   0.0000    10     3
                                        CO     270.0000  190.0000   2.0000   0.0000    10     0
                                         S       3.2435  280.0000   0.0000   0.0000    10     0
                                        CI      10.0000   90.0000   2.0000   0.0000    10     0
                                         S
                                               11.1670    0.0000   0.0000   0.0000    30     1

#
CROSSGEOM TENS-T203_3247  BFLEX 0  0 CI     90.000  135.0000   1.8000   0.0000    10     0
                                       CI    135.000  180.0000   1.8000   0.0000    10     0
                                       CI    180.000  225.0000   1.8000   0.0000    10     0
                                       CI    225.000  270.0000   1.8000   0.0000    10     0
                                        S     10.400  180.0000   0.0000   0.0000    30     1
                                       CI    270.000  315.0000   1.8000   0.0000    10     0
                                       CI    315.000  360.0000   1.8000   0.0000    10     0
                                       CI    360.000  405.0000   1.8000   0.0000    10     0
                                       CI     45.000   90.0000   1.8000   0.0000    10     0
                                        S     10.400    0.0000   0.0000   0.0000    30     0
                        #-------------------------------------------------------------------
#
# BENDING STIFFENER
#
#                        name            type    nbnod  node  id    od      no_th    rks          imno_i          imno_o
CROSSECTION  MYBENDSTIFFENER  NLBENDSTIFF   1   501   360   1096   10   0.1   mat_in   mat_out
                                                8   508   360   1096   10   0.1   mat_in   mat_out
                                                9   509   360   1096   10   0.1   mat_in   mat_out
                                               95   595   360   428    10   0.1   mat_in   mat_out
                                              101   601   360   428    10   0.1   mat_in   mat_out
#-------------------------------------------------------------------
#
# Element property input
#
#          name  type   rad    th   CDr  Cdt  CMr  CMt   wd       ws     ODp    ODw   rks
ELPROP core  pipe  100.0  5.0  1.0   0.1    2.0   0.2  0.00000 0.00  250.0  250.0   0.5
#         name   type        shearm
# GRO: this info is no longer required
#ELPROP tenslayer1  flexpipe shearmat
#
#       name       type    diameter  inside
ELPROP  bscontact bellmouth    336.0     1
#
#---------------------------------------------------------------------
# Boundary condition data
#      Loc    node  dir
BONCON GLOBAL 1      1
BONCON GLOBAL 1      2
BONCON GLOBAL 1      3
BONCON GLOBAL 1      4
BONCON GLOBAL 1      6
BONCON GLOBAL 501    1
```

```
BONCON GLOBAL 501      2 repeat 100 1
BONCON GLOBAL 501      3
BONCON GLOBAL 501      4
BONCON GLOBAL 501      6 repeat 100 1
BONCON GLOBAL 201      2
BONCON GLOBAL 201      3
# fix the relative disp at ends
BONCON GLOBAL 1001      1
repeat        16     201
BONCON GLOBAL 1201      1
repeat        16     201
BONCON GLOBAL 20001     1
repeat        16     201
BONCON GLOBAL 20201     1
repeat        16     201
#-----------------------------------------------
# Constraint input
CONSTR PDISP GLOBAL   1     5  0.0175 100
CONSTR PDISP GLOBAL   501 5  0.0175 100
#-----------------------------------------------
# Cload input
#     hist  dir  no1    r1       no2   r2         n m
CLOAD  200   1   201  100000.0
#-----------------------------------------------
PELOAD 300  400
PILOAD 500   1   20  200  20
#-------------------------------------------------------------
# History data
#
#    pdisp
#
#    no  istp  fac
THIST 100   0   0.0
              2   0.0
            102  3.0
            302 -3.0
            402  0.0
#    cload
#
THIST 200   0     0.0
              1     1.0
            402   1.0
#    ext press
#
THIST 300   0      0.0
            402   0.0
#    gravity
#
THIST 400   0      0.0
            402   0.0
#
#    int pres
#
THIST 500   0    0.0
              1    1.0
            402   1.0
#-------------------------------------------------------------------------
#  Material data
```

```
#
#       name     type    poiss    ro       talfa  tecond  heatc beta   em   gm    em2
#
#                name    type          poiss ro      talfa    tecond  heatc  eps sigma
MATERIAL mat_in  hyperelastic    0.3  1000e-9 11.7e-6   2.0     50     -1000. -150000.0 1000.0 150000.
MATERIAL mat_out hyperelastic    0.3  1000e-9 11.7e-6   2.0     50     -1000. -150000.0 1000.0 150000.
#       name    type    poiss  talfa    tecond  heatc  beta   ea      eiy     eiz      git      em      gm      den
MATERIAL plastic linear    0.3   11.7e-6   50     800   0    1.02e6  3.210e3  3.210e3 2.568e3   300    100     1000E-
9 300
MATERIAL steel   linear    0.4   11.7e-6   50     800   0    1.02e6  3.210e3  3.210e3 2.568e3   200E3  80e3
7850e-9 2E5
#                name     type         alfa poiss ro     talfa    tecond  heatc eps       sigma
MATERIAL nl_steel elastoplastic  1    0.3  7850   1.17e-5   50     800    0         0
                                                    1.691E-03   3.50E+02
                                                    0.005       450
                                                    0.0998      835
#       name         type     alfa   eps    sigma (asphalt 0.1-0.3) (1 MPa for pp)
MATERIAL shearmat  epcurve         1   0.0     0.00
                                       0.2     0.9
                                       1.0     1.0
                                       1000.0    2.0
#
#       Contact coil-swift:
#
#       name         type     rmyx  rmyz  xmat    ymat     zmat
MATERIAL bscontmat1 isocontact  0.30   bellx      bellz
#       name      type     alfa   eps     sig
MATERIAL bellx     epcurve  1      0       0
                                    1.0     1
                                   1000    10
MATERIAL bellz     hycurve       -1000   -5e5
                                    1000    5e5
#       material    name of file
FATPROP  steel      myfatiguedata
```

Appendix B (ITCODE31 gap0)

```
# Trying input to simla
HEAD BFLEX2010 - test - real nonlinear bs - independ node sys. -itcode 31 - 1
#-------------------------------------------------------------------------
# Control data
#
#       maxit  ndim  isolvr npoint ipri  conr   gacc    iproc
CONTROL    100    3    2      16      1    1.e-5  9.81    stressfree
TIMECO       2.0  1.0  1.0    201.0  STATIC  auto   none    all    50   7    1e-5
TIMECO     402.0  1.0  5.0    201.0  static       auto   none    all    20   5    1e-5
#-------------------------------------------------------------------------
# Nocoor input
#                            no        x      y     z
Nocoor Coordinates   1         0       0     0
                           201     10e3    0     0
Nocoor Coordinates 501       0       0     0
                           601     5e3       0     0
#
Visres Integration 1 Sigma-xx-ax Sigma-xx-my Sigma-xx-mz SIGMA-XX fatigue
#-------------------------------------------------------------------------
# Elcon  input
# The core
#           group       elty       material  no  n1   n2  n3   n4
Elcon  core       pipe52     mypipe     1   1   2
#         n    elinc  nodinc
Repeat  200   1        1
# The bend stiffener
#                   group       elty      crossname       elid    n1     n2  n3   n4
Elcon  bendstiffener pipe52    mybendstiffener  501    501    502
#       n   elinc  nodinc
Repeat  100   1        1
#Elcon  hlpbs1 pipe31    hlpbs1 801   501      502
#       n   elinc  nodinc
#Repeat  100   1        1
#
# Tensile Layers
#              group       elty      crossname   elid     n1     n2  n3   n4
Elcon  tenslayer1  pipe52      mypipe      1001     1      2
#       n   elinc  nodinc
Repeat  200   1        1
# Tensile Layers
#           group       elty         crossname   elid     n1     n2  n3   n4
Elcon  tenslayer2  pipe52      mypipe      2001     1      2
#          n   elinc  nodinc
Repeat  200   1        1
#
# Contact between bend stiffener and pipe
#
ELCON  bscontact cont130    bscontmat1  601   1  REPEAT 100 1 1
#-------------------------------------------------------------------------
# Orient input
#
# The core
#                            no     x  y    z
Elorient Coordinates    1      0  1e3  0
                            200       0  1e3  0
#                             no        x  y    z
Elorient Coordinates   501       0  1e3  0
```

```
                          600       0  1e3  0
#Elorient Coordinates   801      0  1e3    0
#                       900      0  1e3    0
# Tensile Layer 1
#                         no     x  y    z
Elorient Coordinates  1001    0  1e3  0
                      1200    0  1e3  0
# Tensile Layer 2
#                         no     x  y    z
Elorient Coordinates  2001    0  1e3  0
                      2200    0  1e3  0
# Contact
Elorient Eulerangle   601     0  0    0
                      700     0  0    0
#             groupn     mname      sname     is1    isn    istx  isty   istz  gt1   gt2
CONTINT bscontact    core    bendstiffener 501    600    2   5001    2    60    1
#-------------------------------------------------------------------------------
#
# Definition of flexible pipe cross-section
# GRO: the cloadnode and cloadhistno is no longer required
#          name    type      ifric  disfac forfac geofac endfac   ID   Timeini itcode prlay ielbfl fimod   content nelgr   el1
el2
CROSSECTION  MYPIPE  FLEXCROSS  1    10000.0  10.0   0.0   -0.001  203.2  2.0    31     12      21     0    1000e-9
3   core tenslayer1 tenslayer2
#
# CTYPE     TH   matname   FRIC  LAYANG  RNUM   TEMP     nlmat      CCODE CFATFL  AREA         IT         INY         IKS
WIDTH
   CARC    7.20     steel   0.1   88.062    1    0.0      none  C203_3247   NONE  0.00   0.000e+00   0.000e+00   0.000e+00      0.00
   THER    3.00   plastic   0.1    0.000    0    0.0      none       NONE   NONE  0.00   0.000e+00   0.000e+00   0.000e+00      0.00
   THER    6.00   plastic   0.1    0.000    0    0.0      none       NONE   NONE  0.00   0.000e+00   0.000e+00   0.000e+00      0.00
   THER    3.00   plastic   0.1    0.000    0    0.0      none       NONE   NONE  0.00   0.000e+00   0.000e+00   0.000e+00      0.00
   ZETA   10.00     steel   0.1   88.868    1    0.0   nl_steel  Z203_3247   fi09  0.00   0.000e+00   0.000e+00   0.000e+00      0.00
   THER    2.50   plastic   0.1    0.000    0    0.0      none       NONE   NONE  0.00   0.000e+00   0.000e+00   0.000e+00      0.00
   TENS    3.60     steel   0.1  -40.000   44    0.0   nl_steel  T203_3247   fi09  0.00   0.000e+00   0.000e+00   0.000e+00      0.00
   THER    2.50   plastic   0.1    0.000    0    0.0      none       NONE   NONE  0.00   0.000e+00   0.000e+00   0.000e+00      0.00
   TENS    3.60     steel   0.1   40.000   46    0.0   nl_steel  T203_3247   fi09  0.00   0.000e+00   0.000e+00   0.000e+00      0.00
   THER    1.30   plastic   0.1    0.000    0    0.0      none       NONE   NONE  0.00   0.000e+00   0.000e+00   0.000e+00      0.00
   THER    2.50   plastic   0.1    0.000    0    0.0      none       NONE   NONE  0.00   0.000e+00   0.000e+00   0.000e+00      0.00
#   TENS    3.60     steel   0.1  -40.000   48    0.0   nl_steel  T203_3247   fi09  0.00   0.000e+00   0.000e+00   0.000e+00      0.00
#   THER    2.50   plastic   0.1    0.000    0    0.0      none       NONE   NONE  0.00   0.000e+00   0.000e+00   0.000e+00      0.00
#   TENS    3.60     steel   0.1   40.000   50    0.0   nl_steel  T203_3247   fi09  0.00   0.000e+00   0.000e+00   0.000e+00      0.00
#   THER    1.80   plastic   0.1    0.000    0    0.0      none       NONE   NONE  0.00   0.000e+00   0.000e+00   0.000e+00      0.00
   THER   10.00   plastic   0.1    0.000    0    0.0      none       NONE   NONE  0.00   0.000e+00   0.000e+00   0.000e+00      0.00
#
#CROSS-SECTION BOUNDARY DATA
#          NAME      type  X0  Y0   CCURV    P1        P2      P3      P4     NINTER    ICODE
CROSSGEOM CARC-C203_3247 BFLEX  0   0   S      6.00     180.00     0.0      1.2       5       2
                                        S      7.20      90.00     0.0      1.2       5       0
                                        S     19.20       0.00     0.0      1.2       5       0
                                        S      7.20     270.00     0.0      1.2       5       0
                                        S     19.20       0.00     0.0      1.2       5       0
                                        S      7.20      90.00     0.0      1.2       5       0
                                        S      6.00     180.00     0.0      1.2       5       2
#
CROSSGEOM ZETA-Z203_3247   BFLEX  0   0  CI     90.0000   187.5000   1.2500   0.0000     10       0
```

```
                                        S     3.6810   97.5000  0.0000  0.0000    10      0
                                       CI   187.5000  330.0000  1.2500  0.0000    10      2
                                        S     1.6155  240.0000  0.0000  0.0000    10      0
                                       CO   150.0000   90.0000  1.2500  0.0000    10      0
                                        S     1.3770  180.0000  0.0000  0.0000    10      3
                                       CO    90.0000   10.0000  2.0000  0.0000    10      0
                                        S     3.2435  100.0000  0.0000  0.0000    10      0
                                       CI   190.0000  270.0000  2.0000  0.0000    10      0
                                        S    11.1670  180.0000  0.0000  0.0000    30      1
                                       CI   270.0000  367.5000  1.2500  0.0000    10      0
                                        S     3.6810  277.5000  0.0000  0.0000    10      0
                                       CI     7.5000  150.0000  1.2500  0.0000    10      2
                                        S     1.6155   60.0000  0.0000  0.0000    10      0
                                       CO   330.0000  270.0000  1.2500  0.0000    10      0
                                        S     1.3770    0.0000  0.0000  0.0000    10      3
                                       CO   270.0000  190.0000  2.0000  0.0000    10      0
                                        S     3.2435  280.0000  0.0000  0.0000    10      0
                                       CI    10.0000   90.0000  2.0000  0.0000    10      0
                                        S    11.1670    0.0000  0.0000  0.0000    30      1
#
CROSSGEOM TENS-T203_3247  BFLEX  0  0 CI    90.000  135.0000  1.8000  0.0000    10      0
                                       CI   135.000  180.0000  1.8000  0.0000    10      0
                                       CI   180.000  225.0000  1.8000  0.0000    10      0
                                       CI   225.000  270.0000  1.8000  0.0000    10      0
                                        S    10.400  180.0000  0.0000  0.0000    30      1
                                       CI   270.000  315.0000  1.8000  0.0000    10      0
                                       CI   315.000  360.0000  1.8000  0.0000    10      0
                                       CI   360.000  405.0000  1.8000  0.0000    10      0
                                       CI    45.000   90.0000  1.8000  0.0000    10      0
                                        S    10.400    0.0000  0.0000  0.0000    30      0
#-------------------------------------------------------------------
#
# BENDING STIFFENER
#
#                          name          type   nbnod  node  id          od        no_th    rks         imno_i  imno_o
CROSSECTION  MYBENDSTIFFENER  NLBENDSTIFF  1   501   360    1096    10     0.1     mat_in    mat_out
                                                 8   508   360    1096    10     0.1     mat_in    mat_out
                                                 9   509   360    1096    10     0.1     mat_in    mat_out
                                                 95  595   360    428     10     0.1     mat_in    mat_out
                                                 101 601   360    428     10     0.1     mat_in    mat_out
                                #-------------------------------------------------------------------
#
# Element property input
#
#            name  type   rad   th   CDr  Cdt  CMr  CMt   wd    ws    ODp   ODw   rks
#ELPROP core  pipe  100.0  5.0  1.0   0.1   2.0    0.2 0.00000 0.00  250.0  250.0 0.5
#              name  type   rad    th   CDr  Cdt  CMr  CMt      wd     ws    ODp   ODw rks
#ELPROP hlpbs1  pipe  100.0  5.0  1.0   0.1     2.0     0.2       0.0    0.0  250.0  250.0 0.5
#       name        type     diameter  inside
ELPROP  bscontact bellmouth     336.0    1
#
#-------------------------------------------------------------------
# Boundary condition data
#              Loc     node  dir
BONCON GLOBAL 1      1
BONCON GLOBAL 1      2
BONCON GLOBAL 1      3
BONCON GLOBAL 1      4
BONCON GLOBAL 1      6
BONCON GLOBAL 501    1
BONCON GLOBAL 501    2 repeat 100 1
BONCON GLOBAL 501    3
```

```
BONCON GLOBAL 501    4 repeat 100 1
BONCON GLOBAL 501    6 repeat 100 1
BONCON GLOBAL 201    2
BONCON GLOBAL 201    3
#-----------------------------------------------
#
# Constraint input
CONSTR PDISP GLOBAL   1  5   0.0175 100
CONSTR PDISP GLOBAL   501 5  0.0175 100
#
#-----------------------------------------------
# Cload input
#
#    hist  dir  no1 r1  no2 r2         n m
#
CLOAD   200   1  201  100000.0
#-----------------------------------------------
PELOAD  300  400
PILOAD  500   1   20   200   20
#-------------------------------------------------------------
# History data
#
#   pdisp
#
#   no  istp  fac
THIST 100   0   0.0
  `              2   0.0
               102  3.0
               302 -3.0
               402  0.0
#   cload
#
THIST 200  0      0.0
               1      1.0
              402   1.0
#
#   ext press
#
THIST 300    0     0.0
              402   0.0
#   gravity
#
THIST 400  0     0.0
             402  0.0
#
#   int pres
#
THIST 500  0       0.0
               1      1.0
              402   1.0
#-------------------------------------------------------------------------------
#  Material data
#       name     type    poiss    ro       talfa  tecond  heatc beta   em   gm    em2
#
#       name    type          poiss  ro      talfa  tecond  heatc   eps   sigma
MATERIAL mat_in  hyperelastic   0.3  1000e-9  11.7e-6   2.0     50    -1000. -150000.0 1000.0 150000.
MATERIAL mat_out hyperelastic   0.3  1000e-9  11.7e-6   2.0     50    -1000. -150000.0 1000.0 150000.
#       name    type    poiss  talfa  tecond  heatc beta  ea      eiy     eiz      git     em    gm    den
```

```
MATERIAL plastic linear   0.3  11.7e-6   50    800   0    1.02e6  3.210e3  3.210e3 2.568e3  300  100.0  1000E-9 300
MATERIAL steel   linear   0.4  11.7e-6   50    800   0    1.02e6  3.210e3  3.210e3 2.568e3  2E5  0.8e5  7850E-9 2E5
#MATERIAL hlpbs1   linear   0.4  11.7e-6   50    800   0    1.02e9  0.0     0.0     1e10     2E5    0.8e5  7850E-9 2E5
#       name     type         alfa poiss ro      talfa    tecond  heatc eps sigma
MATERIAL nl_steel elastoplastic  1    0.3  7850    1.17e-5   50     800  0          0
                                                    1.691E-03   3.50E+02
                                                    0.005       450
                                                    0.0998      835
#       name         type     alfa   eps    sigma (asphalt 0.1-0.3) (1 MPa for pp)
MATERIAL shearmat  epcurve        1    0.0       0.00
                                       0.2       0.9
                                       1.0       1.0
                                     1000.0    2.0
#       Contact coil-swift:
#
#       name         type     rmyx  rmyz  xmat    ymat     zmat
MATERIAL bscontmat1 isocontact  0.30   bellx      bellz
#       name      type     alfa   eps     sig
MATERIAL bellx     epcurve  1      0       0
                                    1.0     1
                                   1000    10
#
MATERIAL bellz     hycurve       -1000   -5e5
                                   1000    5e5
#       material    name of file
FATPROP  steel      myfatiguedata
```